Transmural differences in the properties of ventricular muscle in normal and failing rabbit hearts.

A thesis submitted in fulfilment of the degree of
Doctor of Philosophy

to

University of Glasgow
Faculty of Medicine

by

Alexis Mary Duncan
BSc (Hons)

Institute of Biomedical and Life Sciences, University of Glasgow.

April 2002

Abstract

It is now well established that electrical, metabolic and mechanical properties vary across the wall of the mammalian ventricle. In this thesis, protein expression, intracellular [Ca^{2+}], and myocyte shortening are examined in myocardium from endocardial and epicardial regions of normal rabbit hearts. These properties were compared with those in equivalent regions of hearts with significant left ventricular dysfunction (LVD) resulting from a ventricular apical infarct.

Resting myocyte length was significantly longer in myocytes isolated from LVD hearts but no regional differences in resting myocyte length in sham or LVD myocytes was observed. Fractional shortening was not significantly different between endocardial and epicardial myocytes from both sham and LVD hearts. LVD endocardial myocytes shortened less than myocytes from the comparable region in the sham group. No difference in fractional shortening was observed when comparing epicardial myocytes from sham and LVD hearts. Contraction kinetics were slower in both LVD endocardial and epicardial myocytes. The rest decay effect was more pronounced in endocardial compared with epicardial myocytes in both sham and LVD groups but minimal differences were observed when comparing experimental groups.

Peak systolic $[Ca^{2+}]_i$ was similar in endocardial myocytes from both experimental groups but was significantly lower in the LVD epicardial group than sham. Peak systolic $[Ca^{2+}]_i$ was similar between endocardial and epicardial myocytes in the sham group but LVD epicardial peak systolic $[Ca^{2+}]_i$ was lower than endocardial. These results suggest various changes in $[Ca^{2+}]_i$ transient amplitude and myocyte shortening in LVD that may be explained by changes in myofilament Ca^{2+} sensitivity.

Transmural protein expression of Calsequestrin, SR Ca^{2+}-ATPase (SERCA) and Na^+/Ca^{2+} exchanger was similar in sham and LVD myocytes. Calsequestrin and Na^+/Ca^{2+}exchanger protein expression was significantly increased, and SERCA protein expression was significantly decreased, in LVD myocytes. The link between altered protein expression and altered intracellular [Ca^{2+}] transients in LVD is discussed.

Comparison of the amount of protein retrieved from sham and LVD ventricular homogenate samples showed that protein retrieval was similar throughout a range of ventricular tissue wet weights (60 to 1000mg) and in sham and LVD myocardial samples. In contrast, protein retrieved from crude SR preparations (250 – 1000mg) was significantly greater in LVD preparations than sham samples. In addition, crude SR vesicles derived from ventricular samples weighting less than 250mg proved unsuitable for experimental use because of the variable protein retrieval when using such small sample weights.

Sources of experimental variation within the Western Blotting technique were also investigated. It was concluded that the major sources of variation were attributable to the electroblotting and the antibody binding steps.

Contents

Chapter 3. Cardiac myocyte contractility measurements

List of figures **Page:**

List of tables **Page:**

Acknowledgements

First and foremost I would like to sincerely thank my supervisor Professor Godfrey Smith for his unwavering guidance, support, encouragement and incredible patience throughout the period of my research.

I am also very grateful to Dr Susan Currie for her introduction and guidance through the minefield that is "Gel electrophoresis".

A special thanks goes to Dr Paul Neary for his patient listening ear and advice over the last few years.

Thanks to Ann and Aileen for their ever present technical support, help and advice that they have given to me during my work on the 4th floor. Thanks also to my many colleagues/ friends whom I have had the pleasure of working and socialising with over the last few years. It's been great fun.

I would like to thank The British Heart Foundation for financial support.

A very big thank you also goes to my family and friends (Pam, Julie, Gillian, Debbie, John, Kaska, Rosemary, Eileen, Sarah, Lorraine and Jo who have helped me through the up and downs of the last 4 years and given me invaluable support and advice.

Finally, a special thank you to my parents and brother Peter who as usual have given me their constant love, support and guidance throughout the working of and writing of this thesis.

This thesis is dedicated to the memory of my Grandma, Mary Dawson.

Declaration

Coronary artery ligation and sham operations on all rabbits were performed by technical staff (Mrs Dianne Smillie, Mr Michael Dunne and Mr Graham Deuchar) at the Department of Medical Cardiology, Glasgow Royal Infirmary under the supervision of Dr Martin Hicks. Echocardiography was performed by Mrs Dianne Smillie. All the experimental work contained in this thesis is original work and was undertaken by me. The material has not been submitted previously for any other degree. Some of the results presented here have been published during the period of study, details of which are given below.

Publications

"*Endocardial – epicardial differences in myocyte contractility in normal and failing rabbit hearts*" G.L.Smith and A.M. Duncan. **Biophysical Journal** 2000, Volume 78, P638

" *Transmural differences in Ca^{2+} handling proteins in normal rabbit hearts and hearts with left ventricular dysfunction*" A.M.Duncan, S.Currie and G.L.Smith. **Journal of Physiology** 2001; 536P.

Abbreviations

AB	Assay buffer
ADP	Adenosine diphosphate
ATP	Adenosine triphosphate
BSA	Bovine serum albumin
cAMP	Cyclic adenosine mono phosphate
CICR	Calcium induced calcium release
CrP	Creatine phosphate
CSQ	Calsequestrin
D50	Duration at 50% contraction
DTT	Dithiothreithol
E-C coupling	Excitation- contraction coupling
EDTA	Ethylenediamine – tetra acetic acid
EF	Ejection fraction
EGTA	Ethylene Glycol-bis (β-aminoethyl ether)-N,N,N',N',-tetraacetic acid
ENDO	Endocardial
EPI	Epicardial
FCS	Foetal calf serum
FS	Fractional shortening
gAMP	Guanosine adenosine mono phosphate
HB	Homogenisation buffer
HEPES	(N-[2-Hydroxyethyl] piperazine – N'-[2-ethan esusulfonic acid])
HRP	Horse radish peroxidase
I_{CA}	Sarcolemmal Ca^{2+} current

kDa	Kilo daltons
K_D	Calcium concentration at 50% maximum response
L-type channels	Sarcolemmal calcium channels
LV	Left ventricle
LVD	Left ventricular dysfunction
MF	Myofilaments
Mito	Mitochondrion
mRNA	Messenger ribonucleic acid
MOPS	3-(N-morpholino) propane sulfonic acid
MW	Molecular weight
NCX	Sarcolemmal sodium- calcium exchanger
NO	Nitrous oxide
OD	Optical density
PA	Peak amplitude
PAGE	Polyacrylamide gel electrophoresis
PB	Precipitation buffer
RCC	Rapid cooling contractures
Pi	Inorganic phosphate
PLB	Phospholamban
PRP	Post rest potentiation
R_{min}	Minimum fluorescence ratio
R_{max}	Maximum fluorescence ratio
RyR	Ryanodine receptor
SDS	Sodium dodecyl sulfate
SEM	Standard error of Mean
SR	Sarcoplasmic reticulum
SR Ca^{2+}-ATPase pump	SERCA 2A

TD50	Time to decay at 50 % contraction
TD90	Time to decay at 90% contraction
TTP	Time to peak
TTP50	Time to peak at 50 % contraction
Tris base	2-amino-2- (hydroxymethyl)- 1,3- propanediol
Tris HCL	(Tris[hydroxlmethyl]aminomethane hydrochloride
Triton X-100	T- octylphenoxypolyethoxyethanol
Tween 20	Polyoxthylene sorbitan monolaurate
V	Voltage

Chapter 1

Introduction

Cardiac myocytes generate the contraction required for the pumping action of the heart. Under normal physiological conditions cardiac myocytes of the atria and ventricles function as a syncitium, where electrical and mechanical links between cells ensures that every cell contracts at each beat. The synchrony of cellular contraction is critically important for adequate cardiac function. As with most physiological systems there is no one simple process or mechanism governing cardiac function, rather there is a multitude of distinct complex mechanisms, all functioning together for the common goal; efficient cardiac function.

Clearly, pathophysiological conditions, such as congestive cardiac failure, which disrupt myocyte function and connective tissue structure and function can give rise to severe contractile dysfunction and hereafter potential systemic dysfunction.

It is appropriate at this point to discuss our current understanding of myocyte structure and function, and how myocyte contraction is mediated within mammalian cardiac muscle.

1.1. Ultrastructure of cardiac myocytes

Mammalian cardiac myocyte dimensions are similar between species, for example; human myocytes measure, 19 ± 1.7μm by 141 ± 9 μm (width/length) (Gerdes *et al.* 1992); rabbit; 27.3 ± 1.0μm by 134.8 ± 2.7 μm (sub-epicardium); 29.5 ± 1.1μm by 140.4 ± 2.6 μm (sub-endocardium) (McIntosh *et al.* 2000) and rat 22.1 ± 0.8μm by 149.4 ± 3.9 μm (Gerdes *et al.* 1996). Mammalian myocytes contain either a single or double nucleus and are physically, electrically, and biochemically attached to adjacent myocytes by intercalated discs. The sarcomere is the functional unit of contraction within myocytes, and measures approximately 2μm in length. Sarcomeres are aligned side by side across the cell with their individual boundaries defined by Z lines. The A and I bands of the sarcomere give cardiac (and skeletal) myocytes their

characteristic striated appearance. In ventricular myocytes invaginations of the sarcolemma occur opposite Z lines forming transverse tubules (T-tubules). T-tubules transmit electrical stimuli rapidly into the myocyte interior and thus help activate multiple myofilaments simultaneously (Levick, 1995). Sarcomeres contain 2 main types of contractile proteins, thick (myosin) and thin (actin) filaments, plus additional modulatory proteins, namely tropomyosin, and troponin. Actin filaments project approximately 1μm from the Z lines and appear to be anchored to the latter by intermediate filaments. Myosin filaments are ~1.6μm long and are connected to neighbouring myosin filaments by crosslinks.

The thick filament is composed largely of the protein myosin. The complete myosin molecule consists of 2 heavy chains and 4 light chains. Each of the two heavy chains consist of a long α-helical tail (~ 120nm) and a globular head. The 2 tails are intertwined and form a double-headed structure. The heavy chain itself is further divide into light meromyosin (most of the tail) and heavy meromyosin. Heavy meromyosin consists of subfragments 1 (S1, globular head and enzymatic activity) and 2 (S2) which are composed of the remainder of the tail section and the light chains. The globular heads contain the adenosine triphosphatase (ATPase) (site of ATP hydrolysis; ATP ~high energy molecule,) and the actin (thin filament) binding site (See later for details of crossbridge cycling /sliding filament theory). It is the heavy meromyosin that forms the *crossbridge* which projects from the thick filament and interacts with the thin filament (actin).

The major component of the thin filament is the actin monomer (G-actin). Under physiological concentrations of ATP and Mg^{2+}, G-actin assembles into a helical double stranded F-actin polymer (the backbone of the thin filament). In addition the thin filament contains regulatory proteins; the double stranded protein Tropomyosin and Troponin, a complex of 3 functionally distinct proteins. Troponin consists of Troponin T which is the Tropomyosin binding subunit, Troponin I the inhibitory subunit, and Troponin C the Ca^{2+}-binding subunit. Troponin C possesses 1 Ca^{2+}-specific binding site and 2 Ca^{2+}-Mg^{2+} sites. (Solaro, 1995).

1.2. Calcium activated contraction

During diastole, when $[Ca^{2+}]_i$ is ~100nM, Ca^{2+}-binding sites on Troponin C are unoccupied. This status permits the interaction between Troponin I and Troponin C which appears to enhance the inhibitory effect of Troponin I, strengthening the interaction between Troponin I and actin. Such Troponin I/actin contact shifts the Troponin-Tropomyosin complex out of the actin groove and physically prevents the myosin heads (crossbridges) binding to actin (termed *steric hindrance*), and consequentially prevents crossbridge cycling. During systole, when $[Ca^{2+}]_i$ rises to ~1μM, Ca^{2+} binds to Troponin C (at Ca^{2+} specific sites). This binding alters the interaction of Troponin I and Troponin C and subsequently causes a configurational change between Troponin I and actin. This shifts the Troponin-Tropomyosin complex into the actin groove, removing the *steric hindrance*. In this state, the crossbridges can attach to actin and cross-bridge cycling and consequently contraction (shortening) can occur. Huxley first suggested this steric hindrance model in 1973, using x-ray diffraction studies.

During systole, in the presence of ATP and high $[Ca^{2+}]_i$, attachment of the crossbridges to actin occurs. The ATP molecule bound to the myosin head is hydrolysed (into adenosine di-phosphate; ADP, inorganic phosphate, Pi and H^+) and an energy source is released. This energy is used by the crossbridges to produce a power stroke which causes parallel sliding of the attached actin filament relative to the myosin filament. This sliding mechanism was first proposed in 1954 by two separate groups, H.E.Huxley and A.F. Huxley plus colleagues and was termed the *sliding filament theory.*

It is clear that both Ca^{2+} and ATP are essential metabolic requirements for cardiac contraction. As the active myocyte requires a constant supply of ATP, it comes as no surprise that myocytes possess an exceptionally high density of mitochondria; 35% of cell volume. Mitochondria produce ATP by oxidative phosphorylation for which oxygen is obligatory, hence the reason why cardiac performance is directly dependent on oxygen supply and hence coronary blood flow (Bers, 1993).

1.2.1. Calcium sensitivity of the myofilaments

Briefly, myofilament sensitivity to Ca^{2+} is affected by several factors including; temperature, (Harrison & Bers, 1989), pH_i, (Fabiato & Fabiato, 1978; Kentish & Orchard, 1990; Hajjar *et al.* 2000), sarcomere length (Kentish *et al.* 1986; Schwinger *et al.* 1994), intracellular [Mg^{2+}], (Best *et al.* 1977) and intracellular [Pi] (Kentish, 1986).

1.3. Calcium induced calcium release (CICR)

Initiation of electrical conduction begins within pacemaker cells found in the Sinoatrial node in the atria. Activation then spreads via the atrioventricular node through the specialised conduction system (Purkinje fibres), to the ventricles. Specialised sarcolemmal protein channels called gap junctions found within intercalated discs provide low resistance pathways, which allow electrical and biochemical coupling between adjacent myocytes (Bruzzone *et al.* 1996). These pathways are believed to be responsible for the rapid propagation of electrical excitation that allows the heart to contract as an electrical syncytium.

Electrical excitation of the myocyte surface membrane (sarcolemma) initiates an action potential (electrical signal) which propagates as a wave of depolarisation along the sarcolemma and down into the T-tubules. T-tubules penetrate deep into the myocyte, forming close contact with the junctional region of the sarcoplasmic reticulum (SR). Myocyte depolarisation by the action potential produces a rise in intracellular [Ca^{2+}] ($[Ca^{2+}]_i$) via the Ca^{2+} current (I_{CA}) and possibly a small influx via the sarcolemmal Na^+/Ca^{2+} exchanger (NCX). This rise in $[Ca^{2+}]_i$ triggers an additional and much magnified release of SR Ca^{2+} via Ca^{2+} release channels (Ryanodine receptors). This mechanism is termed Ca^{2+} induced Ca^{2+} release (CICR). These release channels are thought to be closely apposed to the sarcolemmal Ca^{2+} channels (dihydropyridine receptor) (Block *et al.* 1988; Sun *et al.* 1995). This close spatial relationship is necessary for efficient excitation-contraction coupling (E-C coupling). SR Ca^{2+} release is generally accepted to be the dominant source of myofilament activator Ca^{2+} with small contributions from I_{CA} and NCX. The localised increase in $[Ca^{2+}]_i$ activates the nearby myofilaments in a $[Ca^{2+}]$-dependent

manner, and manifests as myocyte contraction/shortening. The CICR mechanism implies a positive feedback system, i.e. the greater the amount of Ca^{2+} released, the greater is the amount of "trigger" Ca^{2+} available to induce further release. If this were the case all of the SR Ca^{2+} content would be released during depolarisation. However, this has been shown not to occur and in fact the magnitude of CICR is graded by the amount of trigger Ca^{2+}, and also the rate of change of $[Ca^{2+}]_i$ surrounding the SR (Fabiato, 1983). Such a graded response suggests some degree of regulation within this system. To date, the CICR theory appears to be the most generally accepted, even though the exact nature of the release mechanism remains somewhat controversial. A schematic diagram of the intracellular Ca^{2+} transport mechanism within cardiac myocytes is shown in figure 1.1.

1.4. Intracellular calcium homeostasis

As Ca^{2+} is one of the most crucial participants in E-C coupling it is important to be aware of the different cellular regulatory mechanisms involved in and affecting its homeostasis. As discussed earlier, Ca^{2+} enters the cell during the action potential either via the sarcolemmal Ca^{2+} channels (L-type) or via the Na^+/Ca^{2+} exchanger working in reverse mode. After contraction (systole) cardiac muscle must relax, in order for this to occur it is essential that $[Ca^{2+}]_i$ is reduced back to diastolic levels (100nM), such that Ca^{2+} will dissociate from Troponin C and the inhibition of Troponin I is removed.

There are 4 main mechanisms which contribute to this process:

1) SR Ca^{2+}-ATPase pump (SERCA 2A)

2) Sarcolemmal Na^+/Ca^{2+} exchanger (NCX)

3) Sarcolemmal Ca^{2+} ATPase

4) Mitochondrial calcium uniporter

1.4.1. SR Ca^{2+} -ATPase pump (SERCA 2A)

A Ca^{2+}/Mg^{2+} dependent ATPase, a 997 amino acid transmembrane protein, pumps Ca^{2+} into the SR during diastole. Three Ca^{2+}-ATPase genes exist, SERCA 1,2 & 3, encoding the 100kDa SR/ER (endoplasmic reticulum) calcium pumps within intracellular membranes. This family of enzymes is well conserved throughout many tissues performing identical functions. The SERCA 2 isozyme is found in cardiac muscle (as well as in slow skeletal, smooth and some non-muscle cells). Variants of SERCA 2; SERCA 2A, and SERCA 2B are found in cardiac and smooth muscle respectively. SERCA 2A transports 2 Ca^{2+} into the SR during one cycle and uses 1 ATP molecule, calcium binding is sequential and cooperative (Colyer, 1993; Simmerman & Jones, 1998). SERCA 2A is a high affinity pump with a K_M = 0.1-0.5 μM, and a V_{Max} of 20-30 nmol Ca^{2+}/mg protein/s at 25^0C (Where K_M is $[Ca^{2+}]$ at which the pump is 50% activated, the lower the concentration the fewer Ca^{2+} are required for pump activation, therefore the greater the pump Ca^{2+} sensitivity). V_{Max} is the maximum Ca^{2+} transport rate across the SR (Carafoli, 1985).

The principal regulator of SERCA 2A in cardiac SR is the SR protein phospholamban (PLB). PLB is a pentamer of 5 identical subunits each containing 52 amino acids (MW~25kDa). This protein can be divided into 2 almost equal parts; a cytoplasmic domain containing the phosphorylation sites (residues 1-30) and the transmembrane domain (31-52). PLB regulation of SERCA 2A depends on the phosphorylation state of PLB; dephosphorylated PLB inhibits SERCA 2A and phosphorylated PLB enhances pump activity. The exact mechanism of this inhibition remains controversial, but may reflect a physical inhibition of the pump by PLB. In vitro studies have identified Serine-16 and Threonine-17 as the residues phosphorylated by cAMP/cGMP-dependent protein kinases, and calcium/calmodulin-dependent protein kinases, respectively (Koss & Kranias, 1996). There is also some speculation that phosphorylation can occur on Serine-10 although this remains controversial. In total, there are 10 potential phosphorylation sites on PLB, five each on Serine-16 and Threonine-17 (Simmerman & Jones, 1998). PLB is one of the few proteins which is phosphorylated in SR by both by cAMP/cGMP-dependent protein kinases, and Ca^{2+}/calmodulin-dependent protein kinases.

Phosphorylation of these residues reduces the inhibitory affect of PLB on SERCA 2A, and enhances the rate of calcium uptake into the SR (Koss & Kranias, 1996). PLB phosphorylation appears to increase the affinity of SERCA 2A for calcium, as even at low $[Ca^{2+}]_i$ when the calcium pump is only marginally active, subsequent PLB phosphorylation causes a substantial increase in calcium transport. The rate of PLB phosphorylation parallels the activity of SERCA 2A and the rate of calcium transport into the SR. All of these processes occur additively (Simmerman & Jones, 1998). PLB is also an important mediator in the regulation of cardiac function during β-adrenergic stimulation, via the cAMP cascade (Koss & Kranias, 1996; Simmerman & Jones, 1998). SERCA 2A is highly dependent on [ATP] and $[Ca^{2+}]$, its activity is also modulated by changes in intracellular pH (Fabiato, 1985). For reasons of brevity SERCA 2A shall subsequently be referred to as SERCA.

1.4.2. Sarcolemmal Na^+/Ca^{2+} exchanger (NCX)

The cardiac Na^+/Ca^{2+} exchanger consists of 970 amino acids (MW~110kDa) including 12 transmembrane domains and 1 large cytoplasmic domain. The Na^+/Ca^{2+} exchanger functions bidirectionally depending on the cell's membrane potential and the extracellular and intracellular $[Na^+]$ and $[Ca^{2+}]$. The Na^+/Ca^{2+} exchanger is the main competitor with SERCA for cytoplasmic calcium during cardiac relaxation, with the latter normally dominant (28:70, Bassani, Bassani & Bers, 1994). The most widely accepted stoichiometry of Na^+/Ca^{2+} exchanger is $3Na^+:1Ca^{2+}$ (Reeves & Hale, 1984), making the pump electrogenic (powered normally by Na^+ gradient, created by Na^+/K^+ exchanger). The Na^+/Ca^{2+} exchanger is a low affinity pump with a K_M (Ca^{2+}) 2-20μM and a V_{Max} of 15-30 nmole Ca^{2+}/mg protein/s at 25^0C (Carafoli, 1985). Again, there are many intracellular factors which can affect the activity of the Na^+/Ca^{2+} exchanger. The Na^+/Ca^{2+} exchanger transports $[Na^+]$ and $[Ca^{2+}]$ and is also regulated by these ions (Philipson & Nicoll, 2000). Na^+/Ca^{2+} activity is modulated by intracellular pH, phosphorylation (Philipson *et al.* 1982) and [ATP] (Hilgemann, 1990). For reasons of brevity Na^+/Ca^{2+} exchanger shall subsequently be referred to as NCX.

1.4.3. Sarcolemmal Ca^{2+}ATPase

The sarcolemmal Ca^{2+}-Mg^{2+} dependent ATPase (sarcolemmal Ca^{2+}-ATPase) as its name suggests is a Ca^{2+}, Mg^{2+}, ATP dependent calcium pump (MW-138kDa). The sarcolemmal Ca^{2+}-ATPase pumps 1 Ca^{2+} out of the cell per ATP molecule hydrolysed. Although, the pump has a relatively high affinity for $[Ca^{2+}]_i$ (K_M 0.5μM) its transport rate is believed to be too slow (V_{Max} 0.5 nmole Ca^{2+}/mg protein/s at 25^0C) to make any substantial contribution to calcium fluxes during the cardiac cycle, however it may be influential for longer term cellular calcium extrusion (Carafoli, 1985).

1.4.4. Mitochondrial calcium uniporter

Under physiological conditions the mitochondrial role in regulating cytoplasmic $[Ca^{2+}]$ appears to be minimal as Ca^{2+} uptake into the mitochondria is thought only to occur once cytoplasmic $[Ca^{2+}]$ reaches approximately 1μm. Calcium enters the mitochondria via a uniporter system down a large electrochemical gradient set up by the extrusion of protons (H^+). Calcium entry exhibits a sigmoidal dependence on $[Ca]_i$. The uniporter has a K_M of 10μM and a V_{Max} of 10 nmole Ca^{2+}/mg protein/s at 25^0C (Carafoli, 1985). The uniporter is blocked by physiological ions such as $[Mg^{2+}]$ and by pharmacological agents such as ruthenium red.

Studies have concluded that SERCA and NCX are the 2 dominant mechanisms responsible for reducing cytoplasmic calcium during relaxation, (the former being more so). SERCA is thought to be responsible for removing 70% of the cytoplasmic Ca^{2+}, NCX removes about 28% and the remaining 2% is removed via the Ca^{2+}-ATPase pump and the mitochondrial uniporter (Bassani *et al.* 1994). Bers *et al.* (1993), make an interesting point in that if ~25% of cytoplasmic Ca^{2+} is removed by the exchanger, then in order to maintain steady state contractions it is likely that 25% of the Ca^{2+} needed to activate the myofilaments must come from outside the cell (via the I_{Ca}, or NCX, working in influx mode (outward)). In the absence of SERCA and NCX relaxation still occurs, albeit slowly, via the sarcolemmal Ca^{2+}-ATPase and the mitochondrial calcium uniporter (Bers *et al.* 1993).

1.5. Ultrastructure and function of Sarcoplasmic reticulum (SR)

The sarcoplasmic reticulum (SR) is an entirely intracellular, membrane bound organelle, separate from the sarcolemma. The SR is the main calcium store within cardiac myocytes. The SR consists of three distinct regions longitudinal, corbular and junctional SR. Ca^{2+} uptake by SERCA is thought to occur throughout the SR whereas Ca^{2+} release occurs predominantly within the junctional SR. Recent studies suggest that SR Ca^{2+} release channels or Ryanodine receptors (RyR) and calsequestrin are localised within the junctional SR (Allen & Katz, 2000).

1.5.1. Longitudinal SR

In 1965, Winegrad using autoradiograph studies proposed the theory that Ca^{2+} is sequestered into the longitudinal SR, and is then transported through the SR to release sites (RyR) at the junctional SR. To date these results have not been reproduced.

1.5.2. Junctional SR

Invaginating T-tubules within the sarcolemma form close contacts with the junctional SR (terminal cisternae), and it is at these areas that large proteins termed "feet" span the gap. These feet proteins are thought to be the RyR, responsible for Ca^{2+} release during CICR. Numerous proteins are associated with the RyR providing structural and regulatory support. Several key proteins; RyR, triadin, junctin and calsequestrin have been reported to form a stable complex localised at the junctional SR and are believed to be required for normal SR Ca^{2+} release (Zhang *et al.* 1997). Furthermore, phosphorylation state (Marx *et al.* 2000) and the physical association of FK 506 binding proteins (FKBP12.6) with RyRs is important for stabilising RyR channel function (Brillantes *et al.* 1994) and facilitates coupled gating between neighbouring RyR channels (Marx *et al.* 2001). The RyR within mammalian cardiac muscle is activated by micromolar [Ca^{2+}], millimolar [ATP], inhibited by millimolar [Mg^{2+}], micromolar [calmodulin] and is modified (activated/inhibited in a [dependent] manner) by the binding of ryanodine, a plant alkaloid (Meissner, 1994). The SR Ca^{2+} binding protein calsequestrin is increasingly believed to have a

modulatory affect on RyR activity (Ikemoto *et al.* 1989; Szegedi *et al.* 1999). Free SR calcium content has been estimated at approximately 1mM, with additional Ca^{2+} bound to intracellular organelles and membranes (Szegedi *et al.* 1999). In addition to the known SR Ca^{2+} release channel (RyR), it is believed that a non-specific RyR insensitive Ca^{2+} leak also exists in the SR (Pessah *et al.* 1997).

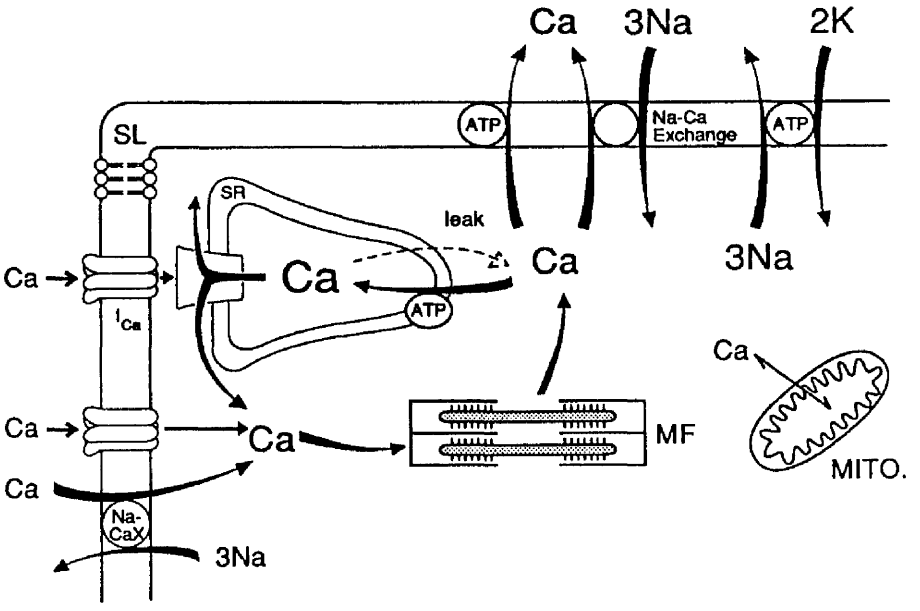

Figure 1.1. Schematic representation of Ca^{2+} transport systems within cardiac myocytes. Including sarcolemmal L-type Ca^{2+} channels, Ca^{2+}/Na^{+} exchanger, Ca^{2+} ATPase pump and Na^{+}/K^{+} ATPase. Intracellular transport systems include the Sarcoplasmic reticulum (SR) Ca^{2+} ATPase pump, SR Ca^{2+} release channel, a non specific Ca^{2+} leak and Mitochondrial Ca^{2+} transporters. Mito-mitochondrion, MF-myofilaments and SL-sarcolemma. (taken from Bers, 1993)

1.6. Heterogeneity of cellular properties within mammalian myocardium

It is now well established that there are regional (transmural) differences in electrical, structural, metabolic and mechanical properties within mammalian myocardium. The myocardium can be subdivided into three regions; an inner sub-endocardium region, a mid-myocardium and an outer sub-epicardium region. For brevity, in future sub-endocardial and sub-epicardial myocytes shall be simply referred to as endocardial and epicardial myocytes.

Transmural gradients in myocardial blood flow (Hoffman, 1995), intramyocardial pressure, capillary distribution and cell cross sectional area have been reported (Gerdes *et al.* 1979). Capillary density is lower in endocardial than the epicardial region, and a reduced blood flow during systole (due to higher intracardiac pressure) implies that endocardium perfusion is more likely to be compromised than that of the epicardium. This, coupled with a larger sub-endocardial cell size, (Hoffman, 1995), workload and a greater oxygen consumption rate (Robitaille *et al.* 1990) make endocardial myocytes more susceptible to insufficient oxygen supplies (anoxia) during ischaemic insults and or in the normal heart during increased workloads. This is consistent with the finding that endocardial myocytes suffer most ischaemic damage post myocardial infarction (Hoffman, 1995).

Transmural differences in myocyte length have been reported by Campbell and Gerdes (1988) and McIntosh *et al.* (2000), who observed that endocardial myocytes were longer than epicardial myocytes. In contrast, other groups report no significant transmural length differences (Bishop *et al.* 1979; Smith *et al.* 1988; Chamunorwa & O'Neill 1995; Bryant *et al.* 1997). Such discrepancies may arise due to species variation. Additional structural differences, such as longer sarcomere lengths (Spotnitz *et al.* 1966) and larger cross-sectional areas have been reported in endocardial cells (Gerdes *et al.* 1979). Bishop *et al.* (1979) reported no transmural differences in myocyte volume.

Differences in action potential characteristics are the most commonly observed transmural electrophysiological feature. Several groups have reported

longer action potential durations in endocardial in comparison to epicardial myocytes (Antzelevitch *et al.* 1991; Cook *et al.* 1997; Bryant *et al.* 1997; McIntosh *et al.* 2000). Analogous differences in action potential duration have been reported between apical and basal regions of guinea-pig (Bryant *et al.*1997) and rat left ventricle (Shipsey *et al.* 1997). However, other apical and basal physiological properties have not been extensively studied. L-type calcium current density (I_{CA}), was found to be similar between endocardial and epicardial myocytes (Bryant *et al.* 1997) or slightly higher in endocardial myocytes (McIntosh *et al.* 2000). McIntosh *et al.* (2000) also observed longer calcium transients in endocardial in comparison to epicardial myocytes in rabbit ventricular myocytes, whereas Chamunorwa & O'Neill (1995) observed no such differences. Transmural differences in intracellular [Ca^{2+}] have also been observed, ranging from higher diastolic and systolic $[Ca^{2+}]_i$ in endocardial in comparison to epicardial myocytes (Figueredo *et al.* 1993), to similar transmural diastolic $[Ca^{2+}]_i$, and a higher epicardial systolic $[Ca^{2+}]_i$ (McIntosh *et al.* 2000). In addition, Cook *et al.* (1997) observed that intracellular $[Na^+]_i$ differed across the rabbit ventricle with $[Na^+]_i$ being significantly higher in epicardial in comparison to endocardial myocytes, at rest and during steady state stimulation.

Transmural metabolic studies by Robitaille *et al.* (1990) reported lower creatine phosphate (CrP) concentrations and a lower CrP/ATP ratio in endocardial in comparison to epicardial myocytes. Furthermore, Humphrey *et al.* (1988) reported that the capacity of ATP resynthesis is lost more rapidly in endocardial in comparison to epicardial myocytes. In contrast, Van der Vusse *et al.* (1990) investigated differences in energy requirements and metabolism but failed to reveal any substantial transmural differences.

Transmural differences in myosin isoforms are also believed to exist, which may have an influence on ATP metabolism and contraction (Eisenberg *et al.* 1985).

Evidently, from the above discussion some aspects of transmural heterogeneity remain controversial. However, it suffices to say that such transmural characteristics serve to co-ordinate myocardial function according to the varying transmural metabolic, mechanical and functional requirements of the ventricle.

1.7. Normal physiological features

1.7.1. The Force-frequency relationship

In normal myocardium an increase in stimulation frequency is accompanied by an increase in myocardial contractile force, termed a positive force-frequency relationship or treppe. Positive force-frequency relationships are observed in human (Davies *et al.* 1995; Pieske *et al.* 1999) and rabbit myocardium (Shattock & Bers, 1989, Maier *et al.* 2000) whereas a negative force-frequency is observed in rat (Orchard & Lakatta, 1985; Maier *et al.* 2000) and mouse myocardium (Wolska & Solaro, 1996).

Essentially, increasing stimulation frequency leads to an increase in diastolic $[Ca^{2+}]_i$ and subsequent increase in SR Ca^{2+} content via increased I_{CA} (Ca^{2+} influx), plus less time between stimulation leads to decreased Ca^{2+} extrusion by NCX (Bers, 2000). Additionally, higher stimulation frequencies increase $[Na^+]_i$ (increased influx during action potential) which reduces the effectiveness of NCX in extruding Ca^{2+} and subsequently $[Ca^{2+}]_i$ increases. Increased diastolic $[Ca^{2+}]_i$ in turn stimulates the activity of SERCA to pump more Ca^{2+} into the SR, raising SR Ca^{2+} content. A high SR Ca^{2+} content allows for greater SR Ca^{2+} release, increasing the amount of Ca^{2+} available for binding to Troponin C, and subsequent myofilament activation and force generation.

A negative force-frequency relationship produces a decrease in the force of contraction as stimulation frequency increases. This phenomenon is thought to reflect the shorter action potential duration and higher $[Na^+]_i$ found in rat hearts (Shattock & Bers, 1989; Maier *et al.* 2000).

1.7.2. Rest Decay

Following long periods of rest (>1 min) (no stimulation), the first contraction of ventricular muscle is reduced in amplitude, a phenomenon known as rest decay. This process is thought to reflect a time-dependent decrease in SR Ca^{2+} content via SR Ca^{2+} leak (Allen *et al.* 1976; Bers, 1985; Macleod & Bers, 1987; Bers, 1989;

Hryshko *et al.* 1989; O'Neill 1993; Chamunorwa & O'Neill, 1995). Evidence for rest decay comes from experiments using rapid cooling contractures (RCC). RCC elicit Ca^{2+} release directly from the SR and is a relative indicator of SR Ca^{2+} content (Bridge, 1986; Bers, 1989; Hryshko *et al.* 1989). For example, Hryshko *et al.* (1989) showed that the amplitude of the RCC declined as a function of the rest duration, parallel to the amplitude of the muscle contraction. As RCC amplitude depends directly on SR Ca^{2+} content, they concluded that rest decay reflects a decrease in SR Ca^{2+} content.

It has been proposed that during rest, both SR and cytosolic $[Ca^{2+}]$ must fall in order for rest decay to occur. If, for example, SERCA was the only means of reducing cytosolic Ca^{2+} then, Ca^{2+} released from the SR would be resequestered back into the SR, SR Ca^{2+} content (intraluminal $[Ca^{2+}]$) would remain constant and rest decay would not occur. As rest decay does occur, this suggests that the Ca^{2+} leaking from the SR is removed completely from the cell by other mechanisms. The most likely candidates for this are the sarcolemmal Ca^{2+} pump and NCX, which normally regulate $[Ca^{2+}]_i$, along with smaller contributions from the sarcolemmal Ca^{2+}-ATPase pump and mitochondrion. Inhibition of NCX, by removing extracellular $[Na^+]$ and/or $[Ca^{2+}]$ abolishes rest decay confirming the critical link between cytosolic $[Ca^{2+}]$ regulation and NCX (Hryshko *et al.* 1989; Bers *et al.* 1993, Bassani & Bers 1994) (See intracellular calcium homeostasis above). It has been concluded that during rest, $[Na]_i$ falls, due to a combination of the cessation of Na^+ influx during the action potential, and the continuous activity of the Na^+/K^+ exchanger. Low $[Na^+]_i$ and increasing $[Ca^{2+}]_i$ leaking from the SR enhances NCX activity and promotes Ca^{2+} extrusion from the cell. Subsequently, extracellular $[Ca^{2+}]$ increases, $[Ca^{2+}]_i$ decreases, SR $[Ca^{2+}]$ content decreases and rest decay arises (MacLeod & Bers, 1987; Shattock & Bers, 1989). Rest decay is observed in several mammalian species, with the exception of rat, ferret, dog ventricle (Bers *et al.* 1993) and rabbit atria (Bers, 1985).

Post rest potentiation is an increase in the amplitude of the first contraction following short rest periods. Post rest potentiation has been observed in mouse (Terracciano *et al.* 1998) rat, ferret and dog ventricle (up to 2 min of rest, beyond which time rest decay ensues) (Bers *et al.* 1993). Post rest potentiation is thought to

reflect an increase in intracellular (and subsequent SR) $[Ca^{2+}]$, suggesting that these myocytes gain Ca^{2+} during rest and electrical stimulation actually reduces intracellular and SR $[Ca^{2+}]$ (Bers, 1989; Hryshko *et al.* 1989; Shattock & Bers, 1989). Rat myocardium has an intrinsically high $[Na^{+}]_i$, which during rest reduces the reversal potential for NCX and favours Ca^{2+} influx hereby increasing $[Ca^{2+}]_i$, SR Ca^{2+} content and produces rest potentiation. However, post rest potentiation observed in ferret ventricle was not paralleled by a raised SR Ca^{2+} content, but was believed to reflect an initial increased fractional release of SR Ca^{2+} in response to electrical stimulation (Bers *et al.* 1993).

A recent study by Pieske *et al.* (1999) observed for the first time that in non-failing human ventricular muscle strips, an increase in rest interval produced a parallel increase in post rest twitch force. This increased twitch force was associated with progressive SR Ca^{2+} loading during rest and increased fractional SR Ca^{2+} release upon restimulation.

Experimentally rest decay is used as a tool to indicate the calcium load of the myocyte, which then can be related to the efficiency of the intracellular Ca^{2+} transporters/pumps and therefore the physiological condition of the myocyte.

1.8. Pathophysiology of failing/hypertrophied cardiac myocytes

Structural and functional remodelling of cardiac myocytes occurs in both compensated and failing mammalian myocardium. Hypertrophy is an enlargement of myocyte size, via a combination of increased cell length and/or width. Hypertrophy within the context of this work refers to myocyte enlargement caused by a pathophysiological disease. However, hypertrophy does not always have deleterious effects on cardiac function, an example being the enlarged heart of the athlete (physiological hypertrophy).

The extent, site and form of myocyte remodelling appears to be dependent on the aetiology and severity of the underlying disease. The initial cellular adaptations associated with the early stages of cardiac hypertrophy (compensatory reactive hypertrophy) are activated as a compensatory mechanisms in an attempt to enable the heart to maintain an adequate cardiac output despite adverse haemodynamic conditions. This is sometimes referred to as the *adaptive phase* (compensated hypertrophy). If these adaptations are insufficient to maintain adequate cardiac output the adaptive phase can deteriorate into decompensated ventricular hypertrophy or heart failure. Progressive changes in myocyte form/function, ventricular cavity volume/pressure, and extracellular matrix structure occur, producing an enlarged, poorly contracting myocardium. Such characteristics are often associated with the syndrome of heart failure. Heart failure can be defined as "a syndrome which develops as a consequence of cardiac disease, and is recognised clinically by a constellation of symptoms and signs produced by complex circulatory and neurohormonal responses to cardiac dysfunction" (Cowie *et al.* 1997).

There is a vast literature concerning heart failure and its pathophysiological consequences, the following is only an overview of some cellular characteristics, which are altered during hypertrophy and heart failure.

1.8.1. Origin of contractile dysfunction in failing/hypertrophic cardiac ventricular myocytes

1.8.1.1. Morphological changes associated with failing/hypertrophied cardiac myocytes

The exact origin of contractile dysfunction in failing myocardium remains controversial, but is thought to reflect many detrimental alterations to cellular form and function. Myocytes isolated from failing myocardium show abnormal structural changes, the nature of which, depends on the cause and severity of the hypertrophy. In general, ventricular pressure overload, induced, for example by hypertension, produces an increase in ventricular wall thickness, which is reflected at cellular level by increased myocyte cross sectional area (diameter) with little change in ventricular chamber diameter. Such remodelling is termed concentric. In comparison, ventricular volume overload, which is commonly associated with myocardial ischaemia, produces eccentric remodelling. Generally a proportional increase in chamber diameter and wall thickness occurs due to a proportional increase in myocyte length and diameter (Gerdes *et al.* 1996). It must be noted that a combination of these length/width changes are possible within any one form of overload.

Numerous studies have observed morphological changes in failing or hypertrophied cardiac myocytes. Increased cell length in myocytes isolated from both hypertrophied and failing myocardium in guinea-pigs, (Bryant *et al.* 1997), rabbits (McIntosh *et al.* 2000), rats (Liu *et al.* 1991;1&2; Smith *et al.* 1988; Bishop *et al.* 1979; Gerdes *et al.* 1996) and humans (Beltrami *et al.* 1994; Gerdes *et al.* 1992; Gerdes *et al.* 1995) have commonly been observed. Del monte *et al.* (1995) in contrast, reported no significant changes in failing ventricular human myocytes. Changes in either myocyte length or width can produce alterations in myocyte length/width ratio. For example, increased length/width ratio has been observed in human (Gerdes *et al.* 1992 & 1995) and rat myocytes (Gerdes, 1996). Increased cell volume (Bishop *et al.* 1979; Smith *et al.* 1988; Lui *et al.* 1991,1&2; Gerdes *et al.* 1992; Olivetti *et al.* 1994) and cross sectional area (Smith *et al.* 1988; Gerdes, 1992 & 1996, Olivetti *et al.* 1994; and del Monte, 1995) have also been described. Such

cellular adaptations increase the normal ventricular wall/lumen diameter ratio which subsequently decrease ventricular wall stress thus acting as a compensatory mechanism. Myocyte loss and subsequent replacement fibrosis has been reported in hypertrophied human hearts (Schaper & Schaper 1986; Olivetti *et al.* 1994). Further, no change (Gerdes *et al.* 1992 & 1996; Del monte *et al.* (1995), or an increase in sarcomere length (Harding *et al.* 1989) have been reported.

1.8.1.2. Abnormal intracellular calcium homeostasis

Diastolic $[Ca^{2+}]_i$ - Studies have reported that failing human myocardium is unable to restore low $[Ca^{2+}]_i$ during diastole (Gwathmey *et al.*1987; Morgan *et al.* 1990; Beuckelmann *et al.* 1992; Arai *et al.* 1993) and diastolic $[Ca^{2+}]_i$ is subsequently raised. Beuckelmann *et al.* (1992) observed that diastolic $[Ca^{2+}]_i$ decay was prolonged in failing myocardium and concluded that a decreased Ca^{2+} uptake into the SR and prolongation of the action potential were responsible. McIntosh *et al.* (2000) observed in the same rabbit model of hypertrophy used in this study, increased and unchanged diastolic $[Ca^{2+}]_i$ in endocardial and epicardial failing myocytes respectively, suggesting transmural heterogeneity in $[Ca^{2+}]_i$ regulation.

Systolic $[Ca^{2+}]_i$ - Reduced peak systolic $[Ca^{2+}]_i$ has been reported in failing myocardium reflecting a decreased SR Ca^{2+} content, secondary to a reduced Ca^{2+} uptake into the SR (Beuckelmann *et al.* 1992; Schmidt *et al.* 1998; Lindner *et al.* 1998). Unchanged peak systolic $[Ca^{2+}]_i$ (Gwathmey *et al.* 1990) has also been observed. Siri *et al.* (1991) observed a decreased peak systolic $[Ca^{2+}]_i$ and unchanged diastolic $[Ca^{2+}]_i$ in a guinea-pig model of heart failure.

Transmural differences in peak systolic $[Ca^{2+}]_i$ were reported in this rabbit coronary ligation model, with an increased endocardial and a reduced epicardial peak systolic $[Ca^{2+}]_i$ (McIntosh *et al.* 2000).

Gwathmey *et al.* (1987) showed prolongation of Ca^{2+} transient duration in failing human heart muscle and observed that these preparations showed two distinct components. They concluded that the second additional component reflected dysfunction of both sarcolemma and SR Ca^{2+} transport, producing a prolongation of the Ca^{2+} transient. These results were further confirmed by later studies (Morgan *et*

al. 1990; Gwathmey *et al.* 1991). McIntosh *et al.* (2000) reported transmural differences in Ca^{2+} transient and action potential duration in failing rabbit myocytes, were duration of both parameters was decreased in endocardial and increased in epicardial myocytes. This data agrees with transmural action potential differences observed in rat hypertrophy (Shipsey *et al.* 1997). Bryant *et al.* (1997) also observed a prolonged action potential in hypertrophic epicardial myocytes but unchanged duration in endocardial myocytes. Prolongation of action potential duration is the most consistently observed electrophysiological abnormality observed in cardiac hypertrophy (Gwathmey *et al.* 1991, Hart, 1994, Milnes & MacLeod, 2001).

There is conflicting evidence regarding changes in Ca^{2+} current density (I_{CA}) (via L-type sarcolemmal channels) in hypertrophic and failing myocardium. Increased Ca^{2+} current in rat hypertrophic myocardium (Keung *et al.*1989), decreased current in guinea-pig myocardium (Ming *et al.* 1994) and cardiomyopathic hamsters (Hatem *et al.* 1994) and unchanged Ca^{2+} current in failing rabbit myocardium have all been observed (Pogwizd *et al.* 1999). McIntosh *et al.* (1999) reported transmural differences in I_{CA} in failing hearts, (epicardial higher than endocardial) and I_{CA} had a tendency to be higher in endocardial failing myocytes in comparison to control myocytes. No differences in I_{CA} between control and failing epicardial myocytes was observed. Assessment of Ca^{2+} current density in failing human myocardium remains controversial with Beuckelmann *et al.* (1992) observing no reduction whereas Ouadid *et al.* (1995) found a reduction in patients undergoing cardiac transplantation (severe failure).

1.8.1.3. Alterations in intracellular gene and protein expression

Intracellular Ca^{2+} homeostasis within myocytes is precisely regulated by both sarcolemmal and SR Ca^{2+} handling proteins. Therefore, alterations in gene and protein expression may have serious effects on intracellular Ca^{2+} homeostasis.

Human studies

SERCA protein expression in human studies remains controversial as several studies have reported reduced SERCA protein expression in failing human myocardium (Hasenfuss *et al.* 1994; Meyer *et al.* 1995; Hasenfuss, 1998 (review);

Ravens, 2000 (review) as well as no change (Movesian *et al.* 1994; Hasenfuss, 1998; Ravens, 2000 (review). Decreased SERCA mRNA expression has been reported by Mercadier *et al.* (1990) and Arai *et al.* 1993. Several groups have observed reduced SERCA and phospholamban activity and mRNA levels without accompanying alterations in protein expression (Schwinger *et al.* 1995; Linck *et al.* 1996 and Flesch *et al.* 1996). Flesch *et al.* (1996) concluded that these proteins were either subjected to posttranscriptional or posttranslational regulation.

Levels of NCX protein expression in human failing myocardium were found to be either unchanged (Schwinger *et al.* 1999, Prestle *et al.* 1999) or increased (Reinecke *et al.* 1996; Hasenfuss *et al.* 1999). Hasenfuss *et al.* (1999) subdivided their failing human heart results (which included preparations from dilated cardiomyopathy and ischaemic cardiomyopathy) into two groups according to diastolic function. The phenotype with disturbed diastolic function expressed a decreased SERCA and unchanged NCX expression, and the other group with preserved diastolic function expressed increased levels and activity of NCX and unchanged SERCA expression. They concluded that increased NCX expression was activated as a compensatory mechanism to preserve diastolic function. This is in agreement with previous work by Studer *et al.* (1994) on dilated cardiomyopathy and ischaemic heart failure in humans.

It is generally accepted that calsequestrin protein expression is unchanged in failing human myocardium in comparison to control myocardium (Takahashi *et al.* 1992 (mRNA), Movesian *et al.* 1994; Meyer *et al.* 1995; Schwinger *et al.* 1999; Prestle *et al.* 1999). As calsequestrin protein levels appear to be unchanged in human hypertrophy and heart failure it is often used as a protein standard with which to compare alterations in other intracellular protein expression levels.

Reduced SR Ca^{2+} release channel or Ryanodine receptor protein (RyR) mRNA levels were found in end stage human heart failure (Takahashi *et al.* 1992; Arai *et al.* 1993; Go *et al.* 1995;). Brilliantes *et al.* (1992) reported decreased RyR mRNA expression in myocardium taken from patients with ischaemic cardiomyopathy, but observed a small increase in RyR mRNA taken from patients

with dilated cardiomyopathy. In contrast, Meyer *et al.* (1995) reported unchanged protein expression in human dilated cardiomyopathy.

Animal studies

The literature regarding SERCA expression in animal studies is fairly clear with most studies reporting reductions in SERCA protein (Hasenfuss 1998 [review]; O'Rourke *et al.* 1999; Ravens & Dobrev 2000, [review]) and mRNA expression (Hasenfuss 1998,[review]; Pogwizd *et al.* 1999; Ravens & Dobrev 2000,[review]). Currie & Smith, (1999), using the same rabbit model described in this study (volume overload model), and Kiss *et al.* (1995) (pressure overloaded guinea -pig model) reported reductions in SERCA expression with concomitant decreases in phospholamban expression (PLB). Currie & Smith (1999) also observed increased PLB phosphorylation. Arai *et al.* (1996) reported increased SERCA mRNA expression in mild hypertrophy with a subsequent reduction in severe hypertrophy.

Increased NCX protein (O'Rourke *et al.* 1999; Pogwizd *et al.* 1999) and mRNA expression (Pogwizd *et al.* 1999) have been reported in failing hearts. Increased NCX activity was reported by Hatem *et al.* 1994; Pogwizd *et al.* 1999, whereas, Dixon *et al.* (1992) and Naqvi & Macleod, (1994) observed decreased NCX activity in a coronary ligated rat model and a guinea pig (volume overloaded) model of heart failure respectively. In a rat hypertrophy model (volume overloaded) CSQ mRNA expression was unaltered over a range of hypertrophic severity (Arai *et al.* 1996). Matsui et al. (1995) observed a decrease in mRNA calsequestrin expression whereas, in contrast, a recent study by Naqvi *et al.* (2001) observed a significant increase in calsequestrin protein expression (65%) in a rabbit model of cardiac hypertrophy.

Increased RyR protein levels have been observed in a mild rat hypertrophy model (volume overloaded) but levels subsequently diminished in severe hypertrophy (Arai *et al.* 1996). In contrast, Hisamatsu *et al.* (1997) reported a reduction in RyR numbers during early changes in a volume overloaded rat model of heart failure. Milnes & MacLeod (2001) recently reported a 34% reduction in RyR density in a rabbit model of left ventricular dysfunction.

Clearly, there is conflicting evidence regarding protein/gene expression of NCX and SR Ca^{2+} transporting proteins in both hypertrophied and failing myocardium. These differences may reflect species differences and/or the mode and severity of the failure. In addition, mRNA and protein expression levels do not always follow the same trend in expression, such differences may represent post – translational or post-transcriptional regulation.

In summary, it has been established that a correlation between intracellular Ca^{2+} handling mechanisms and contractile dysfunction exists in both human and animal models of heart failure. Experimental evidence suggests that mRNA and /or protein expression encoding SR Ca^{2+} transporting proteins is altered in cardiac hypertrophy and heart failure both in humans and in experimental animal models. These changes may be partly responsible for the altered contractile function observed in failing and hypertrophic myocytes. Furthermore, changes in electrophysiological parameters and myofilament Ca^{2+} sensitivity in failing and hypertrophic myocytes may also contribute to contractile dysfunction.

1.8.1.4. Changes in physiological features

In general, the force-frequency relationship observed in failing or hypertrophied myocytes is depressed or reversed. This phenomenon has been observed in human papillary muscles (Schwinger *et al.* 1993; Schmidt *et al.* 1994); ventricular muscle strips (Muliere *et al.* 1992); ventricular trabeculae (Morgan *et al.* 1990; Pieske *et al.* 1999) and studies on whole rabbit hearts (Ezzaher *et al.* 1992). Studies suggest that the most likely cause for this depressed force-frequency relationship is a disruption of intracellular Ca^{2+} handling, producing abnormal diastolic and systolic $[Ca^{2+}]_i$ (Morgan *et al.* 1990; Gwathmey *et al.* 1991).

Minimal work has been carried out on the effect of rest decay in failing/hypertrophic cardiac myocytes. A recent study by Pieske *et al.* (1999) using failing human muscle strips showed signs of rest decay as rest interval duration was increased. This was the opposite of the behaviour displayed by non-failing myocytes. Pieske *et al.* (1999) concluded that a combination of reduced SERCA and increased

NCX activity in failing preparations would bias Ca^{2+} extrusion from the cytosol rather than its reuptake into the SR and subsequently rest decay would ensue.

It is possible to correlate the kinetics of contraction with the kinetics of the Ca^{2+} transients and subsequent mechanical dysfunction. Similar to prolongation of the Ca^{2+} transient duration, both the contraction and relaxation velocity of myocytes are slowed in failure preparations, thus confirming their association (Gwathmey *et al.* 1987; Morgan *et al.* 1990; Gwathmey *et al.* 1991, Beuckelmann *et al.* 1992). Prolonged contraction kinetics have also been attributed to reduced peak systolic $[Ca^{2+}]$ (*Siri et al.* 1991) a variety of intracellular abnormalities (del Monte *et al.* 1995) and defective SR Ca^{2+} release (Milnes & MacLeod, 2001). Contractile dysfunction may also by affected by decreased myofilament Ca^{2+} sensitivity, although this theory remains controversial (Gwathmey *et al.* 1990; Perez *et al.* 1999).

1.9. Thesis Aims

As discussed in the Introduction, minimal experimental work has been performed investigating transmural physiological properties in isolated cardiac myocytes. In order to properly understand the functions of mammalian myocardium it is essential to be aware of any differences in transmural physiological properties. The purpose of the work reported here was to study transmural properties in normal rabbit hearts and hearts with left ventricular dysfunction, induced by coronary artery ligation (LVD). Contractile function, intracellular [Ca^{2+}] and protein expression of cardiac Ca^{2+} handling proteins were assessed in endocardial and epicardial myocytes in sham operated hearts and hearts with LVD. Experimental results from sham operated and LVD hearts were then compared.

Chapter 2 outlines the general methods used in the experimental work described in this thesis. These include:

a) The coronary artery ligation procedure involved in producing the coronary ligation model of left ventricular dysfunction.

b) Assessment of left ventricular function using Echocardiography

c) Physiological solutions

d) Isolation procedure of single cardiac myocytes

e) Biochemical tissue preparation

f) Western blotting technique

Chapter 3 of this thesis describes measurements of isolated myocyte contractile function and contraction kinetics. All measurements were made from myocytes isolated from sub-endocardial (Endo) and sub-epicardial (Epi) regions of sham operated and hearts with left ventricular dysfunction. These experiments were undertaken to explore possible differences in transmural and sham/LVD contractile function.

Chapter 4 describes measurements of intracellular [Ca^{2+}] in the above mentioned experimental groups (Sham - Endo/Epi; LVD - Endo/Epi). Transmural and Sham/LVD comparisons were made. These experiments were performed to investigate whether changes in intracellular [Ca^{2+}] were responsible for possible changes in contractile function.

Chapter 5 aims to assess and compare protein retrieval in homogenate and SR vesicle preparations isolated from sham operated and hearts with LVD. This part of the study also assessed the suitability of a range of sample sizes for use in experimental protocols, the criterion of which depended on protein retrieval efficiency.

Chapter 6 explains the sources of experimental variation observed in the standard Western Blotting technique. Potential experimental and technical improvements to minimise variation were assessed and implemented in the experiments performed in chapter 7.

Chapter 7 describes the quantification of specific cardiac Ca^{2+} handling protein expression. Protein expression was assessed in the fore mentioned experimental groups (Sham - Endo/Epi; LVD - Endo/Epi). Correlation between protein expression and intracellular [Ca^{2+}] was subsequently investigated.

Finally, chapter 8 summarises the experimental results and attempts to correlate changes in contractile function with changes in intracellular [Ca^{2+}]. Further, attempts to relate changes in intracellular [Ca^{2+}] to changes in Ca^{2+} handling protein expression were also investigated. The results are also related to our current understanding of the pathophysiology of heart failure or left ventricular dysfunction.

Chapter 2

General Methods

2.1. Animal Model

The model of left ventricular dysfunction used in this study was a rabbit coronary artery ligation model described by Pye *et al.* (Pye *et al.* 1996).

New Zealand male white rabbits (2.5–3.5kg) were anaesthetised using Midazolam (1-2 mg kg^{-1}) via a marginal ear vein, and were intubated and ventilated throughout the surgical procedure using an O_2, NO & Halothane mixture (1:1:1). A left thoracotomy was performed, and the ventricular branch of the left coronary artery was ligated mid way between the artery's origin and the cardiac apex. This procedure produced a significant apical infarct. Sham operated animals underwent the same surgical procedure except that no coronary artery was tied off. Post-operative analgesics and antibiotics were administered and the animals were allowed to recover. Left ventricular size and function were assessed by echocardiographic and haemodynamic examination 8 weeks post-operatively, prior to sacrifice for *invitro* experimentation. Echocardiographic assessment was performed under light sedation using a Toshiba SSH160 A echocardiograph. Left ventricular (LV) size (LV end diastolic internal diameter) and area ejection fraction (EF-%) (end-diastolic area – end-systolic area / end-diastolic area) were measured (Pye *et al.* 1996).

2.1.1. Assessment of *In vivo* left ventricular function

The degree of left ventricular dysfunction (LVD) induced by this coronary artery ligation model was quantified by analysing ejection fraction (%) and left ventricular end-diastolic dimension (LVEDD) (mm) using *In vivo* echocardiography (table 2.1). Table 2.1 below shows the mean ejection fraction (%) and LVEDD obtained for all sham operated and LVD animals used throughout this study. Significant haemodynamic dysfunction is observed in the LVD animals in terms of decreased ejection fraction ($p<0.001$) and increased LVEDD ($p<0.001$) in comparison to the sham data.

Experimental group	Mean ejection Fraction (%)	Mean LVEDD (mm)
Sham (n=60)	**73.4 ± 0.7**	**17.2 ± 0.2**
LVD (n=69)	**45.3 ± 0.8 ***	**21.0 ± 0.3 ***

Table 2.1. Mean echocardiographic parameters in sham and LVD animal groups. Data are mean ± SEM. n= number of animals. * significant difference between sham and LVD animals at the level of $p<0.001$.

Previously published data using this model of LVD also observed significant decreases in left ventricular ejection fraction and significant increases in LVEDD and left atrial dimension (Ng *et al.* 1998; McIntosh *et al.* 2000) in comparison to sham operated animals. Furthermore, significant increases in heart, lung and liver wet weights where also observed in this model (Ng *et al.* 1998; McIntosh *et al.* 2000 (liver & lung only).

This coronary ligation procedure produces a volume overload condition due to a dysfunctional left ventricle with clinical signs of liver and lung congestion and heart and liver enlargement. This condition is similar to that observed in human subjects with valvular regurgitation or post myocardial infarction. Eccentric remodelling occurs in this model of LVD with increases in myocyte length and width (McIntosh *et al.* 2000). In addition, a degree of left ventricular wall thinning occurs (Burton, McPhaden, & Cobbe, 2000).

In this study coronary ligated animals were categorised according to their ejection fractions into moderate (≥ 45%) or severe (≤ 45%) LVD. Animals were subdivided and referred to as either sham operated (sham), moderate left ventricular dysfunction (Moderate LVD) and severe left ventricular dysfunction (severe LVD), (chapter 5) unless stated otherwise. Where no significant differences in the results between moderate LVD and severe LVD where observed, these two groups where combined and classed together as the LVD group (chapter 3,4,7).

2.2. Physiological studies

2.2.1. Physiological saline solutions

Accurate electrolyte concentrations within physiological solutions are vital during any scientific experiments using animals. Optimum electrolyte concentrations vary between species, therefore it is critically important to use as near as possible a species specific physiological saline solution during experimentation. With this in mind, arterial blood samples were taken from both sham operated and coronary ligated rabbits (LVD) to verify normal rabbit arterial electrolyte concentrations. Electrolyte analysis was performed using standard clinical methods by the Department of clinical Biochemistry, Glasgow Royal Infirmary. These blood results combined with current literature solution values enabled suitable physiological solutions to be calculated, and hereafter used experimentally. The electrolyte levels for sham and LVD animals were indistinguishable from each other and were therefore combined (table 2, this study). Blood electrolyte concentrations from three rabbit studies are shown in table 2.2. Note that ionised Ca^{2+} is approximately 1/3 of total Ca^{2+} concentrations, suggesting that the other 2/3 are bound to plasma proteins, such as albumin. Table 2.3 shows physiological solutions used by a variety of researchers using various animal species. The original superfusate solution used in this study (Solution A) was modified to solution B after the blood data was collected.

References	Sample	Na^+	K^+	Ca^{2+}	Cl^-	Mg^{2+}
De Mulder* *et al.*(1997)	Plasma	137 ± 1	4.15± 0.2	1.31 ± 0.1$^+$	101±2	
Yu** *et al.* (1979)	serum	141.4 ± 2.6	3.94 ± 0.36	3.4 ± 0.36^{++}	103.6 ± 2.8	1 ± 0.05
This study*	serum	133 ± 2.8	3.6 ± 0.13	3.14 ± 3.1	96 ± 2.61	0.8 ± 0.02

Table 2.2. Rabbit electrolyte concentrations (mM L^{-1}). *SEM, ** SD. Ionised (free) Ca^{2+} indicated by $^+$, total [Ca^{2+}] (bound and free) by $^{++}$. This study n= 14 except K^+ were n=11.

References	Species	NaCl	KCl	$MgCl_2$	Ca Cl_2	Hepes	Glucose	Na_2HPO_4	Others	pH
Levi *et al.* 1996	Rabbit	140	4	1	2.5	5	10			7.4
Fedida & Giles 1991	Rabbit	121	5	1	2		5.49	1.0	Na acetate - 2.8 $NaHCO_3$ –24	7.4
Bers & Berlin 1995	Rat	145	4	1	2	10	10			7.4
Bryant *et al.* 1997	Guinea pig	134	5.4	1.2	1.8	5	11.1			7.4
This study: Sol A (orig)	Rabbit	144	5.4	1	1.8	5	11.1	0.3		7.3
Sol B	Rabbit	140	4	1	1.8	5	11.1	0.3		7.4

Table 2.3. Superfusate solutions (mM L^{-1}) used in isolated cardiac myocyte experiment.

2.2.2. Single cardiac myocyte isolation

In this study both sham (control) and rabbits with left ventricular dysfunction (LVD) were used. All rabbits were terminally anaesthetised with pentobarbitone sodium (200mg) mixed with heparin (5000 units) via the marginal ear vein. Animals were deemed terminally anaesthetised when both stretch and corneal reflex were absent. All procedures were undertaken in accordance with the United Kingdom Animals (Scientific Procedures) Act 1986. The following procedure was used to isolate cardiac myocytes for use in both contraction (chapter 3) and fluorescent experiments (chapter 4).

Hearts were quickly excised and mounted onto a Langendorff perfusion apparatus. The heart was perfused retrogradely at 37°C via the aorta with a Ca^{2+} free Krebs solution (in mM: 140 NaCl, 20 Hepes, 5.4 KCl, 0.52 NaH_2Po_4, 3.5 $MgCl_2$, 20 Taurine, 10 Creatine, and 11.1 Glucose, pH 7.25 at 37°C). The heart was perfused with approximately 350mls of Krebs to clear blood from the coronary circulation (10 min). The heart was then digested (approximately 10 min) with 75 ml of an enzyme solution containing Collagenase 1.5mg ml^{-1} (type1, Worthington Chemicals) and Protease 25mg ml^{-1} (type XIV, Sigma). Enzyme perfusion was carried out until the ventricular tissue became soft to touch, indicating digestion of the heart's connective tissue. The right ventricle and atria were dissected from the heart and discarded. The left ventricle was removed from the Langendorff apparatus and placed in a petri dish containing 1% bovine serum albumin solution (BSA) in Krebs with 0.1mM $CaCl_2$. Layers of tissue from basal endocardial and epicardial surfaces of the left ventricular free wall were then dissected out. This tissue was finely chopped, shaken to enhance individual cell separation and filtered through a nylon mesh (250μm) into 0.1mM $CaCl_2$ Krebs/BSA. This cellular suspension was then gently spun in a hand operated centrifuge (30 - 60 s) until a pellet of cells lay at the bottom of the tube. The supernatant was discarded and the cells were resuspended in 0.5mM $CaCl_2$ Krebs/BSA. The cells were allowed to settle (15 min), the supernatant was removed and the pellet was resuspended in 1mM $CaCl_2$ Krebs/BSA. The cells were stored in this 1mM $CaCl_2$ Krebs/BSA solution at room temperature until use.

Amendments to the above myocyte isolation protocol were implemented between the time that the contraction experiments and the fluorescent experiments were carried out. These amendments greatly improved the yield of viable myocytes. The amended protocol is as follows. Briefly, hearts were isolated as previously described and perfused with 150ml of Krebs instead of 350ml. Enzyme concentrations and digestion times were as before, except that 0.05mM $CaCl_2$ was added to the recirculated enzyme. In addition, 100ml of BSA was perfused through the heart prior to its removal from the apparatus. Sub-endocardial and sub-epicardial chunks were dissected as before but were placed into a flask and shaken in a water bath (37^0C) for 60min to allow gentle separation of single myocytes. The supernatant was removed and hand centrifuged until a pellet of cells was formed. The supernatant was discarded and the pellet was resuspended in Krebs/BSA containing 0.125mM $CaCl_2$. This suspension was allowed to settle (approx.15 min), the supernatant was removed and the pellet resuspended in Krebs/BSA (1%) containing 0.25mM $CaCl_2$. This resuspending procedure was repeated for 0.5 and 1mM $CaCl_2$ Krebs/BSA solutions. The cells were stored in the final Krebs/BSA (1mM $CaCl_2$) solution until use.

2.2.2.1. Statistical Analysis

All data are expressed as mean (± SEM). Students *t* tests or paired *t* test were used to compare two groups and ordinary ANOVA analysis (parametric) was used to compare multiple groups (followed by Tukey post test when appropriate). Value of $p < 0.05$ was considered statistically significant.

2.3. Biochemical studies

2.3.1. General tissue preparation

In this study both control (sham operated) and rabbits with left ventricular dysfunction (LVD) were used. All rabbits were terminally anaesthetised with Pentobarbitone sodium (200mg, mixed in heparin 1000units) via the marginal ear vein. Hearts were quickly excised, rinsed in ice cold Ringer solution to clear them of blood (in mM: 150 NaCl, 5 Hepes, 5 KCl, 1 $MgCl_2$, 2 CaCl, pH 7.4 at 37°C) and kept on ice until use.

Tissue samples were dissected from endocardial and epicardial regions of the left ventricle and immediately placed in cold homogenisation buffer (in mM: – 300 Sucrose, 20 Histidine, 10 Imidazole, 1 Dithiothreithol (DTT; reducing agent), Protease inhibitors Leupeptin 5mg/ml, Aprotinin 10mg/ml at pH 7.2). Care was taken when dissecting tissue from LVD hearts that fibrotic, adipose and infarcted tissue was not removed, thus ensuring that only viable muscle tissue was used in these samples. The above procedure was used to prepare tissue samples for experiments detailed in chapters 5,6 and 7.

2.3.2. Homogenate tissue samples for Western blot analysis

Initially, samples for Western blot analysis were prepared as described in the 2.3.1 and stored in ice cold Ringer solution until use. A vertical incision was made from apex to base up the left side of the septum, allowing exposure of the left ventricular free wall (LV). The LV was pinned down onto a petri dish with the LV free wall endocardium facing upwards, and covered in ice cold Ringer solution. Approximately 1mm thick strips of basal endocardium tissue were dissected, the heart was turned over and similar sized epicardial samples were dissected. Papillary muscles were not used in any samples. These endocardial and epicardial tissue samples were weighed (blotted to remove excess Ringer solution) and resuspended in 5 volumes of homogenisation buffer (taken as 1ml = 1mg).

Prior to Western blot analysis of proteins, experiments were performed on transmural homogenate samples to assess homogenate and SR protein retrieval (see chapter 5). Based on the amount of variation observed within intracardiac samples

during the protein retrieval experiments it was considered essential to prepare every future tissue sample, irrespective of use, in exactly the same way to avoid any unnecessary variation in protein content. Therefore, all samples underwent equal homogenisation times at the same temperature and were resuspended in equal volumes of homogenisation buffer. All endocardial and epicardial tissue samples were finely chopped with scissors and then homogenised using an ultra-turrax T_8 (IKA Labortechnik) for two 30s periods on ice. Samples were removed for protein assay (2.3.3.) and the remainder was frozen at -80^0 C until use.

2.3.3. Protein assay

The assaying of total protein content (mg ml^{-1}) for all tissue samples (homogenate, SR vesicles, endocardial, epicardial sham and LVD samples) was performed in the following way.

Protein content (mg ml^{-1}) was determined using the Coomassie Plus protein reagent (Pierce) and Bovine serum albumin (BSA) 0.1-1mg ml^{-1} as standard (Bradford method). Figure 2.1. below shows a typical sigmoidal calibration curve produced by the BSA standards. Protein samples were assayed on a 96 well plate (triplicate samples) and protein content was determined by measuring the optical density of the samples at a wavelength of 595nm (Reader program, Dynatech Laboratories.

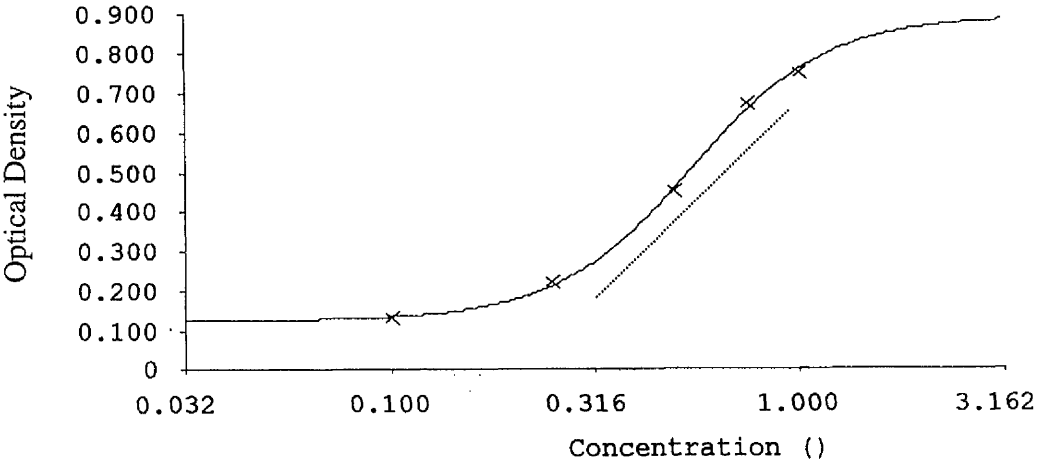

Figure 2.1. BSA standard calibration curve. Standard concentrations (0.1-1mg ml^{-1}), $mg.ml^{-1}$ (abscissa) vs optical density (ordinate). Dashed line indicates optimum area for accurate protein measurements.

Filters within the spectrophotometer are set (595nm) to allow specific measurements of absorption at that wavelength. The amount of absorption measured at that wavelength is standardised using the calibration curve and converted into a protein concentration. To improve the accuracy of this assay, sample values were taken on the *straight line* of the curve (indicated by the dashed line in figure 2.1). This avoids the upper and lower optical density readings where the resolution of protein concentrations is the least accurate.

2.3.3.1. Statistical Analysis

All data are expressed as Mean (± SEM) unless stated otherwise. ANOVA multi variant analysis (parametric) was used to compare multiple groups. A value of $p<0.05$ was considered statistically significant.

2.3.4. Western blot technique

After tissue isolation and preparation (see 2.3.1 & 2) homogenate samples were prepared for electrophoresis according to manufacture's instructions. Briefly, samples were diluted with deionised water and sample buffer (Invitrogen) to desired concentration. All samples were reduced (Dithioreithol (DTT)- 0.5M) and heated at 70^0C for 10 min prior to loading into the gel. In order to maximise the number of comparisons that could be made within one gel both sham and LVD endocardial and epicardial homogenate samples were loaded into a 15 well gel. For each sample three different total protein amounts 0.5, 1, and 2μg were loaded.

Such a gel set-up allowed comparisons of protein expression between:

Sham – Endo: Epi

LVD – Endo: Epi

ENDO -Sham: LVD

EPI - Sham: LVD

The 12 individual samples were loaded into 15 well polyacrylamide gels (Bis-Tris 4–12%) Rainbow Marker (Amersham, Life sciences) or See Blue Plus 2 (Invitrogen) were used as molecular weight standards. SDS-polyacrylamide gel electrophoresis (PAGE) was then performed as described by Laemmli (1970) with antioxidants included in the buffers. Electrophoresis running times were optimised at 200 volts for 90 min (Biorad power/pac 1000). Proteins were transferred to nitrocellulose membranes using the X cell II Blot module. The "Gel sandwich" was made up according to manufacturer's instructions (Invitrogen). Protein transfer times were optimised at 30 volts for 75 min. After protein transfer, nitrocellulose membranes were cut horizontally at the 66 kDa marker to allow parallel but separate antibody incubations for proteins with different molecular weights. Non specific protein binding sites on the membranes were blocked using Blocking buffer for various time periods depending on the protein of interest. Blocking times, antibody concentrations and incubation times varied and were optimised for each protein of interest (see table 2.4). Nitrocellulose membranes were incubated with primary antibodies (in incubation buffer) washed in low/high/low salt buffers (3x10min),

incubated in secondary antibody (in incubation buffer) and the washes were repeated. All secondary antibodies were conjugated with Horseradish peroxidase (HRP) which when mixed with the chemoluminescence assay ECL reagent mix catalyses a chemical reaction which emits light (chemiluminescence). This emitted light is detected on the autoradiograph film (Hyperfilm, Amersham). Nitrocellulose membranes were incubated in ECL reagent mix (Amersham) for 60s placed in a film cassette and exposed to autoradiograph film. Exposure time varied according to the intensity desired, and was optimised for each protein of interest. Films were developed using the Kodak X-OMAT processor (ME-3).

After film development, the nitrocellulose membranes probed with the NCX primary antibody (antiserum) were stripped of this antibody using Restore western blot stripping buffer (Pierce) for 30 min at 37^0C (gentle mixing). To test the efficiency of the stripping buffer, ECL reagent was reapplied to the membranes and reexposed to autoradiographic films. No residual antibody was detected on the films.

Nitrocellulose membranes were then washed (3x10min) and the antibody incubation procedure was repeated for the detection of the SERCA 2 protein.

2.3.4.1. Coomassie stained gels

Staining gels directly after electrophoresis enables a good visual indication of the size and abundance of proteins present in any one sample. Samples and molecular weight markers were loaded into 14% Tris –glycine gels and were subjected to electrophoresis at a constant current of 25mA for 2.5 hr. Gels were stained for 3hrs using Colloidal Blue stain (Invitrogen), and destained overnight in distilled water. Gels were then dried at 80^oC for 2hrs on a gel dryer (Biorad). See image (figure 5.2).

An additional staining method to assess protein transfer involved running and transferring gels (Bis-Tris 4–12%) as described above in 2.3.4. Gels were stained after transfer in 0.125% Coomassie Brilliant blue (R-250, Biorad) for 60 min to verify transfer efficiency. Gels were then destained in Destain I for 2hr and Destain II overnight and stored in Destain II until use. Coomassie stained gels were also used to determine total protein values within individual bands and lanes. Consistently a 200 kDa protein remained largely untransferred under the above conditions. The

suitability of total lane protein and this 200kDa protein as normalisation standards was subsequently assessed (see chapter 6).

Target protein	Blocking time	Primary antibody	Secondary antibody
SERCA	Overnight	1:20,000 - 45min (monoclonal, Affinity)	1:2,000 - 45min (Goat anti-mouse Ig G: HRP) (Transduction Laboratories, (TL))
Sodium-calcium exchanger (NCX)	60 min	1:5,000-overnight (antiserum,Swant)	1:5,000-120min (Goat anti-rabbit Ig G: HRP) (TL)
Calsequestrin (CSQ)	Overnight	1:80,000 - 30 min (antiserum,Swant)	1:20,000 - 30min (Goat anti-rabbit Ig G: HRP) (TL)

Table 2.4. Details of optimised blocking times, antibody dilutions and incubation times for the specific proteins investigated; SERCA , NCX and CSQ.

2.3.4.2. Biochemical solutions:

All solutions were made up in ultra pure (deionised) water (using either Maxima, Elga or Milli-Q, Millipore water systems).

Running buffer contained: NuPage 20 X MOPS SDS running buffer (Invitrogen) diluted with deionised water. Antioxidant (500µl in 200ml) of 1X running buffer (inner chamber).

Transfer buffer contained: NuPage 20 X transfer buffer, diluted with deionised water and 10% Methanol, SDS (0.1g, denatures proteins) and antioxidant (500µl in 500ml)

Incubation Buffer contained: 100 mM $MgCl_2$, 0.5% Tween 20, 1% Triton X-100, 100 mM Tris HCl, pH'd to 7.5, then BSA 5%, Foetal calf serum (FCS) 5% and Thimerosal 0.01% were added.

Blocking buffer contained:3% BSA added to incubation buffer

Low salt buffer contained in mM 150 NaCl, 1 EDTA, 0.1% TritonX-100, 10 Tris-HCl, 0.05% Tween 20, at pH 7.5.

High salt buffer contained in mM: 600 NaCl, 1 EDTA, 0.1% TritonX-100, 10 Tris-Base, 0.05% Tween 20, at pH 7.5.

Coomassie stain contained: 1% stock made up in distilled water, then diluted to 0.125% in Destain I.

Destain I contained: 50% Methanol, 10% Acetic acid, 40% deionised water.

Destain II contained: 5% Methanol, 7% Acetic acid, 88% deionised water.

2.3.5. Quantification of Immunoreactive Bands

Auotoradiographs were scanned using an AGFA imaging densitometer (ARCUS II). The densitometer was internally calibrated for optical density using a step tablet standard. Prior to scanning every film additional calibrations were performed. Imaging parameters were adjusted according to the image to be scanned (film or gel). Films were scanned using maximum resolution in transmissive mode and files were saved using the software package Quantity One (4.2.1, Biorad).

Mean band intensity was calculated using the following basic steps.

1) Initial images were filtered (5x5 median filter).
2) Lanes were created and inserted through each protein band profile.
3) Background signal was deducted from the protein band profile on a lane to lane basis (example figure 2.2).
4) Brackets were inserted, adjusted in size and numbered around each protein band (in figure 2.2).
5) Intensity profiles (optical density) were calculated for each protein band and data was exported directly into Excel 97 (Microsoft).

Average optical density readings for Sham and LVD endocardial and epicardial samples were calculated. Protein optical density readings were normalised to the nominal protein loads of 0.5, 1 and 2 μg. The slopes of the linear regression lines fitted to the data at 0.5, 1 and 2 μg determined the relative protein expression within each sample. Coomassie stained gels were scanned and analysed in the same way as the developed films using Quantity One software program.

In order to maximise the accuracy of the Western blotting technique (minimise variation) the protein gradient results were expressed relative to another sample type i.e. endocardial:epicardial; sham:LVD within the same gel. Alternatively, protein expression can be expressed relative to another protein developed from the same nitrocellulose membrane.

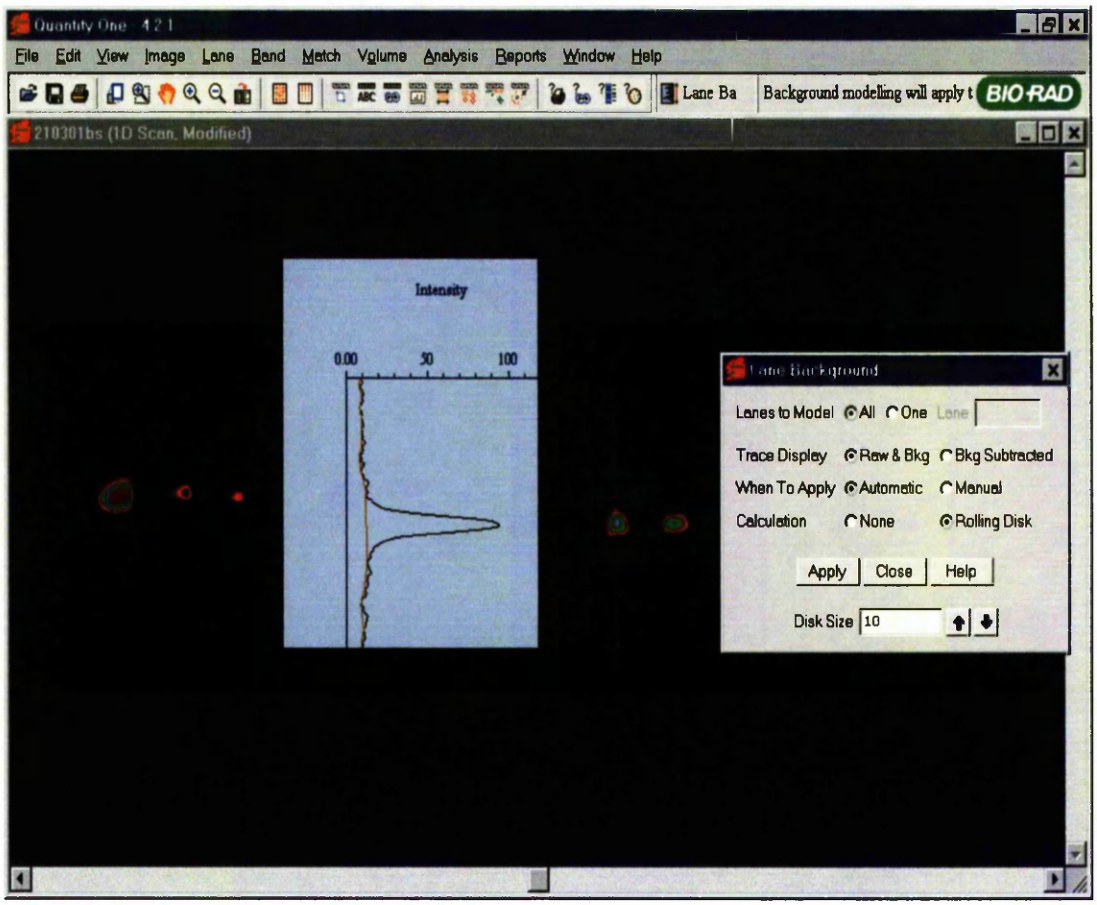

Figure 2.2. Typical trace from Quantity One showing the Intensity reading of an individual band and the background signal (brown solid line, inset) to be deducted. In addition, individual lane profiles and bands can be seen.

RESULTS

Chapter 3

Cardiac myocyte contractility measurements

3.1. Background

This chapter describes work aimed at assessing cardiomyocyte contractility in endocardial and epicardial myocytes in sham and LVD groups. Alterations from normal contractile function at the myocyte level are thought to be the basis of ventricular dysfunction in the whole heart. Cellular contractile function can be affected by many intracellular mechanisms such as changes in protein expression and activity or concentration of intracellular ions including those that affect intracellular pH regulation and myofilament Ca^{2+} sensitivity.

Much experimental evidence is available in the literature regarding changes in contractile parameters in hypertrophied and failing cardiac myocytes yet, to date, little experimental work has been performed to assess contractile parameters in the endocardial and epicardial regions of the ventricular wall.

Contractile function can be measured by assessing contractile features such as the force-frequency relationship and contraction kinetics. Additionally, the rest decay phenomenon can be used to assess Ca^{2+} handling processes within cardiac myocytes. More details of the above contractile features are described in chapter 1 (Introduction). Therefore, only a brief resume is mentioned here.

In most mammalian species (Orchard & Lakatta 1985; Davies *et al.* 1995; Pieske *et al.* 1999) a positive force-frequency relationship is observed, i.e. increasing stimulation frequency results in an increase in the force of contraction (increased myocyte shortening). In general, the force-frequency relationship observed in hypertrophied or failing preparations is depressed or reversed. This phenomenon has been observed in many human and animal models of failure (Muliere *et al.* 1992; Schwinger *et al.* 1993; Schmidt *et al.* 1994, plus see Introduction).

In healthy cardiac myocytes, contraction kinetic velocity (contraction and relaxation) increases as stimulation frequency increases (Davies *et al.* 1995; Perez *et al.* 1999). In general, studies have observed a slowing of contraction kinetics in hypertrophied or failing preparations in human (Gwathmey *et al.* 1987; del Monte *et al.* 1995; Perez *et al* 1999) and animal models (Naqvi & MacLeod, 1994; Bryant, Shipsey & Hart 1997; plus see Introduction). Transmural differences in contraction kinetics were investigated in control and hypertrophied guinea-pig myocytes by Bryant *et al.* (1997) but no significant differences were observed. A study by Perez *et al.* (1999) investigated the effect of changing extracellular $[Ca^{2+}]$ and observed an increase in time to 50% decay (relaxation) in the heart failure group in comparison to control as extracellular $[Ca^{2+}]$ was increased. Increasing extracellular $[Ca^{2+}]$ has a similar experimental affect to increasing stimulation frequency, i.e. both produce a subsequent rise in $[Ca^{2+}]_i$, and an increase in contraction amplitude and kinetics.

Following prolonged periods of rest (no electrical stimulation) the force of contraction of cardiac muscle is reduced, a phenomenon known as rest decay. Rest decay is thought to reflect a time dependent decrease in SR Ca^{2+} content via SR Ca^{2+} leak (see introduction for references and more details on rest decay). Transmural differences in rest decay have been investigated by O'Neill (1993) who observed that the amplitude of the first twitch after rest (3min) was 77.5% and 52.3% of control in epicardial and endocardial myocytes respectively. They suggested that the SR of endocardial myocytes was less able to retain its SR Ca^{2+} store than epicardial myocytes. An extension of this study (Chamunorwa & O'Neill, 1995) observed that the rest decay of cell shortening was faster and the recovery from the rested state slower in endocardial in comparison to epicardial rabbit myocytes. They concluded that changes in factors that affect myofilament calcium sensitivity produced the regional differences observed in rest decay. An alternative explanation could be that transmural differences in SR function exist which affect rest decay.

3.2. Methods

Isolation of single cardiac myocytes was performed as described in the general methods chapter (2.2.2). Cardiac myocytes were loaded into a small perfusion bath (300µl) mounted on an inverted Nikon Diaphot 200 microscope. The bath was perfused at 1ml min^{-1} with Krebs superfusate between 35.5- 37.5^{0}C (solution A in mM: 144 NaCl, 5 Hepes, 5.4 KCl, 0.3 $NaHPo_4$, 1.0 $MgCl_2$, 11.1 Glucose, 1.8 $CaCl_2$, pH 7.3 at 37°C). Single cells were stimulated using a silver-silver chloride electrode system, with electrodes placed either side of the bath, allowing current to pass between them. Stimulation pulse rate was controlled via the dT-Max computer programme Version 1.1 (F.L.Burton, 1992) and was delivered to the electrodes by a Digitimer DS2 stimulator at 80-100V for durations of 2-4 ms. Cell length was recorded as a voltage (V) every 5ms via a Photodiode array system (Cairn Research Limited). Enhancement of cell edge contrast was achieved by minimising a window around each single cell. Single cell length measurements were recorded on video, paper trace and computer and digitised using the software program WCP (John Dempster (1993-4).

Stimulation protocols were performed as follows; 0.3, 0.5, 1, 2, and 3Hz for the force-frequency protocol and 1Hz only interspersed with periods of 30, 60, and 180s rest for the rest decay protocol.

3.2.1. Data analysis

Steady state contraction records throughout the frequency range were averaged using WCP and converted to microns (µm) using conversion factors and data from the calibration curve (figure 3.1). Resting myocyte length was measured at the end of a 3min rest interval during the rest decay protocol.

Electrical stimulus was applied 20ms after the beginning of the sweep and diastolic myocyte length was taken as the length recorded between 10 –20 ms from the beginning of the sweep. Systolic lengths were recorded at their peak contraction values (minimum length). Diastolic and systolic lengths were measured to assess changes in myocyte length and to calculate fractional shortening throughout a range of stimulation frequencies. Diastolic and systolic length changes were expressed relative to diastolic length at 0.3Hz.

Fractional shortening was calculated by the following formula:

(Diastolic length - Systolic length)/ Diastolic length x 100

= % fractional shortening

Only myocytes that responded to the complete stimulus frequency range (0.3 to 3Hz) were included in the data. WCP recordings were started only after steady state contraction had been achieved for each stimulation frequency.

Averages of diastolic, systolic, fractional shortening and rest decay values were calculated for each experiment (1-8 myocytes, average 2), each experimental average (n = number of hearts) was then used to calculate group results. Data comparisons were subsequently made between the following experimental groups:

- Sham - endo: epi
- LVD - endo: epi
- Endo - Sham: LVD
- Epi - Sham: LVD

Kinetic measurements were calculated from averaged shortening records at all 5 stimulation frequencies (figure 3.2). Contraction values for peak amplitude (PA), time to reach peak amplitude i.e.100% (TTP), time to reach 50% peak amplitude (TTP50) were measured. Relaxation values for time to 50% and 90% decay/relaxation, (TD50, TD90) and duration at 50% contraction (D50) were also calculated. Calculations of TD90 proved to be less reliable and consistent than TD50, therefore only TD50 measurements were included in the final analysis.

A schematic diagram of the experimental apparatus used in the contraction experiments is shown in figure 3.3.

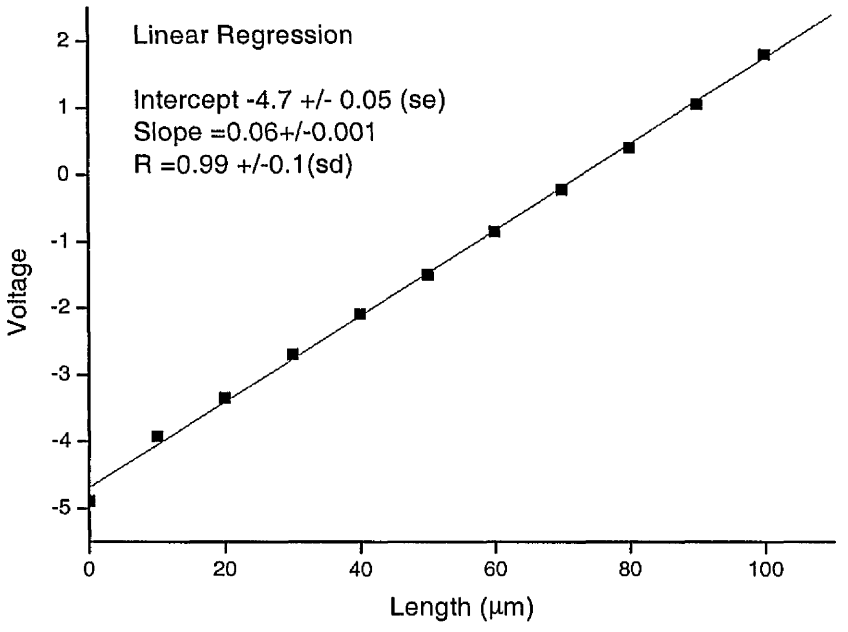

Figure 3.1. Length/voltage calibration curve. Linear regression analysis produced an r value of 0.99 and a slope of 0.06.

3.2.1.1. Statistical analysis

All data are expressed as mean ± SEM. Either *t* tests (one sided) or ordinary ANOVA (parametric) analysis was used to compare single or multiple groups respectively. A value of $p < 0.05$ was considered statistically significant.

3.2.1.2. In vivo left ventricular echocardiographic parameters

Mean ejection fractions (EF) were 74.7 ±1.1 and 44.4 ± 1.9% and LVEDD values were 16.9 ± 0.3 and 21.0 ± 0.3mm for sham (n=28) and LVD (n=16) respectively. The above values were not statistically different from the mean EF and LVEDD values calculated for this whole study (table 2.1).

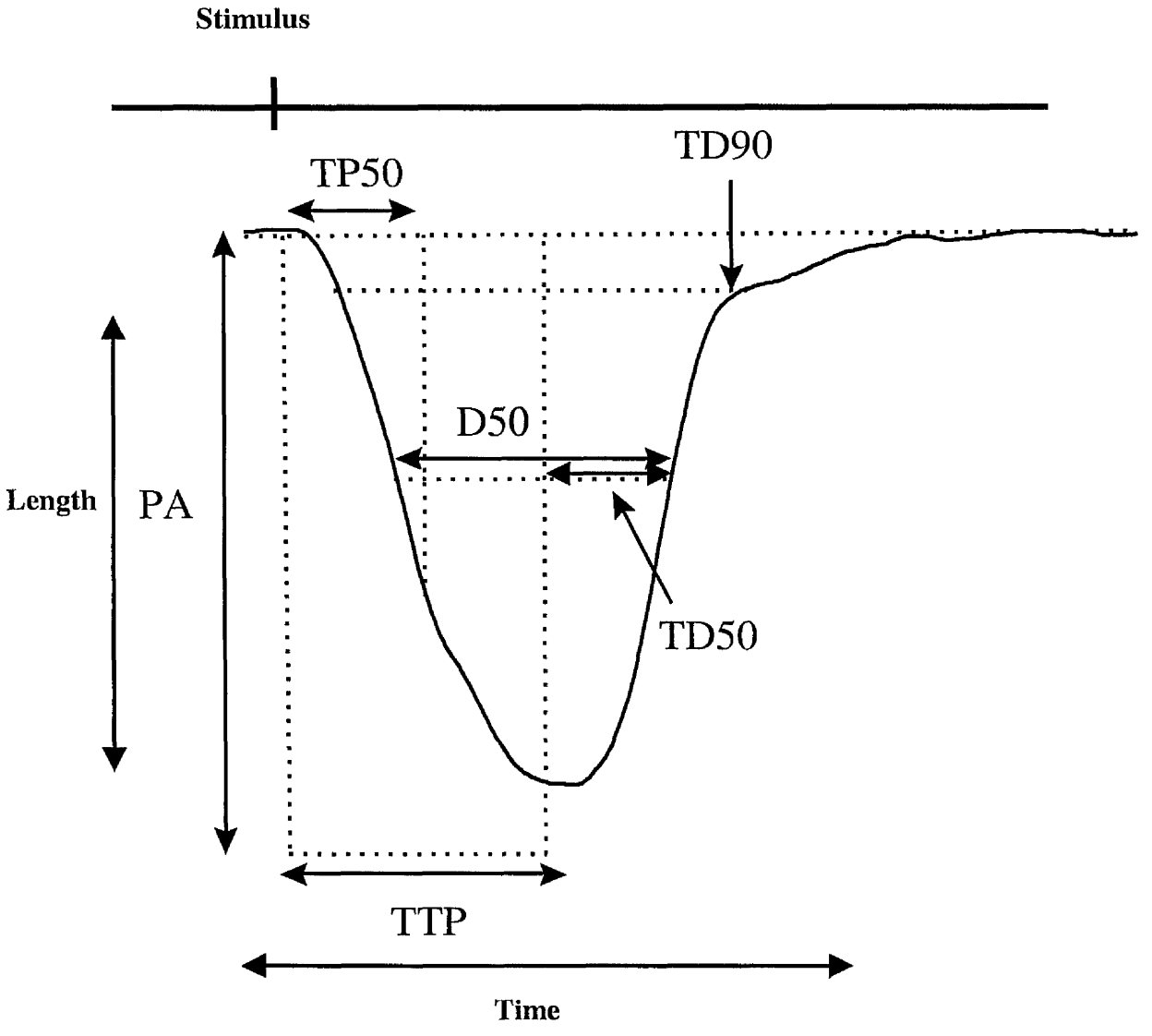

Figure 3.2. Schematic showing Kinetic parameters measured to show contraction characteristics of single cardiac myocytes isolated from rabbit myocardium. TTP, Time to peak contraction; PA, peak amplitude; TP50, time to 50% peak amplitude; D50, duration of contraction at 50%; TD50, time to 50% contraction decay; TD90, time to 90% contraction decay. Stimulus line represents point at which stimulus begins.

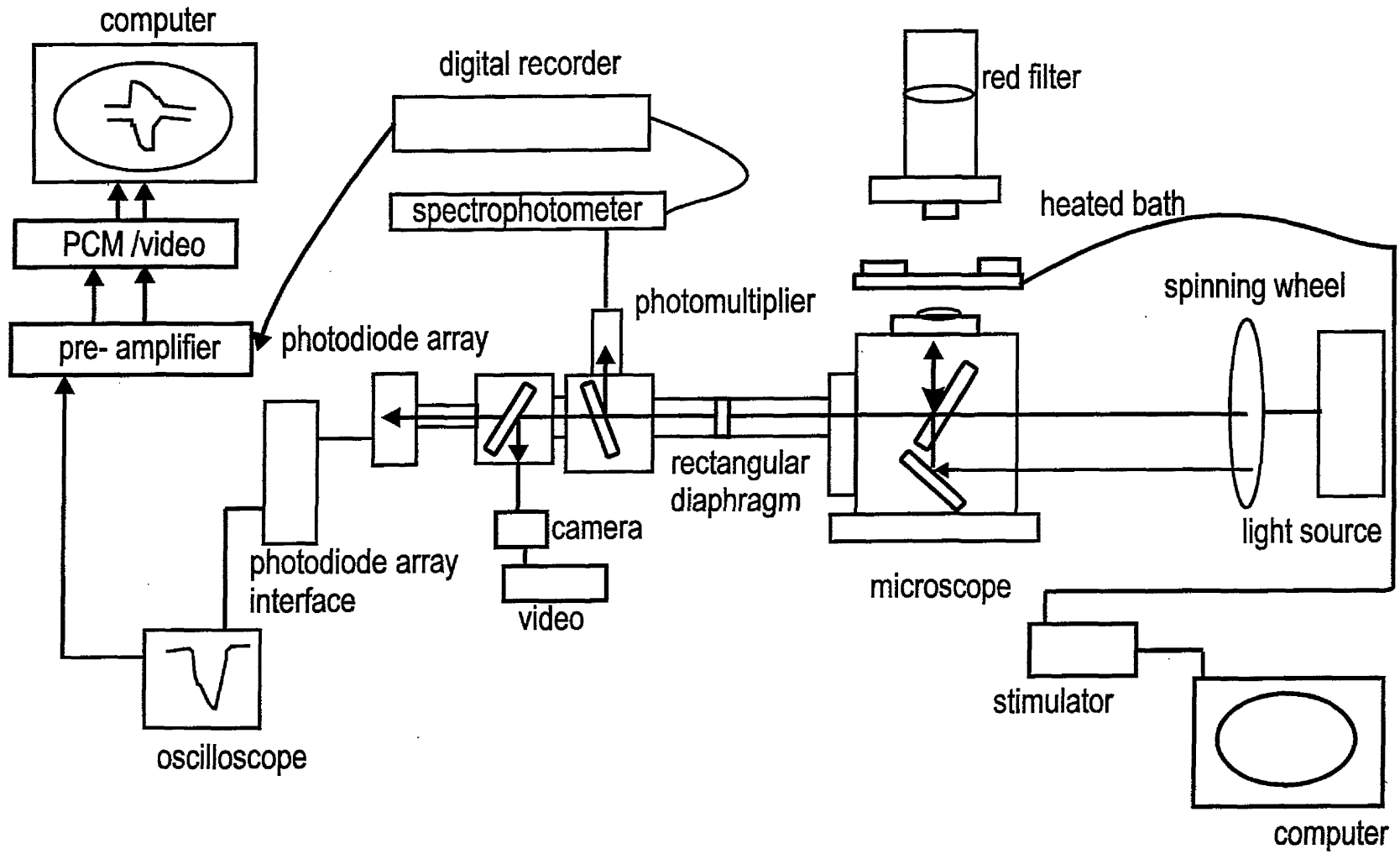

Figure 3.3. Experimental set-up for measuring myocyte length and intracellular fluorescence signal.

3.3. Single myocyte contraction measurements

Normally as stimulation frequency is increased a concomitant increase in fractional shortening is observed (positive force-frequency relationship). This relationship is observed in figure 3.4. Decreases in both diastolic and systolic length occur as stimulation frequency is increased. Furthermore, an increase in contraction amplitude is observed (change in myocyte length). Figure 3.5 shows individual contraction traces enlarged and superimposed upon one another. This diagram clearly shows that with increasing stimulation frequency, diastolic length (D) decreases and contraction amplitudes increases.

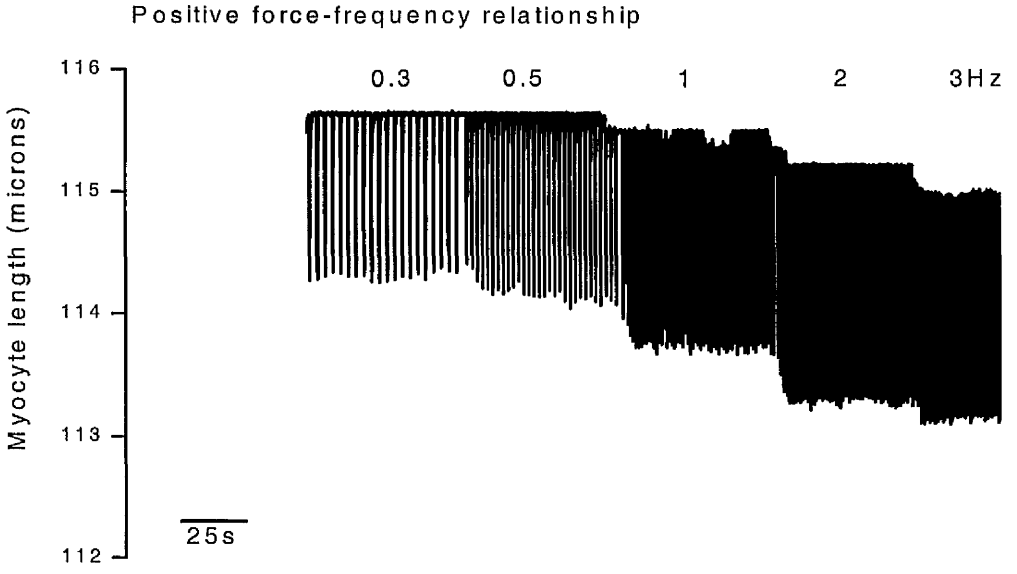

Figure 3.4. Example trace of positive-force frequency relationship showing the change in myocyte length associated with increasing stimulation frequency (0.3, 0.5,1,2 & 3Hz). NB -The fractional shortening for this example was lower than the average fractional shortening.

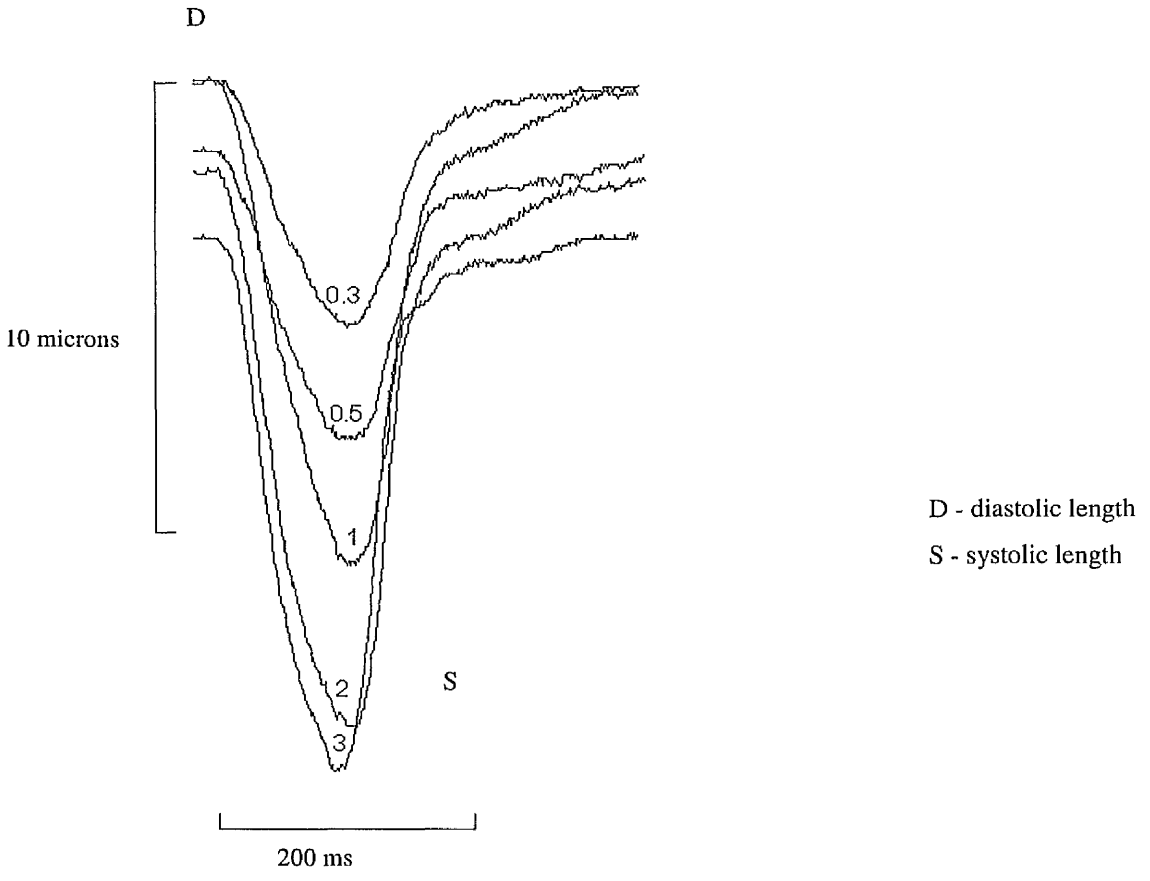

Figure 3.5. Enlarged individual contraction traces produced at various stimulation frequencies (0.3, 0.5,1,2 & 3Hz) and superimposed upon one another. Time and length (μm) scales are represented by solid lines.

3.3.1. Resting myocyte length

Resting myocyte length was measured at the end of a 3min rest interval during the rest decay protocol (see 3.2). No transmural difference in resting length existed in both the sham (endocardial 126.2 ± 6.45 μm & epicardial 124.1 ± 3.1μm, n=14 &15 respectively) and the LVD (endocardial 149.7 ± 3.2 μm & epicardial 149.8 ± 7.8μm, n=14 &10 respectively) data sets. However, a significant increase in resting length was observed when sham and LVD endocardial ($p<0.002$) and epicardial ($p<0.002$) myocytes were compared (figure 3.6). The endocardial and epicardial LVD myocyte lengths were approximately 20% greater than the corresponding values in sham hearts.

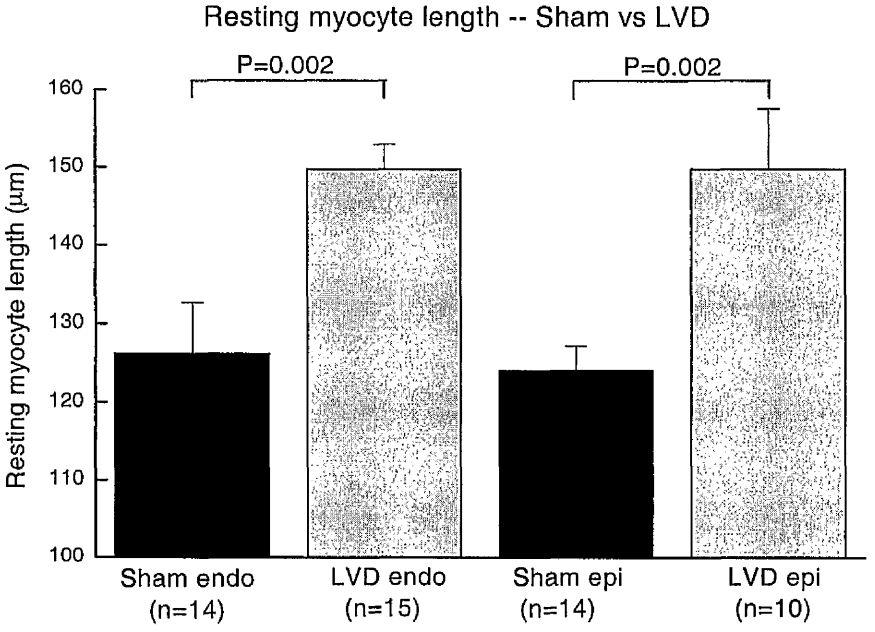

Figure 3.6. Comparisons between sham and LVD resting myocyte lengths (microns). n indicates number of hearts. $p<0.05$ are considered statistically significance. Data are Mean ± SEM.

3.3.2. Changes in diastolic length

3.3.2.1. Transmural diastolic length differences

Diastolic length decreased as stimulation frequency increased in both sham and LVD myocytes. No significant difference in relative diastolic length change was observed between endocardial and epicardial myocytes in both sham and LVD groups (table 3.1). Transmural relative diastolic length changes ranged from 1 to 0.97 at 0.3 and 3Hz respectively in both sham endocardial and epicardial myocytes. A similar range was observed in LVD myocytes with relative length changes ranging from 1 to 0.97 and 1 to 0.96 in endocardial and epicardial myocytes respectively (table 3.1).

3.3.2.2. Comparisons between sham and LVD diastolic length

Comparisons of relative diastolic length changes between sham and LVD revealed minimal differences in both endocardial and epicardial myocytes. LVD endocardial and epicardial length changes had a tendency to be smaller in comparison to sham myocytes. None of the above data showed any statistical differences when analysed using ANOVA.

Cell Type		Relative changes in Diastolic length				
		0.3Hz	0.5Hz	1Hz	2Hz	3Hz
Sham endo	Mean (n=22)	1.0	0.997	0.996	0.978	0.966
	SEM	0	0.001	0.005	0.002	0.002
Sham epi	Mean (n=19)	1.0	0.996	0.991	0.978	0.971
	SEM	0	0.002	0.003	0.002	0.003
LVD endo	Mean (n=15)	1.0	0.999	0.993	0.985	0.969
	SEM	0	0.001	0.001	0.004	0.005
LVD epi	Mean (n=10,*9)	1.0	0.999	0.995	0.984	0.963*
	SEM	0	0.001	0.001	0.003	0.012

Table 3.1. Mean relative changes in diastolic length for Sham and LVD endocardial and epicardial myocytes associated with increasing stimulation frequency (0.3 to 3Hz). Data are Mean ± SEM and expressed relative to diastolic length at 0.3 Hz. n indicates number of hearts.

3.3.3. Changes in systolic length

3.3.3.1. Transmural systolic length differences

A small transmural difference in relative systolic length changes was observed in the sham data. A trend towards greater relative systolic length changes were observed in sham endocardial myocytes in comparison to epicardial myocytes, although this did not reach statistical significance. Endocardial changes ranged from 0.92 ± 0.01 to 0.86 ± 0.01 (0.3 to 3Hz) whereas epicardial changes ranged from 0.93 ± 0.01 to 0.88 ± 0.01(0.3 to 3Hz) (figure 3.7, A). In contrast, changes in LVD endocardial relative systolic length were smaller than epicardial length changes. Endocardial changes ranged from 0.93 ± 0.01 to 0.87 ± 0.01 (0.3 to 3Hz) whereas epicardial changes ranged from 0.92 ± 0.01 to 0.85 ± 0.014 (0.3 to 3Hz). (figure 3.7, B). These data suggest that the small transmural differences in relative systolic length changes that exist in the sham data are not maintained in LVD although the differences were not statistically significant (ANOVA).

3.3.3.2. Comparisons between sham and LVD systolic length

Comparisons in systolic length changes between sham and LVD endocardial myocytes showed that frequency-dependent systolic length changes were slightly greater in sham than LVD endocardial myocytes although not significantly (figure 3.8, A). The opposite trend occurred in epicardial myocytes where systolic length changes were slightly greater in LVD in comparison to sham myocytes (figure 3.8,B).

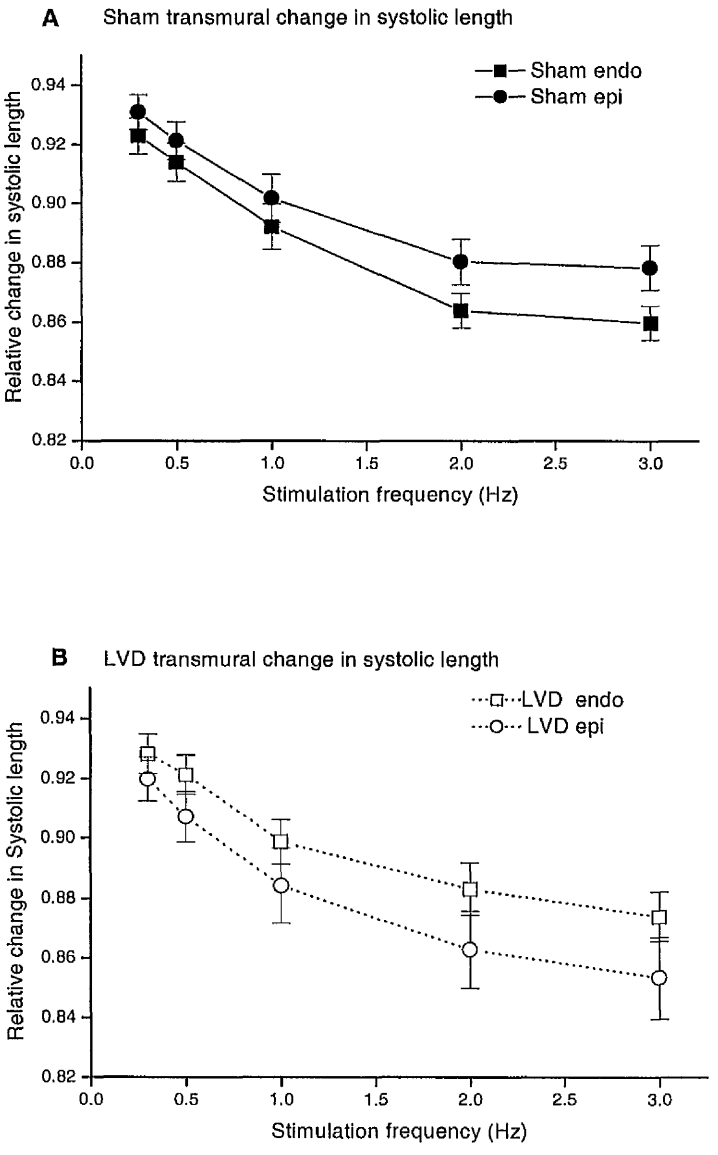

Figure 3.7. Transmural change in relative systolic length in sham (A) and LVD (B) myocytes associated with increasing stimulation frequency (0.3 to 3Hz). n is same as diastolic length (table 3.1). No statistical differences were observed within the data sets.

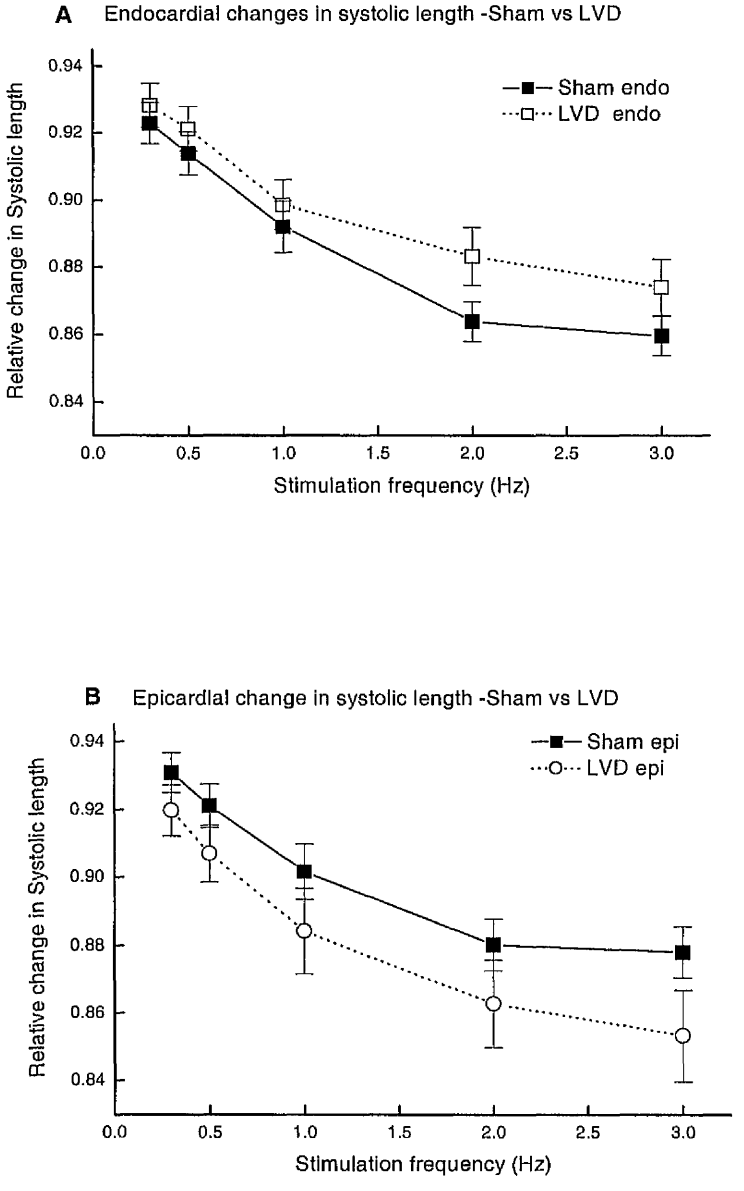

Figure 3.8. Comparisons between sham and LVD endocardial (A) and epicardial (B) relative systolic length changes associated with increasing stimulation frequency (0.3 to 3Hz). No statistical differences were observed within the data sets.

3.3.4. Fractional shortening

3.3.4.1. Transmural fractional shortening

Endocardial and epicardial myocytes from both sham and LVD hearts displayed a positive force-frequency relationship up to 2Hz with a levelling off of fractional shortening occurring at 3Hz, close to physiological resting rate. The reason for the plateauing of the relationship at 3Hz is unknown. *In vivo*, myocytes shorten with both isometric and isotonic phases, furthermore there is significant autonomic influence even at rest. The absence of these conditions in vitro may explain the apparent maximal shortening at 2Hz.

A small transmural difference in fractional shortening was found to exist between sham endocardial and epicardial data. Fractional shortening in endocardial myocytes was found to be greater especially at higher stimulation frequencies in comparison to epicardial myocytes although the differences were not significant (ANOVA, figure 3.9,A). Fractional shortening ranged from 7.16 ± 0.51 to 10.87 ± 0.55% (0.3 to 3Hz) and from 6.94 ± 0.77 to 9.74 ± 0.6% (0.3 to 3Hz) in endocardial and epicardial myocytes respectively.

Endocardial and epicardial fractional shortening in LVD was almost identical (figure 3.9,B). Although a small trend is present indicating greater fractional shortening in endocardial myocytes. LVD fractional shortening in endocardial myocytes ranged from 7.18 ± 0.64 to 9.5 ± 0.6% and from 5.83 ± 0.66 to 9.9 ± 0.8% in epicardial myocytes. None of the above data were significantly different when analysed using ANOVA.

3.3.4.2. Comparisons between sham and LVD fractional shortening

Comparisons in fractional shortening between sham and LVD endocardial myocytes showed that sham endocardial myocytes shorten more than LVD myocytes (not statistically different) at all except the lowest stimulation frequency (figure 3.10, A). In contrast, minimal differences in fractional shortening appear to exist between sham and LVD epicardial myocytes (figure 3.10,B), although sham epicardial myocytes have a tendency to shorten more than LVD epicardial myocytes.

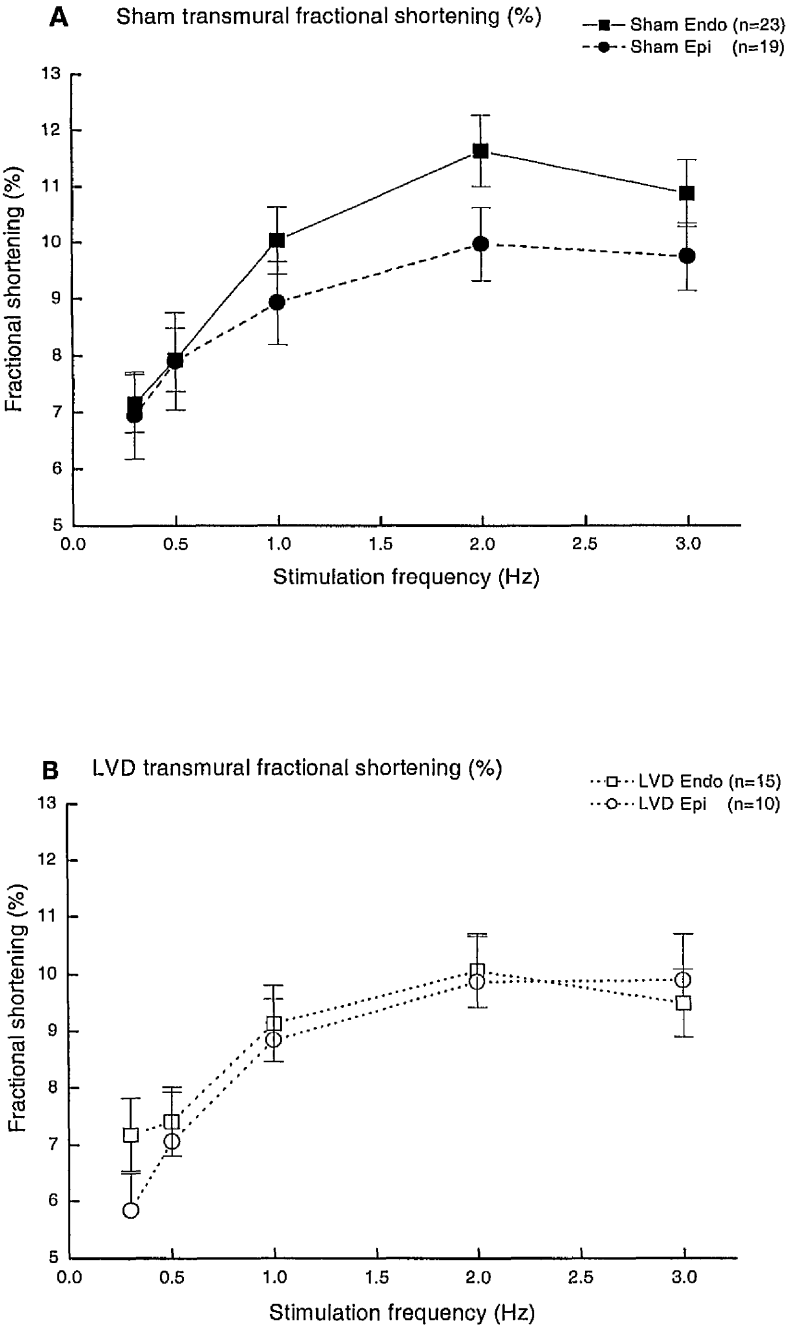

Figure 3.9. Effect of increasing stimulation frequency (0.3 to 3Hz) on transmural (endocardial/epicardial) fractional shortening (%) in sham (A) and LVD (B) myocytes. Data are mean ± SEM. n = number of hearts.

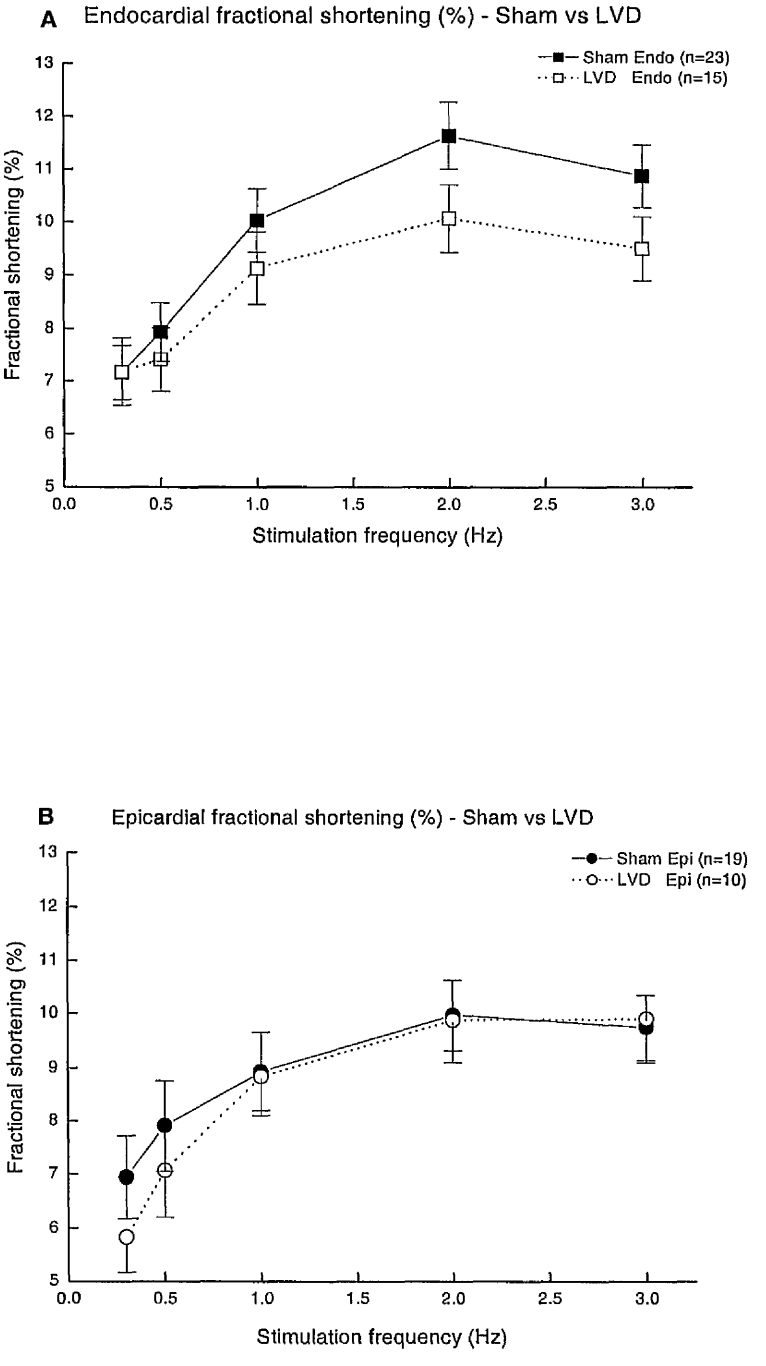

Figure 3.10. Comparisons between sham and LVD endocardial (A) and epicardial (B) fractional shortening as stimulation frequency is increased (0.3 to 3Hz). Data are mean ± SEM. n = number of hearts.

3.4. Single myocyte kinetic measurements

3.4.1. Transmural and Sham vs LVD kinetic measurements

Details of all contraction kinetic measurements are shown in figure 3.2. Increasing stimulation frequency (0.3 to 3Hz) resulted in an increase in peak amplitude in all myocytes types (endocardial and epicardial) from both sham and LVD groups (table 3.2). Transmural comparisons in peak amplitude revealed increased peak amplitude in endocardial myocytes in both sham and LVD groups in comparison to epicardial myocytes. These differences were not statistically different (ANOVA). Peak amplitudes of both endocardial and epicardial LVD myocytes were slightly higher than sham myocytes although LVD epicardial peak amplitude was less than shams at the two lowest stimulation frequencies (0.3 & 0.5Hz).

Increasing stimulation frequency produced an overall decrease in time to peak amplitude (table 3.2). Time to peak amplitude had a tendency to be slower in both sham and LVD endocardial myocytes in comparison to epicardial, although these differences were not statistically significant (ANOVA). Time to peak amplitude in LVD endocardial and epicardial myocytes were slower at all stimulation frequencies when compared to sham (not significantly different).

Myocyte type	Peak amplitude (μm)				
	0.3Hz	0.5Hz	1Hz	2Hz	3Hz
Sham endo (n=18)	8.9 ± 0.8	9.8 ± 0.8	12.3 ± 0.7	13.7 ± 0.7	12.4 ± 0.7
Sham epi (n=17)	8.8 ± 1.1	10.0 ± 1.2	11.1 ± 0.9	12.2 ± 0.8	11.2 ± 0.7
LVD endo (n=15)	10.0 ± 1.0	10.9 ± 1.0	13.3 ± 1.0	14.5 ± 1.0	13.4 ± 1.0
LVD epi (n=10)	8.3 ± 1.0	9.1 ± 1.1	11.9 ± 1.1	13.3 ± 1.2	13.2 ± 1.2
	Time to peak amplitude (ms)				
Sham endo (n=18)	145.5 ± 5.5	142.1 ± 6.3	142.8 ± 5.6	129.9 ± 5.8	117.8 ± 4.2
Sham epi (n=18)	129.0 ± 6.2	123.6 ± 6.1	127.1 ± 5.6	114.8 ± 4.0	105.7 ± 3.3
LVD endo (n=15)	148.4 ± 7.1	149.5 ± 6.4	145.8 ± 6.5	135.9 ± 5.0	126.4 ± 4.3
LVD epi (n=10)	136.5 ± 7.0	133.1 ± 6.6	135.7 ± 6.5	119.3 ± 6.2	112.6 ± 6.5

Table 3.2. Effect of increasing stimulation rate (0.3 to 3Hz) on peak amplitude (μm) and Time to peak amplitude (ms) in sham and LVD endocardial and epicardial myocytes. All data are mean ± SEM. n indicates number of hearts.

Similar prolongation of contraction kinetics was observed in the LVD data set when measuring time to 50% peak amplitude (table 3.3). In all myocyte types and experimental groups time to 50% peak amplitude decreased as stimulation frequency increased. Time to 50% peak amplitude had a tendency to be slower in both sham and LVD endocardial myocytes in comparison to epicardial. Comparisons between sham and LVD endocardial and epicardial myocytes showed that generally both LVD myocyte types were slower in comparison to sham, although epicardial values were similar at 2 and 3Hz. These differences were not significant.

The general trend in duration at 50% contraction showed a decrease in all cell types and groups as stimulation frequency increased (table 3.3). At all frequencies endocardial sham and LVD myocyte durations were longer than the corresponding epicardial values. Sham and LVD comparisons showed that endocardial durations were almost identical to one another. LVD epicardial duration at 50% was longer than sham especially at higher stimulation frequencies (1,2 & 3Hz), although this was not significant (ANOVA).

As stimulation frequency increased, time to 50% decay decreased in all cell types and groups (table 3.3). Sham endocardial decay was longer in comparison to epicardial myocytes at all frequencies, whereas in LVD endocardial myocytes decay was longer than epicardial at lower 0.3, 0.5 & 1Hz, and was the same at higher frequencies. None of these differences were statistically significantly. LVD endocardial decay at 50% contraction was slightly faster than sham at all stimulation frequencies except 0.3Hz. LVD epicardial decay was faster at 0.3 and 0.5Hz and similar at higher frequencies. However, no statistical differences were observed (ANOVA).

Myocyte type	Time to 50% peak amplitude (ms)				
	0.3Hz	0.5Hz	1Hz	2Hz	3Hz
Sham endo (n=18)	**55.7** ± 3.2	**52.8** ± 2.7	**43.7** ± 2.7	**36.9** ± 2.9	**35.9** ± 2.3
Sham epi (n=18)	**44.7** ± 4.2	**42.7** ± 4.3	**42.1** ± 3.8	**34.7** ± 2.8	**34.8** ± 3.8
LVD endo (n=15)	**54.1** ± 2.7	**54.5** ± 3.5	**47.6** ± 2.2	**41.5** ± 2.2	**39.7** ± 2.3
LVD epi (n=10)	**49.7** ± 8.1	**48.7** ± 6.4	**43.9** ± 4.6	**33.9** ± 2.9	**32.0** ± 3.2
	Duration at 50% contraction (ms)				
Sham endo (n=18)	**139.9** ± 6.1	**144.7** ± 6.1	**144.6** ± 5.5	**139.9** ± 4.9	**127.0** ± 4.7
Sham epi (n=18)	**133.0** ± 5.7	**132.9** ± 6.3	**128.4** ± 6.2	**122.3** ± 5.5	**113.5** ± 5.6
LVD endo (n=15)	**142.9** ± 7.5	**144.9** ± 7.2	**143.4** ± 7.9	**136.5** ± 6.1	**126.7** ± 5.1
LVD epi (n=10)	**125.7** ± 8.0	**127.6** ± 8.7	**136.1** ± 6.4	**133.1** ± 7.6	**120.9** ± 6.9
	Time to 50% decay (ms)				
Sham endo (n=18)	**53.6** ± 2.9	**55.2** ± 2.9	**52.7** ± 2.7	**50.0** ± 1.5	**47.8** ± 1.9
Sham epi (n=18)	**53.3** ± 2.5	**52.2** ± 2.2	**47.4** ± 2.5	**45.5** ± 2.9	**44.9** ± 2.7
LVD endo (n=15)	**55.5** ± 3.4	**53.6** ± 2.5	**51.2** ± 3.0	**49.6** ± 2.9	**46.3** ± 2.8
LVD epi (n=10)	**50.0** ± 4.5	**47.8** ± 3.3	**49.8** ± 3.1	**49.6** ± 3.0	**45.7** ± 3.0

Table 3.3. Effect of increasing stimulation rate (0.3 to 3Hz) on Time to 50% peak amplitude (ms), Duration at 50% contraction (ms) and Time to 50% Decay (ms) in sham and LVD endocardial and epicardial myocytes. All data are mean ± SEM. n indicates number of hearts.

3.5. Single myocyte Rest decay measurements

3.5.1. Transmural rest decay measurements

A typical example of the rest decay phenomenon is shown in figure 3.11. Post rest potentiation is observed in the first contraction after 10s rest (panel A) and rest decay (smaller contraction amplitude) is observed as the rest interval is increased to 30 (B) and 180s (C). The fractional shortening data described here are normalised relative to the average steady state contraction prior to beginning the rest intervals. Steady state values quoted in table 3.4 and figures 3.12 - 3.14 are values measured approximately 1-2min after recommencing stimulation depending on rest interval duration. These steady state values show that relative fractional shortening returned to normal after the various rest interval protocols.

Relative fractional shortening for the first contraction and the steady state values after rest intervals of 10, 30 and 180s are shown in table 3.4.

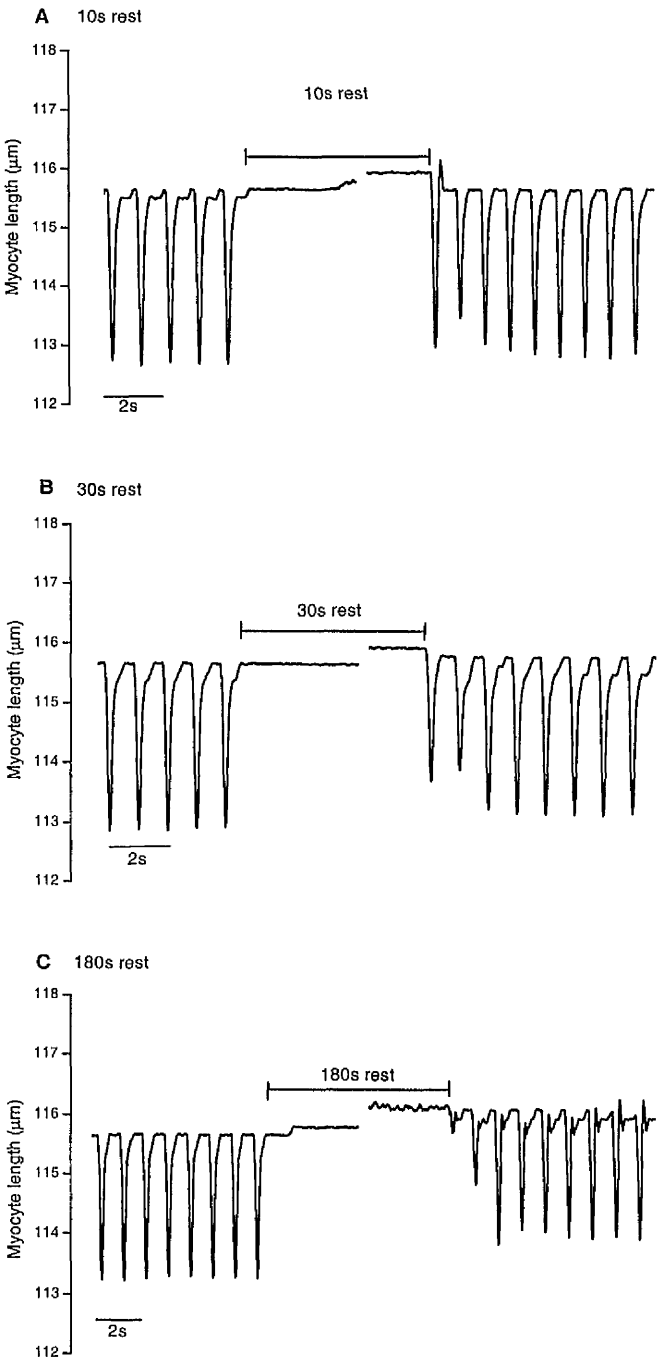

Figure 3.11. Single myocyte contractions after 10 (A), 30 (B) and 180s (C) rest intervals. Electrical stimulation was 1Hz prior to rest interval. 2s time scale is indicated by solid line (left hand side). Solid bracketed bar indicates duration of rest.

	Rest Interval (s)					
	10s		30s		180s	
Cell type	1st contraction	SS	1st contraction	SS	1st contraction	SS
Sham endo	**0.92** ± 0.09	**1.02** ± 0.03	**0.86** ± 0.08	**1.01** ± 0.02	**0.81** ± 0.09 *	**0.95** ± 0.02
Sham epi	**1.14** ± 0.05 *	**1.07** ± 0.04	**1.06** ± 0.08	**0.97** ± 0.02	**0.87** ± 0.09	**0.99** ± 0.03
LVD endo	**0.98** ± 0.02	**0.99** ± 0.01	**0.84** ± 0.04 *	**1.02** ± 0.02	**0.67** ± 0.07 *	**0.99** ± 0.03
LVD epi	**1.04** ± 0.05	**0.98** ± 0.02	**1.02** ± 0.08	**1.02** ± 0.03	**0.76** ± 0.12 *	**0.97** ± 0.03

Table 3.4. Relative fractional shortening of first and steady state contractions after rest intervals of 10, 30 and 180s in sham and LVD endocardial and epicardial myocytes. SS values are contraction values measured 1-2 min after electrical stimulation was recommenced. All data are mean ± SEM. * denotes significantly different value from SS values (prior to cessation of electrical stimulation).

The amplitude of the first contraction after rest is the most important as it reflects SR Ca^{2+} content after rest. The subsequent results and discussion therefore focus only on the relative fractional shortening of the first contraction after rest. Transmural comparisons between sham and LVD show an almost identical trend in rest decay at all three rest intervals measured (10, 30 and 180s). Table 3.4 shows that post rest potentiation is present in the first contraction after 10s rest in both sham and LVD epicardial ($p < 0.05$) but not in endocardial myocytes. After 30s rest, the first contraction in both sham and LVD epicardial myocytes shows similar relative fractional shortening to steady state values. In contrast, rest decay is observed in sham and LVD endocardial myocytes ($p < 0.001$). After 180s rest, significant rest

decay is observed in both endocardial and epicardial sham (endo; $p < 0.05$) and LVD myocytes (endocardial; $p < 0.001$, epicardial, $p < 0.05$). Interestingly, epicardial relative fractional shortening is consistently higher than endocardial irrespective of rest interval duration. These results are more clearly shown in figure 3.12, which shows the relationship between relative fractional shortening of the first contraction and 10, 30 and 180s rest intervals. Both Sham and LVD epicardial first contractions tend to be larger than endocardial, with this trend being more defined in the sham data. Post rest potentiation is also more apparent in sham than LVD epicardial myocytes.

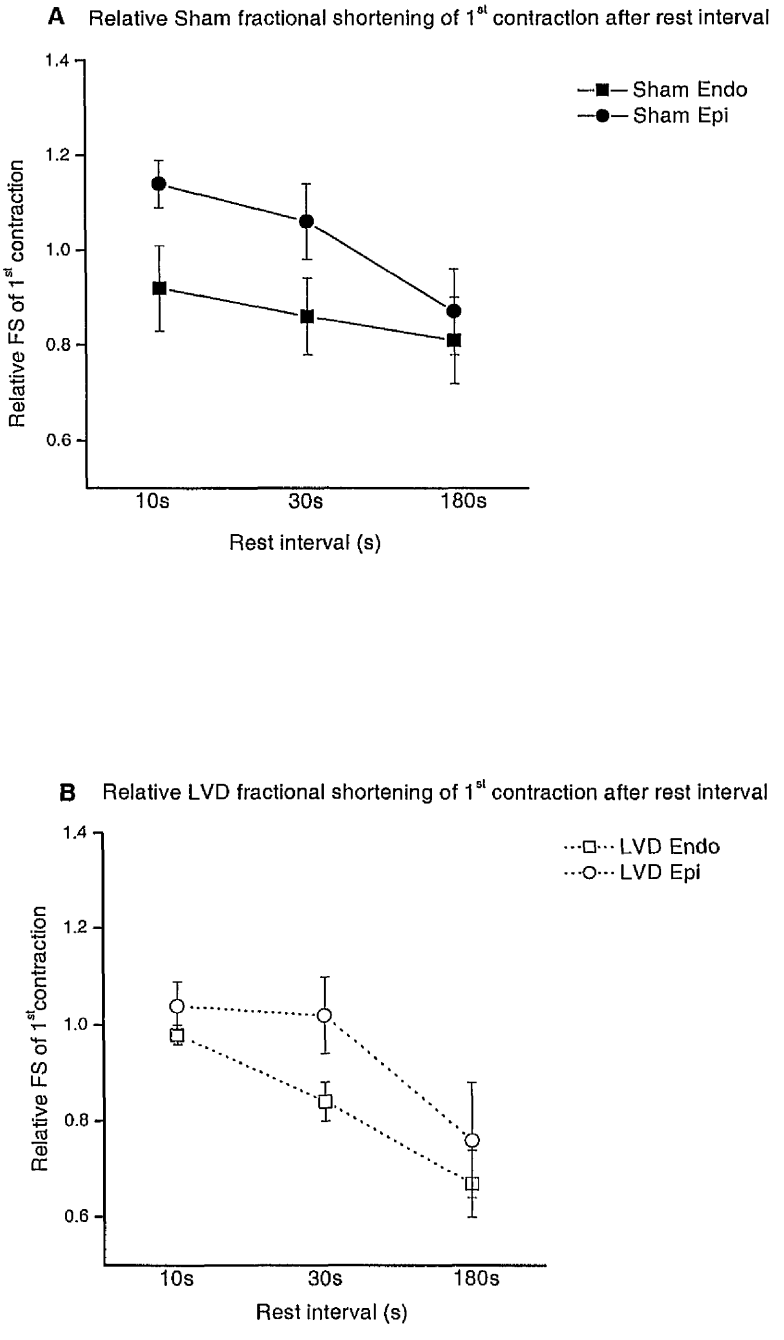

Figure 3.12. Relationship between first contraction (relative fractional shortening) and rest interval in sham (A) and LVD (B) endocardial and epicardial myocytes. Data plotted are mean ± SEM. Data are expressed relative to steady state fractional shortening prior to rest intervals.

3.5.2. Sham vs LVD endocardial rest decay measurements

Comparisons between sham and LVD endocardial rest decay measurements show no differences in relative fractional shortening of the first contraction after a 10s rest interval. The first contraction in each experimental group is not significantly different to the steady state value prior to the rest interval (sham 0.92 ± 0.09 LVD; 0.98 ± 0.02), suggesting that neither post rest potentiation or rest decay has occurred after 10s rest (figure 3.13,A). Prolongation of the rest interval to 30 and 180s produces a progressive post rest decay of the first contraction in both sham (30s; 0.86 ± 0.1 & 180s; 0.81 ± 0.1, $p<0.05$) and LVD endocardial myocytes (30s; 0.84 ± 0.04, $p<0.001$ & 180s; 0.67 ± 0.1, $p<0.001$) (see figures 3.14 & 3.15, panel A). p values indicate values that are significantly different from SS values prior to cessation of stimulation.

3.5.3. Sham vs LVD epicardial rest decay measurements

In contrast, both sham and LVD epicardial myocytes show post rest potentiation in the first contraction after a 10s rest interval (sham; 1.14 ± 0.05, $p< 0.05$) and LVD; 1.04 ± 0.05; figure 3.13,B). No statistical differences were observed between the sham and LVD data sets. Increasing the rest interval to 30s reduced the relative fractional shortening of the first contraction to values similar to steady state (sham; 1.06 ± 0.1, & LVD 1.02 ± 0.1) and relative fractional shortening was reduced further still after 180s rest (sham; 0.87 ± 0.09 & LVD; 0.76 ± 0.12, $p <0.05$) (figures 3.14 & 3.15, B).

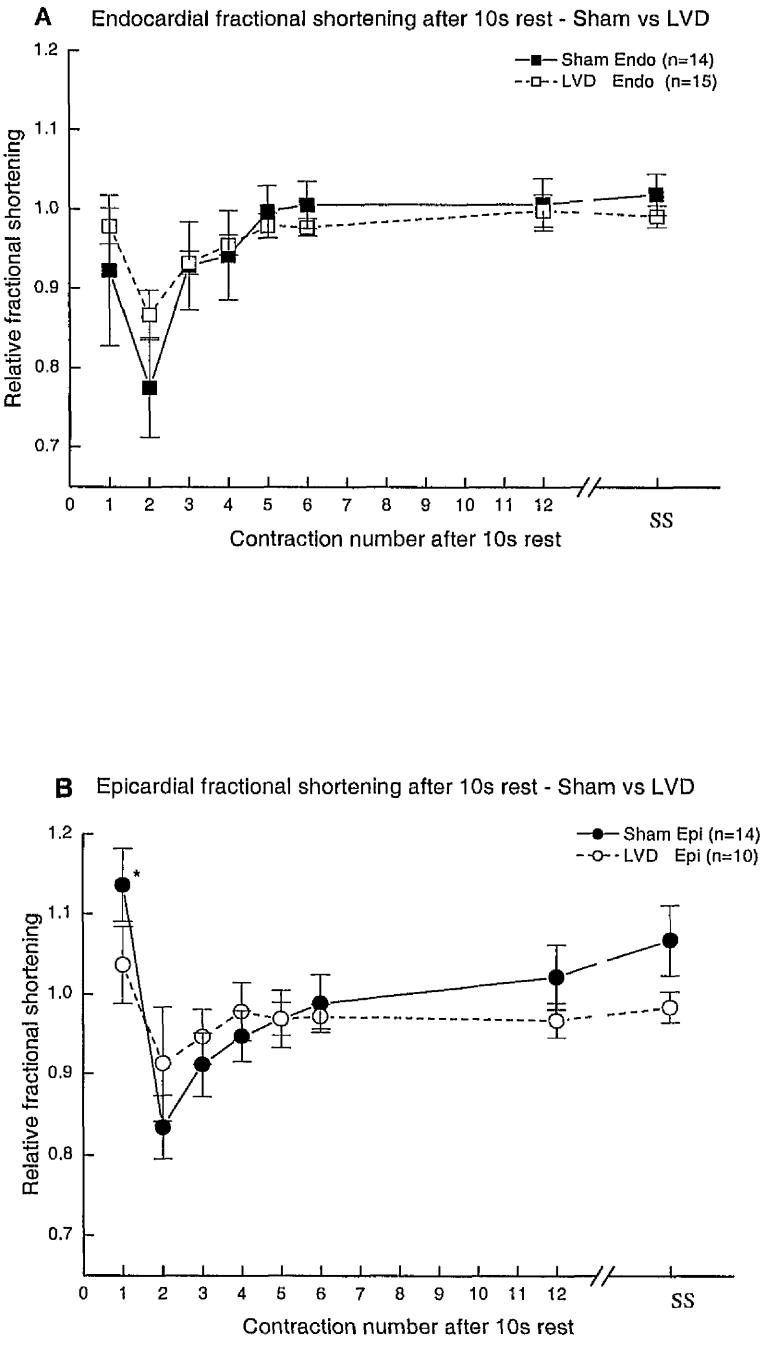

Figure 3.13. Effect of 10s rest interval on relative fractional shortening in sham and LVD endocardial (A) and epicardial (B) myocytes. SS value on graph indicates steady state contraction value after recommencing stimulation. Data are expressed relative to steady state fractional shortening prior to rest intervals. n= number of hearts. * indicates significant difference ($p<0.05$) from SS contraction before rest.

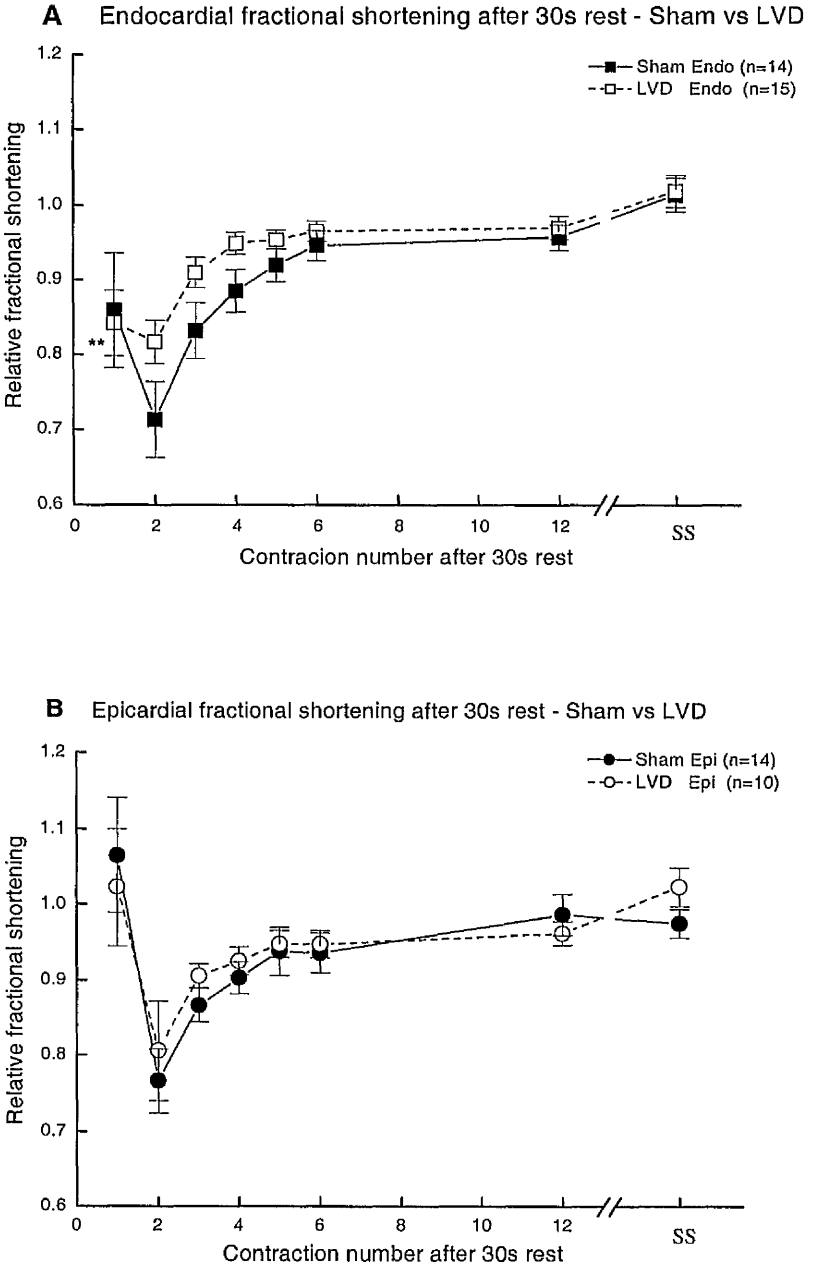

Figure 3.14. Effect of 30s rest interval on relative fractional shortening in sham and LVD endocardial (A) and epicardial (B) myocytes. SS indicates steady state contraction value after recommencing stimulation. Data are expressed relative to steady state fractional shortening prior to rest intervals. n= number of hearts. ** indicates significant difference $p<0.001$.

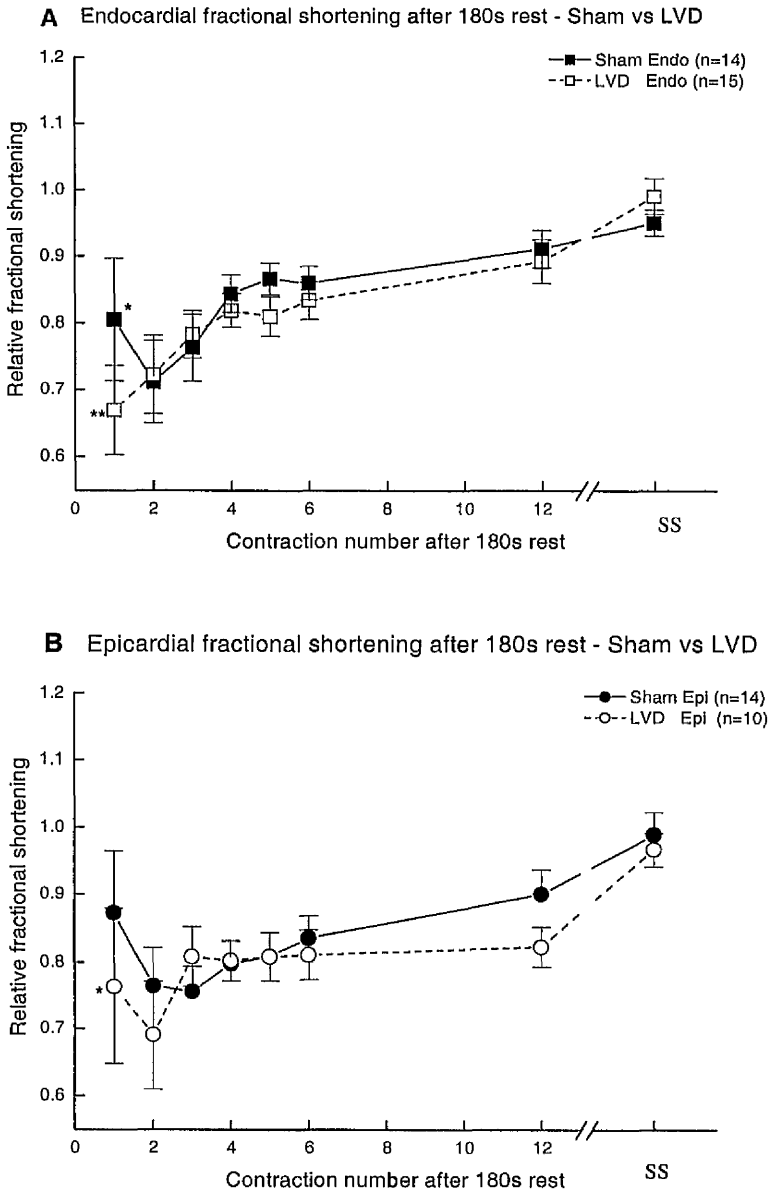

Figure 3.15. Effect of 180s rest interval on relative fractional shortening in sham and LVD endocardial (A) and epicardial (B) myocytes. SS indicates steady state contraction value after recommencing stimulation. Data are expressed relative to steady state fractional shortening prior to rest intervals. n= number of hearts. * indicates statistical significance $p<0.05$, ** indicates statistical significance $p<0.001$.

3.6. Discussion

3.6.1. Myocyte length

An increase in myocyte length has been observed in many volume overload models of hypertrophy or heart failure in both human and animal studies (see introduction for references). These cellular changes are thought to reflect an *in vivo* compensatory cellular hypertrophy initiated by the failing myocardium to maintain cardiac output. The results observed in this study are consistent with previously published data. A significant increase in myocyte length occurred to the same extent in both endocardial and epicardial LVD myocytes (figure 3.6). The increased myocyte length observed in failing myocardium is thought to be achieved by the addition, in series, of more sarcomeres rather than increasing sarcomere length as sarcomere length is reportedly unchanged (Gerdes *et al.* 1992 & 1996).

Decreases in relative diastolic length were observed in all myocyte types and experimental groups as stimulation frequency increased. As stimulation frequency increases, diastolic $[Ca^{2+}]_i$ rises (chapter 4) and a subsequent decrease in diastolic length ensues. No transmural differences in sham and LVD diastolic length were observed and comparisons between sham and LVD endocardial and epicardial diastolic lengths suggested a trend towards a longer relative diastolic length in LVD, although these differences were not significant. The longer relative diastolic length may reflect either a lower diastolic $[Ca^{2+}]_i$ or a reduced myofilament Ca^{2+} sensitivity in both endocardial and epicardial LVD myocytes (chapter 4, & general discussion).

Relative systolic length decreased as stimulation frequency increased. A small transmural difference in systolic length change was observed in the sham data set with epicardial systolic length changing less than endocardial (figure 3.7, A). The reverse trend was observed in LVD with endocardial systolic length changing less than epicardial myocytes. Endocardial and epicardial differences within the sham and LVD data sets revealed no significant differences. The reason for the reversal in systolic length changes in LVD may reflect differences in systolic $[Ca^{2+}]_i$ between sham and LVD myocytes (chapter 4). Systolic length changes were less evident in LVD endocardial and greater in epicardial in comparison to sham myocytes (figure 3.8), although not statistically significant. The reason for greater change in systolic length in LVD epicardial myocytes is unknown, especially as diastolic length

changes appear similar in both endocardial and epicardial myocytes. This difference may be due to lower $[Ca^{2+}]_i$ in LVD epicardial myocytes in comparison to LVD endocardial (see chapter 4 & general discussion).

3.6.2. Fractional shortening

In line with normal force-frequency relations, greater fractional shortening was observed as stimulation frequency increased. In agreement with previous observations (Bryant *et al.* 1997), transmural fractional shortening was slightly greater in sham endocardial than epicardial myocytes (not significant). This trend was maintained in LVD at all frequencies except 3Hz, although the differences were not as distinct (figure 3.9). These fractional shortening differences may be due to transmural differences in systolic $[Ca^{2+}]_i$, and/or myofilament Ca^{2+} sensitivity (see chapter 4 & general discussion). There was no significant difference in fractional shortening between sham and LVD endocardial myocytes although there was a marked reduction in fractional shortening in LVD in comparison to sham myocytes. In contrast, fractional shortening was the same in sham and LVD epicardial myocytes. The reduced fractional shortening in LVD endocardial myocytes may reflect either lower systolic $[Ca^{2+}]_i$, and/or alterations in myofilament Ca^{2+} sensitivity (chapter 4 & general discussion).

3.6.3. Contraction kinetics

As stimulation frequency was increased, peak amplitude increased in all cell types and groups. These results are in agreement with previously published data (Davies *et al.* 1995). Peak amplitude was slightly greater in both sham and LVD endocardial myocytes in comparison to epicardial and in general, LVD peak amplitude was greater than sham (endo -all frequencies; epi 1,2 & 3Hz) (table 3.2) although not significantly. Peak amplitude is an absolute measure of shortening (diastolic –systolic length) and is therefore directly related to cell length. As LVD myocytes are significantly longer than sham myocytes then a greater peak amplitude in LVD myocytes would be expected. However, as there are no apparent transmural differences in cell length within the two experimental groups (figure 3.6), this does not explain the slightly greater peak amplitude observed in endocardial sham and LVD myocytes in comparison to epicardial myocytes. This difference may reflect transmural differences in $[Ca^{2+}]_i$ (chapter 4).

Time to peak amplitude was longer in sham and LVD endocardial myocytes in comparison to epicardial myocytes and overall, time to peak amplitude was longer in LVD endocardial and epicardial myocytes in comparison to sham (table 3.2). An almost identical trend was observed in time to 50% peak amplitude (table 3.3).

It has previously been reported that increasing stimulation frequency causes an increase in contraction amplitude (positive force-frequency relationship), (Orchard & Lakatta 1985) and produces faster contraction kinetics (Davies *et al.* 1995). The observed increase in contraction kinetic speed as stimulation frequency is increased is most likely due to an increased rate of intracellular Ca^{2+} cycling processes (Ca^{2+} uptake and release). Increased Ca^{2+} cycling rates are required to ensure that adequate $[Ca^{2+}]_i$ is available for normal contractile function when stimulation frequency is increased. Furthermore, increased stimulation rate means less time for Ca^{2+} extrusion per unit time, leading to an increase in diastolic $[Ca^{2+}]_i$ and hereafter increased SR Ca^{2+} uptake and subsequent release. This process is believed to be responsible for the increasing amplitude observed as stimulation frequency is increased. Even though peak amplitude increases as stimulation frequency increases the time to peak amplitude decreases (due to faster Ca^{2+} cycling rates). LVD peak amplitude was generally larger yet time to peak amplitude tended to be longer. One possible explanation for the slower time to peak in LVD myocytes is that the velocity of contraction kinetics is related to cell size, i.e. longer myocytes have slower contraction kinetics. This relationship was investigated by plotting time to peak verses myocyte length. The data in figure 3.16 represent endocardial data only, however the same trend was observed when epicardial sham and LVD myocytes were compared (data not shown). These data suggest that the velocity of contraction is unrelated to myocyte length in both sham and LVD myocytes ($r = -0.048$ & -0.28, $p = 0.85$ and 0.31, sham and LVD respectively). These results agree with previously published data (del Monte *et al.* 1995). Alternative reasons for the slower contraction kinetics observed in LVD myocytes may be either a slower and/or reduced Ca^{2+} transient amplitude or that the response to changes in $[Ca^{2+}]_i$ in LVD myocytes is reduced (see chapter 4). In general, the slowing of LVD contraction kinetics presented here are in agreement with previously published data. Prolonged contraction times have been reported in human (Davies *et al.* 1995; del Monte *et al.* 1995) rat myocytes (Perez *et al.* 1999) and rabbit myocytes (Milnes & McLeod 2001).

Alterations in transmural contraction kinetics were investigated by Bryant *et al.* (1997), who observed no change in hypertrophic endocardial myocyte time to peak amplitude but a marked prolongation in epicardial time to peak amplitude. Bryant *et al.* (1997) also observed a small prolongation in hypertrophied endocardial time to 10% relaxation and a more marked prolongation in hypertrophied epicardial myocytes.

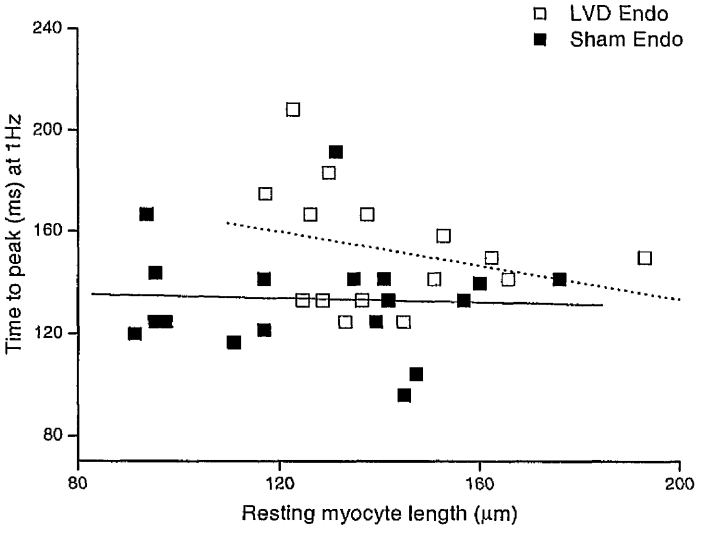

Figure 3.16. Relationship between time to peak amplitude (ms) and resting myocyte length (μm) in sham (solid squares) and LVD (open squares) endocardial myocytes. Solid and dotted lines represent the best fit to a linear correlation with gradient values of -0.040 and -0.28 for sham and LVD data respectively, r = -0.04 and -0.28 and p= 0.85 and 0.31 for sham and LVD respectively.

Duration at 50% contraction was increased in endocardial sham and LVD myocytes at all stimulation frequencies in comparison to epicardial myocytes (not significant). Comparisons between sham and LVD endocardial duration showed no differences and LVD epicardial duration was shorter at 0.3 and 0.5 Hz but longer at 1, 2 and 3Hz (not significant). Electrophysiological studies using this model

observed a slight decrease in LVD endocardial and an increase in epicardial action potential duration (McIntosh *et al.* 2000). These electrophysiological changes may explain the alterations in the contraction duration observed in this study, i.e. decrease in both action potential duration and contraction duration in LVD endocardial myocytes and an increase in both action potential duration and contraction duration in LVD epicardial myocytes.

In general, the results presented here observed slower contraction kinetics in LVD myocytes in comparison to sham and are in agreement with previous reports showing prolongation of cell decay/relaxation times in failing myocytes. Interestingly, time to 50% decay was faster in LVD endocardial in comparison to sham myocytes although not significantly. This finding was unusual and the reasons are unknown. Whether this finding is important remains to be determined, as the difference in decay rate was not significantly faster and all other LVD contraction kinetics were slower in comparison to sham. Additional experiments are required to confirm these results.

In summary, the slower contraction kinetics observed in endocardial myocytes (sham & LVD) and the LVD group may reflect either reduced peak systolic $[Ca^{2+}]_i$, a slower rate of rise in $[Ca^{2+}]_i$ (slow SR Ca^{2+} release) and/or a decrease in myocyte myofilament responsiveness to $[Ca^{2+}]_i$ (chapter 4). Expression and functional activity of Ca^{2+} handling proteins such as SERCA and NCX determine rate, amplitude of contraction and extent of relaxation of cardiac myocytes by affecting $[Ca^{2+}]_i$. Therefore alterations in protein expression may have significant affects on myocyte contractility (see chapter 7).

Although there was a trend towards less fractional shortening (endocardial myocytes) and prolonged contraction kinetics in LVD myocytes no statistically significant differences were observed. Even though these findings imply that a degree of dysfunction has occurred in these LVD myocytes the data do not suggest that major abnormalities exist. Previously published data investigating contractile function have observed significant contractile dysfunction in hypertrophic and/or failing myocytes (see 1.8.1.4). The question that now arises is; Why were no significant differences observed between sham and LVD myocytes in this study?
Was the left ventricular dysfunction severe enough to produce cellular dysfunction? The echocardiography results suggest that significant LVD was present as ejection fraction was significantly decreased and LVEDD values were significantly increased

in the LVD animals used in this study. Such contractile abnormalities are not only observed in single myocytes as studies using the same animal model as this study observed contractile dysfunction in isolated working whole hearts (Pye *et al.* 1996; Ng *et al.* 1998). It is possible that during the myocyte isolation procedure the unhealthiest LVD myocytes do not survive leaving the *healthiest* LVD myocytes alive, which will subsequently be used for experiments. These healthy LVD myocytes may have only slight contractile dysfunction, making it difficult to distinguish significant contractile differences between sham and LVD myocytes.

Although some of the differences within the data sets are almost significant, for example, endocardial fractional shortening at 2 & 3Hz (figure 3.10, A). The high variation within the data sets indicates that a high *n* number would be required in order to reveal any significant differences (n ~ 40 – 50 hearts in each group).

3.6.4. Rest decay

In line with previously published data, the results in this study showed a progressive decrease in contraction amplitude of the first contraction as rest intervals increased (figure 3.12). At all three rest interval durations both sham and LVD epicardial relative fractional shortening was noticeably higher than endocardial although this difference was not significant. Similar results have been observed by O'Neill (1993) and Chamunora & O'Neill (1995) who investigated transmural differences in rest decay recovery in normal rabbit myocytes. The data presented here suggest that the SR of sham and LVD epicardial myocytes are either able to retain SR Ca^{2+} longer (lower SR Ca^{2+} leak) or have a larger SR Ca^{2+} storage capacity in comparison to endocardial myocytes. Several factors such as rate/expression of SR Ca^{2+} pump (SERCA), rate of SR leak and rate of Ca^{2+} efflux from the cell (NCX) may influence SR Ca^{2+} content. Alternatively, higher $[Na^+]_i$ may be responsible for the greater relative fractional shortening observed in the first contraction after rest in sham and LVD epicardial myocytes. As discussed previously, (Introduction) higher $[Na^+]_i$ reduces the reversal potential for NCX favours Ca^{2+} influx and increase $[Ca^{2+}]_i$. Raised $[Ca^{2+}]_i$ reduces the rest decay affect. Transmural $[Na^+]_i$ was assessed in rabbit left ventricular myocytes by Cook *et al.* (1997) who observed significantly increased $[Na^+]_i$ in epicardial in comparison to endocardial myocytes. Higher $[Na^+]_i$ may be responsible for the reduced rest decay observed in epicardial myocytes but

assessment of endocardial and epicardial $[Na^+]_i$ would be required to verify this hypothesis in both sham and LVD myocytes.

No significant differences in relative fractional shortening of the first contraction after rest were observed between sham and LVD endocardial and epicardial myocytes (10, 30 and 180s rest intervals, figures 3.12). A trend to lower relative fractional shortening of the first contraction in LVD endocardial and epicardial myocytes after all rest intervals was observed, although the differences were not significant. These results may suggest that LVD endocardial and epicardial myocytes are either less able to retain (greater leak) and/or have a lower SR Ca^{2+}storage capacity in comparison to sham myocytes during rest intervals. Additional SR functional measurements would have to be performed in order to assess transmural and sham LVD differences in SR Ca^{2+} content (see chapter 4). It is unlikely that lower $[Na^+]_i$ is responsible for the slightly greater rest decay in LVD myocytes as studies have commonly observed increases in $[Na^+]_i$ rather than decreases in hypertrophied human and guinea-pig myocardium (Gray *et al.* 2001) and in isolated whole guinea-pig hearts with compensated hypertrophy (Jelicks and Siri, 1995). This suggests that alternative cellular mechanisms are affecting rest decay.

3.7. Summary

No transmural resting myocyte length differences were observed within either sham or LVD groups. LVD endocardial and epicardial resting myocyte lengths were significantly longer than sham myocytes. No significant transmural differences were observed in both sham and LVD diastolic myocyte length changes as stimulation frequency was increased. Comparisons in diastolic length changes between LVD and sham myocytes revealed no significant differences. Sham transmural systolic length changes revealed a smaller rate-dependent change in epicardial in comparison to endocardial myocyte length, the opposite difference was observed in LVD (endocardial length changed less than epicardial). Endocardial sham verses LVD comparisons showed that the change in LVD endocardial systolic length was less than sham, but epicardial LVD systolic length changes were greater than sham. However, none of the sham vs LVD differences were statistically significant.

Sham fractional shortening was slightly larger in endocardial in comparison to epicardial myocytes, however LVD fractional shortening appeared similar in both

regions. Sham endocardial myocytes shortened more than LVD, but sham and LVD epicardial myocytes showed similar shortening, although sham myocytes had a tendency to shorten more at lower stimulation frequencies. No statistical differences were observed when transmural and sham vs LVD comparisons were made.

Peak amplitude was slightly larger in endocardial sham and LVD myocytes in comparison to epicardial, and peak amplitude in LVD myocytes was larger than sham, although not statistically significant. In general, contraction kinetics (contraction and relaxation) in sham and LVD endocardial myocytes were longer in comparison to epicardial myocytes (not significantly). Duration at 50% contraction was slightly longer in sham endocardial myocytes in comparison to epicardial, but minimal transmural differences were observed in LVD. Overall contraction kinetics were slower in LVD in comparison to Sham, although such differences never reached statistical significance. Duration at 50% contraction was similar in LVD endocardial and slower in epicardial myocytes. Time to 50% decay was faster in LVD endocardial (not significant) and slower at the higher frequencies (1, 2 & 3Hz) in epicardial myocytes in comparison to the corresponding sham values.

Sham and LVD transmural rest decay was similar and showed post rest potentiation after 10 and 30s rest and rest decay after 180s. Throughout the range of rest intervals, epicardial sham and LVD myocytes showed noticeably higher fractional shortening of the first contraction in comparison to endocardial myocytes. Relative fractional shortening in sham and LVD endocardial and epicardial myocytes were similar, with a trend to lower fractional shortening in LVD myocytes.

A cascade of intracellular factors are responsible for contractile function in cardiac myocytes. The expression of sarcolemmal and SR Ca^{2+} handling proteins directly affects SR Ca^{2+} content which subsequently influences $[Ca^{2+}]_i$. Hereafter, coupled with myofilament Ca^{2+} sensitivity, changes in $[Ca^{2+}]_i$ are responsible for myocyte contraction. Some of these intracellular factors are addressed in subsequent chapters (chapter 4 & 7) and their influences on contractile function are discussed in the general discussion (chapter 8).

Chapter 4

Intracellular Calcium measurements

4.1. Background

Measurement of intracellular Ca^{2+} transients using fluorescent indicators like Fura-2 are used to assess intracellular Ca^{2+} homeostasis within isolated cardiac myocytes. Accurate measurements of end diastolic and peak systolic $[Ca^{2+}]_i$ can subsequently be determined from intracellular calcium transients. The aim of this study was 2 fold; one, to assess transmural (endocardial:epicardial) $[Ca^{2+}]_i$ in Sham and LVD myocytes and two; to compare $[Ca^{2+}]_i$ between sham and LVD myocytes.

To date, minimal work has been published on transmural $[Ca^{2+}]_i$ differences in either normal or failing myocardium. A previous study using the same model of LVD described in this study investigated transmural differences in action potentials and intracellular calcium transients (McIntosh *et al.* 2000). They observed no significant transmural differences in either end diastolic or peak systolic $[Ca^{2+}]_i$ in sham myocytes. However, there was a trend towards lower peak systolic $[Ca^{2+}]_i$ in sham endocardial myocytes. Figuerdo *et al.* (1993) observed higher end diastolic and peak systolic $[Ca^{2+}]_i$ in the endocardium in comparison to epicardium in their perfused whole rat heart study (control). McIntosh *et al.* concluded that the differences in results between the two studies was due to either the differences in action potential duration between rat and rabbit or that the mechanical stresses between endocardial and epicardial were different between single dissociated myocytes and those intact within the whole myocardium.

McIntosh compared sham and LVD end diastolic $[Ca^{2+}]_i$ and observed higher endocardial end diastolic $[Ca^{2+}]_i$ but minimal changes in LVD epicardial end diastolic $[Ca^{2+}]_i$. In contrast, LVD endocardial end diastolic $[Ca^{2+}]_i$ and peak systolic $[Ca^{2+}]_i$ was higher in comparison to the corresponding sham data. Figuerdo *et al.* (1993) observed that during ischaemia, endocardial diastolic $[Ca^{2+}]_i$ rose to a greater degree than epicardial levels.

In human heart failure, increased end diastolic $[Ca^{2+}]_i$ (Gwathmey *et al.* 1987; Beuckelmann *et al.* 1992; Arai *et al.* 1993,), decreased peak systolic $[Ca^{2+}]_i$ (Beuckelmann *et al.* 1992) and unchanged peak systolic $[Ca^{2+}]_i$ (Gwathmey *et al.*

1990) have been observed. In addition, prolongation of Ca^{2+} transient duration has also been observed (Gwathmey *et al.* 1987 &1991, Beuckelmann *et al.* 1992).

Similar results have been observed in animal models of heart failure. Siri *et al.* (1998) in their guinea pig model of heart failure observed a decrease in peak systolic $[Ca^{2+}]_i$ but observed no change in end diastolic $[Ca^{2+}]_i$. McIntosh *et al.* (2000) observed a reduced peak systolic and an unchanged end diastolic $[Ca^{2+}]_i$ in failing epicardial myocytes in comparison to sham epicardial myocytes. In contrast, failing endocardial myocytes showed an increased peak systolic and end diastolic $[Ca^{2+}]_i$. Ca^{2+} transient duration was also increased in epicardial but decreased in endocardial failing myocytes.

4.2. Methods

4.2.1. Fluorescent measurements

Changes in intracellular Calcium concentration ($[Ca^{2+}]_i$) during electrical stimulation (termed Ca^{2+} transients) were recorded using the fluorescent Ca^{2+} indicator Fura-2 AM (Molecular probes). Fluorescence excitation at 340 and 380nm was produced by a Xenon arc light source and a spinning wheel system at 60Hz (Cairn Research Systems). Fluorescence emissions above 500nm were collected using an interference filter (long pass 500nm) and passed through a dichroic mirror to the photomultiplier. Output (V) from the photomultiplier was measured by a spectrophotometer (Cairn Research Systems). The adjustable window surrounding each single cell was minimised to reduce external fluorescence and a red filter was introduced within the microscope to allow the cell image to be monitored. Changes in intracellular $[Ca^{2+}]$ ($[Ca^{2+}]_i$) were calculated by the ratiometric measurement of the excited fluorescence signals at 340 and 380nm. These two wavelengths and the 340:380 ratio value were recorded on a chart recorder (Gould Instruments Ltd), video and digitised onto a computer.

The bath and perfusion system used to measure intracellular fluorescence differed from that used in the cell length set-up. Firstly, a smaller bath, 200µl volume was used thus enhancing the speed of solution changes. Secondly, the inflow tube was positioned by micromanipulators directly above the cell of interest. Such a system localises and optimises the effect of solution changes. All other apparatus and

recording equipment was identical to that used in the cell length measurements (figure.3.3).

Myocytes were loaded by incubation with 5μM Fura-2 AM (5μl ml^{-1}) for 10 min at room temperature, subsequently diluted with Krebs by a factor of 2, left for a further 10 min then used as required, up to a maximum of 60min. Myocytes were placed into the heated bath and perfused with Krebs (Sol^n B, Ca^{2+} 1.8mM). Fluorescence ratios from individual myocytes were recorded during the following protocol. Myocytes were electrically stimulated at 0.5 Hz until steady state contraction was reached. Simultaneously, stimulation was ceased and perfusion was switched from Krebs to Krebs containing 20mM caffeine for 5s. Electrical stimulation was recommenced 15 s later for 1min followed by a second caffeine application. This protocol was repeated at 1 and 2Hz stimulation. Only myocytes that responded to the complete stimulus frequency range were included in the data set. Rapid caffeine application allows accurate quantification of SR [Ca^{2+}]. Data from such experiments can be used to compare SR Ca^{2+} release produced by caffeine application (pharmacological) and that produced by electrical stimulation.

4.2.2. Calibration of Fura-2 fluorescence ratio

Ideally, calibration should be calculated on each and every individual cell, however, due to time and technical constraints this is not always practical. A relatively quick and simple method to obtain approximate individual myocyte R_{min} (minimum fluorescence ratio) and R_{max} (maximum fluorescence ratio) values was used in these experiments. Isolated myocytes that had been quiescent for 4-8 hours were placed in the perfusion bath and Fura-2 fluorescence ratio was measured prior to commencing electrical stimulation. This value was taken as $R_{min,}$ assuming that after periods of quiescence the $[Ca^{2+}]_i$ within the myocyte had reduced to levels that cannot be distinguished from R_{min} using EGTA (Ca^{2+} buffer). Additional R_{min} values obtained by perfusing myocytes with a 10 EGTA solution ([Ca^{2+}] ~0.1nM) using either β-escin permeabilisation or microelectrode impalement techniques were not significantly different from the calculated resting R_{min}. Therefore, in this study resting fluorescence ratio could be confidently used as an accurate R_{min} value. After each experimental protocol had been carried out a maximum fluorescence ratio (R_{max}) was obtained by perfusing the cell with a high Ca^{2+} solution (in mM: 120 KCl,

20 Hepes, 10 $CaCl_2$, 1 $MgCl_2$, 10 Caffeine at pH 7.4). This produced a large Ca^{2+} influx resulting in instant hypercontraction of the myocyte i.e. without significant loss of any Fura-2 ratio signal via cell permeabilisation techniques. Intracellular calibration of Fura-2 was performed by another member of the laboratory on the set-up used in this study. Using a Fura-2 calibration curve a value for K_D was determined using data from a group of myocytes. The best fit for the data calculated a K_D of 1.64μM (1.64 ± 0.14 $x10^{-6}$ μM). Fluorescence ratios were converted to free $[Ca^{2+}]$ according to equation [1] (Grynkiewicz *et al.* 1985) using individual R_{min} and R_{max} values and the mean K_D.

$$Ca^{2+} = K_D \, x \left(\frac{R - R_{MIN}}{R_{MAX} - R} \right) \qquad [1]$$

It is unknown what $[Ca^{2+}]_i$ individual myocytes adopt after 4-8 hrs of quiescence (after dissociation from heart). Based on the sensitivity of Fura–2 for Ca^{2+}, cytosolic levels < 20nM would generate a Fura-2 fluorescence within 10% of R_{min}. Previous measurements from Bassani *et al.* (1995) suggest that after 2hrs of quiescence, $[Ca^{2+}]_i$ in rabbit myocytes is ~ 80nM, this would produce a Fura-2 ratio considerably above R_{min}. Therefore, it would appear that the longer period of quiescence in this study resulted in a $[Ca^{2+}]_i$ considerably less than 80nM.

A typical example of an experimental trace including R_{min} and R_{max} ratio values is seen in figure 4.1, panel A. Fura-2 fluorescence ratio values increase as stimulation frequency increases. Using the same experimental trace Fura –2 fluorescence ratio is converted into $[Ca^{2+}]_i$ (panel B) according to equation [1] (see Fura-2 calibration).

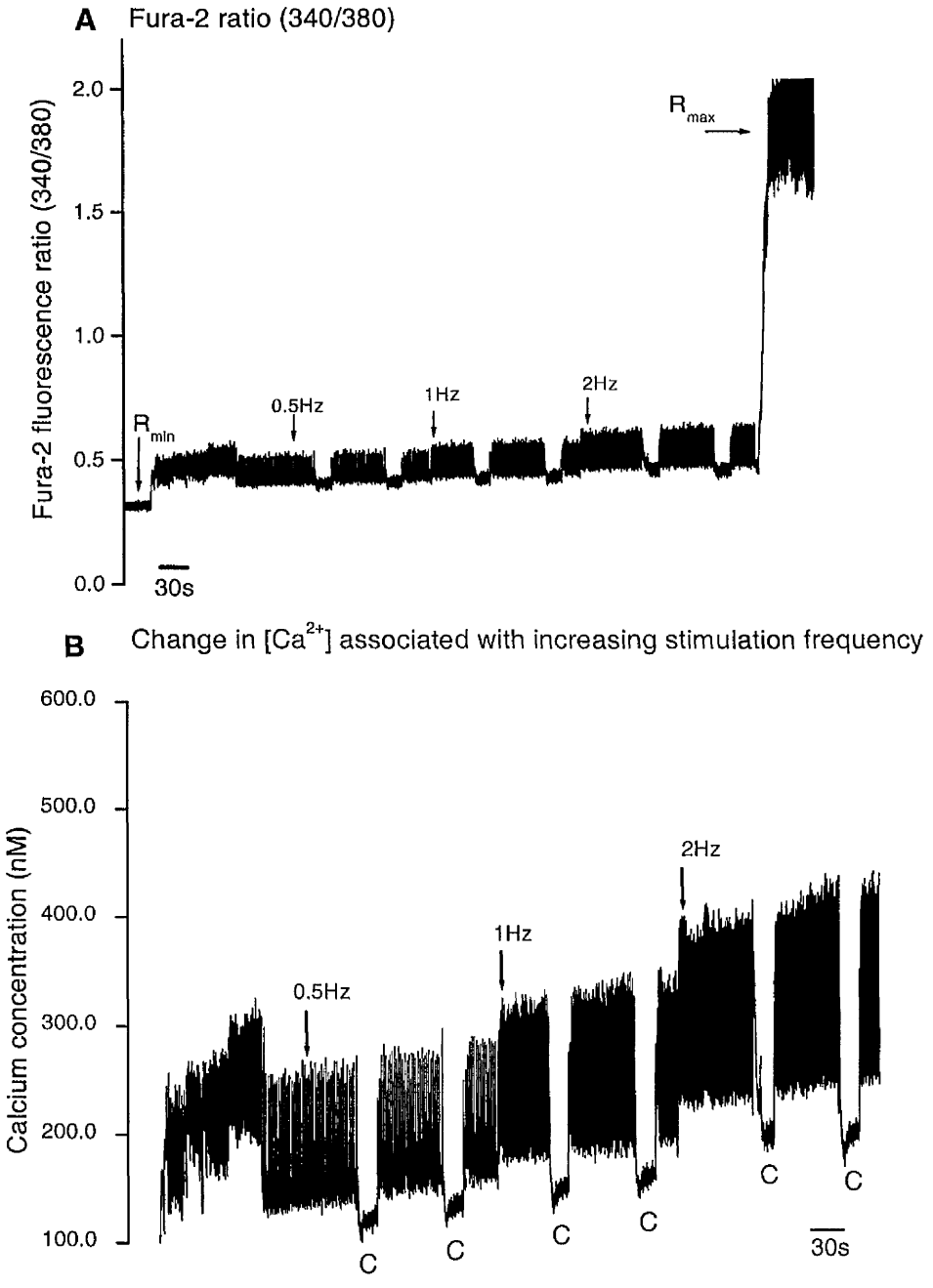

Figure 4.1. Typical experimental trace of Fura-2 fluorescence ratio (A) produced during complete frequency protocol: including Fura-2 ratio at 0.5, 1 & 2 Hz, R_{min} and R_{max} ratios. Changes in $[Ca^{2+}]_i$ associated with increasing stimulation frequency (B). Solid line represents 30s time scale. Gaps in trace B represent cessation of electrical stimulation during caffeine application (c). The amplitude and time-course of the steady state Ca^{2+} transients were analysed prior to caffeine application.

4.2.3. Data analysis

Diastolic and systolic fluorescent Fura-2 ratios were recorded by the software Chart program. The data was converted to Ca^{2+} values using R_{min} and R_{max} values from the experimental record and the previously measured K_D value (see 4.2.2). Diastolic $[Ca^{2+}]_i$ (resting) was measured at 0- 20ms post stimulation and peak systolic $[Ca^{2+}]_i$ was measured at the peak of the calcium transient. To increase the accuracy of the data and to ensure that steady state fluorescence had in fact been attained, diastolic and systolic $[Ca^{2+}]_i$ were averaged over two periods of stimulation (immediately prior to caffeine application). Two caffeine-induced peak systolic $[Ca^{2+}]_i$ values were also measured for each stimulus rate and each cell (figure 4.1).

4.2.3.1. Statistical analysis

All data are expressed as mean ± SEM. Unpaired t tests were used to compare two groups and ordinary ANOVA analysis was used to compare multiple groups. A value of $p < 0.05$ was considered statistically significant.

4.2.3.2. In vivo left ventricular echocardiographic parameters

Mean ejection fractions were 72.0 ± 1.3 and 45.5 ± 1.9% and LVEDD values were 17.8 ± 0.4mm and 19.45 ± 1.81mm for sham (n=12) and LVD (n=11) animals respectively. The above values were not statistically different from the mean EF and LVEDD values calculated for this whole study (table 2.1).

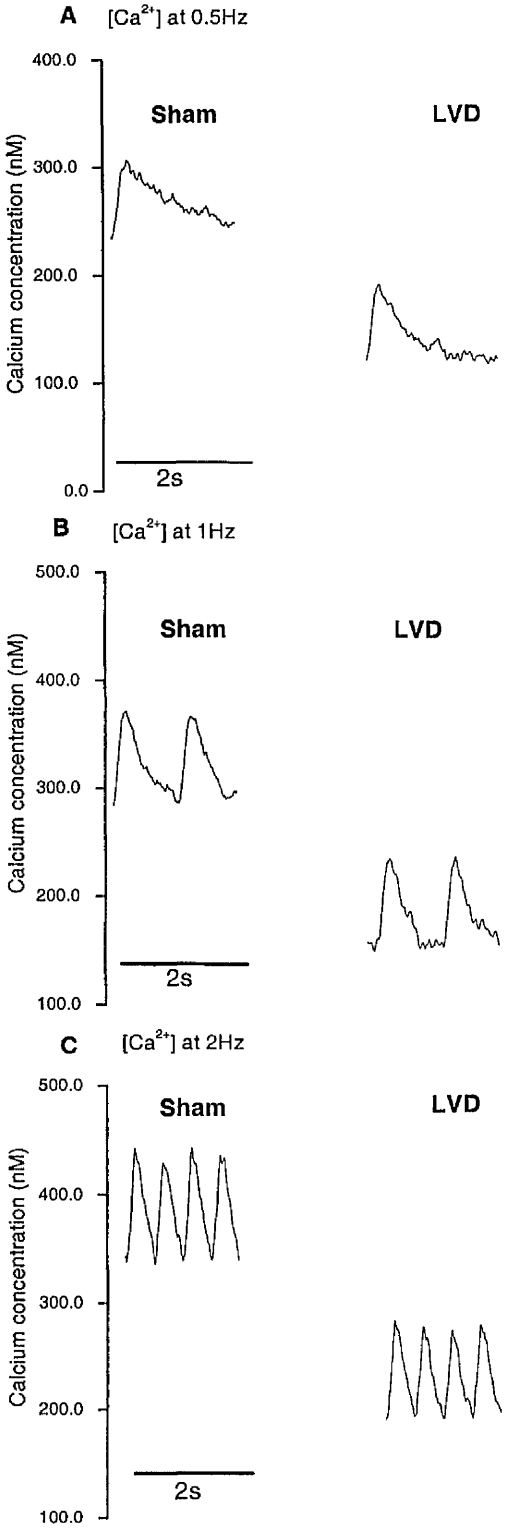

Figure 4.2. Typical examples of calcium transients recorded from sham and LVD epicardial myocytes. Records were produced from a range of stimulation frequencies; A:0.5, B:1 & C: 2Hz. Solid lines represent 2s time scale.

4.3. Transmural intracellular calcium measurements

Although previous intracellular [Ca^{2+}] has been measured in this model of LVD (McIntosh *et al.* 2000), the experiments performed in this study were undertaken using different experimental conditions and protocols. Most importantly, the experiments undertaken in the McIntosh study were performed on cardiac myocytes impaled with a micro-electrode.

Typical examples of calcium transients obtained from sham and LVD myocytes during electrical stimulation at 0.5, 1 and 2Hz are shown diagrammatically in figure 4.2. Note the increase in both diastolic and systolic $[Ca^{2+}]_i$ when stimulation frequency is increased.

4.3.1. Calcium measurements in Sham operated myocytes

End diastolic and peak systolic $[Ca^{2+}]_i$ were calculated from intracellular Ca^{2+} transients elicited by electrically induced stimulation at 0.5,1 & 2Hz.
Measurements of end diastolic $[Ca^{2+}]_i$ for sham endocardial and epicardial myocytes are shown in table 4.1, A. Increasing stimulation frequency from 0.5 to 1 to 2Hz produced an increase in end diastolic $[Ca^{2+}]_i$ in both sham endocardial and epicardial myocytes. At all stimulation frequencies sham endocardial end diastolic $[Ca^{2+}]_i$ was smaller than in epicardial myocytes although these differences were not statistically significant (table 4.1,A; ANOVA analysis).

Similar to the trend observed in end diastolic $[Ca^{2+}]_i$, sham endocardial and epicardial myocytes showed a frequency related increase in peak systolic $[Ca^{2+}]_i$ (figure 4.3;A). Throughout the frequency range applied endocardial peak systolic $[Ca^{2+}]_i$ was slightly lower than epicardial (endocardial range: 259.3 ± 24.2nM at 0.5 Hz to 505.8 ± 37.5nM at 2Hz; epicardial range: 272.6 ± 25.9nM at 0.5 Hz to 608.1 ± 83.9nM at 2Hz).

A	Sham endocardial			Sham epicardial		
Stimulation frequency (Hz)	**Mean diastolic Ca^{2+} (nM)**	**SEM**	**(n)**	**Mean diastolic Ca^{2+} (nM)**	**SEM**	**(n)**
0.5	139.0	15.5	(33)	164.5	18.5	(23)
1	183.5	16.2	(29)	240.3	22.0	(22)
2	300.7	26.0	(23)	370.0	45.5	(21)

B	LVD endocardial			LVD epicardial		
Stimulation frequency (Hz)	**Mean diastolic Ca^{2+} (nM)**	**SEM**	**(n)**	**Mean diastolic Ca^{2+} (nM)**	**SEM**	**(n)**
0.5	98.8	14.0	(25)	85.2 *	10.4	(29)
1	149.9	12.2	(20)	123.7 **	14.4	(29)
2	235.0	19.1	(24)	205.4 *	17.3	(24)

Table 4.1. Mean end diastolic $[Ca^{2+}]_i$ produced by electrical stimulation (0.5, 1 and 2Hz) for sham (A) and LVD (B) endocardial and epicardial myocytes Data shown are mean ± SEM. (n) indicates number of myocytes. Hearts used equals sham endo; 11, sham epi 10; LVD endo 9; LVD epi 10. *denotes statistical significance in comparison to sham data (* $p<0.01$, ** $p<0.001$).

4.3.2. Calcium measurements in LVD myocytes

Similar to the results observed in the sham data, increasing stimulation frequency from 0.5 to 2 Hz produced an increase in end diastolic and peak systolic $[Ca^{2+}]_i$ in both endocardial and epicardial LVD myocytes. At all stimulation frequencies LVD endocardial end diastolic $[Ca^{2+}]_i$ had a tendency to be higher than epicardial end diastolic $[Ca^{2+}]_i$ (table 4.1,B) although this did not reach statistical significance. Peak systolic $[Ca^{2+}]_i$ rose as stimulation frequency increased and the transmural difference remained, i.e. endocardial $[Ca^{2+}]_i$ was higher than epicardial. Endocardial peak systolic $[Ca^{2+}]_i$ ranged from 233.2 ± 19.8 to 448 ± 36.7nM and epicardial peak systolic $[Ca^{2+}]_i$ ranged from 188.8 ± 18.7 to 360 ± 30.1nM (figure 4.3,B). None of these results were statistically different (ANOVA). In contrast to the sham data, LVD endocardial end diastolic and peak systolic $[Ca^{2+}]_i$ were higher than epicardial. This suggests that the normal transmural differences in end diastolic and peak systolic $[Ca^{2+}]_i$ were reversed in LVD.

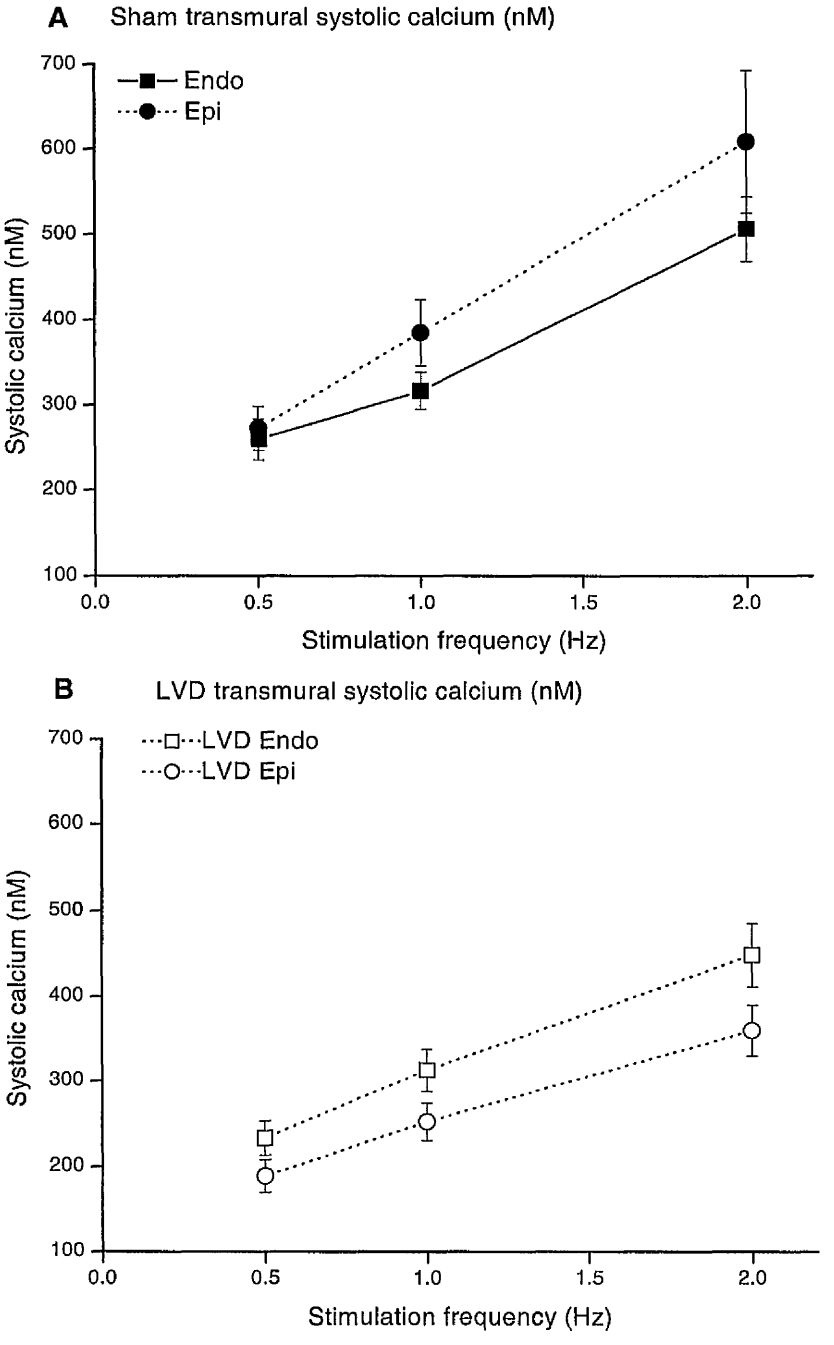

Figure 4.3. Transmural (endocardial/epicardial) changes in peak systolic $[Ca^{2+}]_i$ (nM) associated with increasing electrical stimulation frequency (0.5 to 1 to 2Hz) in sham (A) and LVD (B) myocytes. Data are mean ± SEM.

4.3.3. Comparisons between Sham and LVD $[Ca^{2+}]_i$

4.3.3.1. Endocardial comparisons

A marked difference between Sham and LVD endocardial end diastolic $[Ca^{2+}]_i$ was present at all stimulation rates although this was not statistically significant (table 4.1; A, B). Comparisons between sham and LVD endocardial peak systolic $[Ca^{2+}]_i$ are shown in figure 4.4 (A) where minimal differences were observed.

4.3.3.2. Epicardial comparisons

In marked contrast to the endocardial data, there was a significant difference between sham and LVD epicardial end diastolic and peak systolic $[Ca^{2+}]_i$. End diastolic $[Ca^{2+}]_i$ was significantly lower in LVD epicardial myocytes in comparison to sham at all three stimulation frequencies ($p<0.01$, $p<0.001$, $p<0.01$ at 0.5, 1 and 2 Hz respectively; see tables 4.1., A & B). Similarly, LVD epicardial peak systolic $[Ca^{2+}]_i$ was significantly lower than sham at all stimulation frequencies (figure 4.4, ANOVA, $p<0.05$ at 0.5, 1Hz & 2Hz).

In general, end diastolic and peak systolic $[Ca^{2+}]_i$ are lower in the LVD group (epicardial myocytes particularly) than sham myocytes.

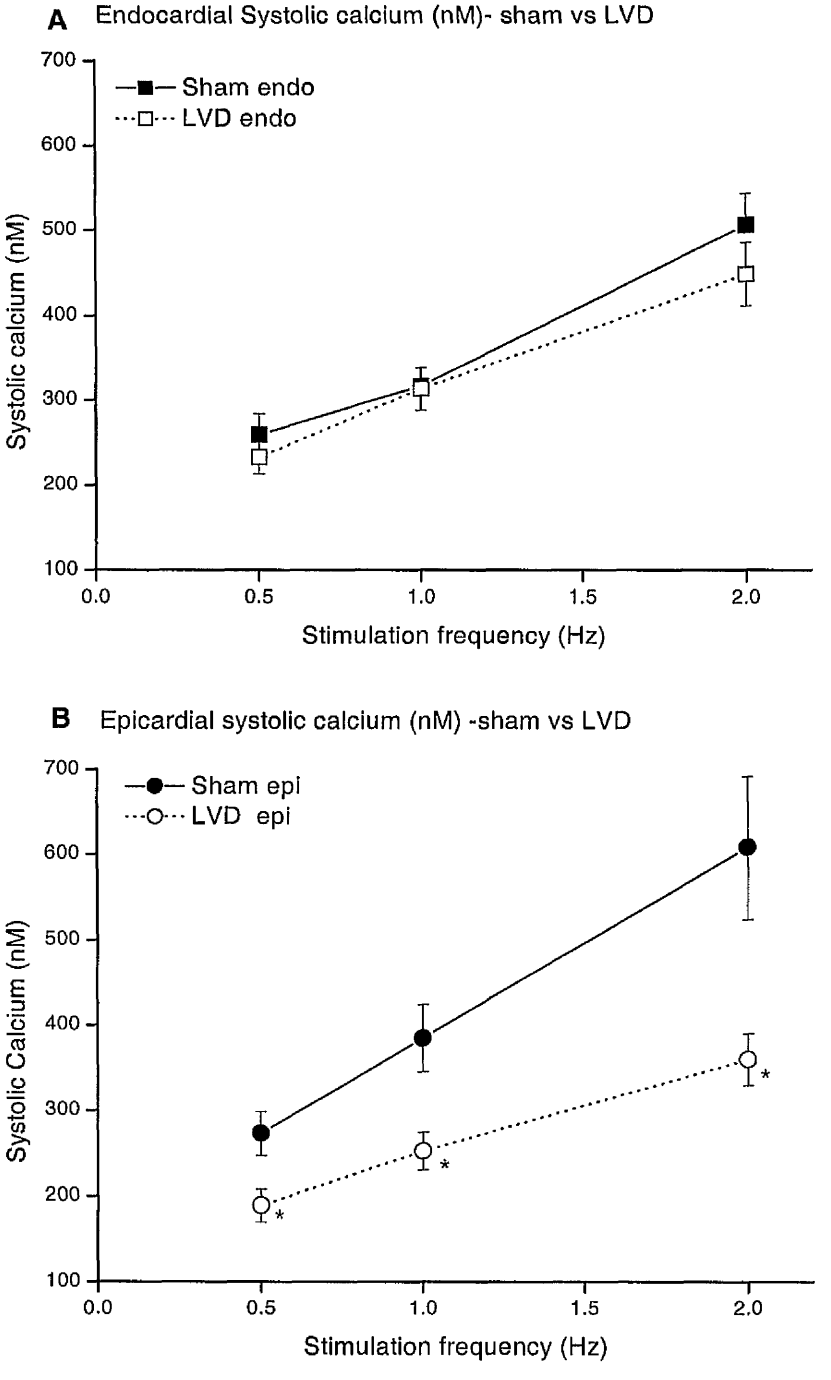

Figure 4.4. Comparisons between Sham and LVD endocardial (A) and epicardial (B) peak systolic $[Ca^{2+}]_i$ produced by electrical stimulation (0.5,1 & 2Hz). * indicates statistical significance of $p<0.05$.

4.4. Caffeine induced Ca^{2+} transients

4.4.1. Background

Caffeine binds to a specific site on the cytosolic side of the ryanodine receptor (RyR) and increases the open probability of the calcium-activated calcium release channel (RyR) without altering the duration of open events (Sitsapesan & Williams, 1990). Rapid caffeine exposure at millimolar concentrations is thought to induce complete release of SR Ca^{2+} and is often used to assay total SR Ca^{2+} content (Bers, 1987; Varro *et al.* 1993).

Briefly, in this study, steady state systolic $[Ca^{2+}]_i$ was attained at the desired electrically stimulated frequency (0.5,1 & 2Hz). Electrical stimulation was ceased and 20mM caffeine (5s) was applied, 15s later electrical stimulation was recommenced for 1 min and a second caffeine pulse was applied. Typical examples of calcium transients produced by electrical stimulation (0.5, 1 & 2Hz) and those produced by the application of caffeine (20mM) after stopping stimulation are shown in figure 4.5. This figure also shows that the peak amplitude of the caffeine induced transient is comparable to transients produced by electrical stimulation. These results are in line with previously published caffeine experiments (Frampton *et al.* 1990). Prolonged duration of caffeine induced transients are observed in caffeine experiments. This phenomenon is thought to reflect the inability of SERCA to resequester Ca^{2+} into the SR due to the increased open probability of ryanodine receptors (Bers, 2000) and continuous release of SR Ca^{2+} during caffeine application. As the rate constant of NCX to remove Ca^{2+} from the cytosol is less than SERCA (Bassani *et al.*1994), the Ca^{2+} transient in caffeine is slower to decay.

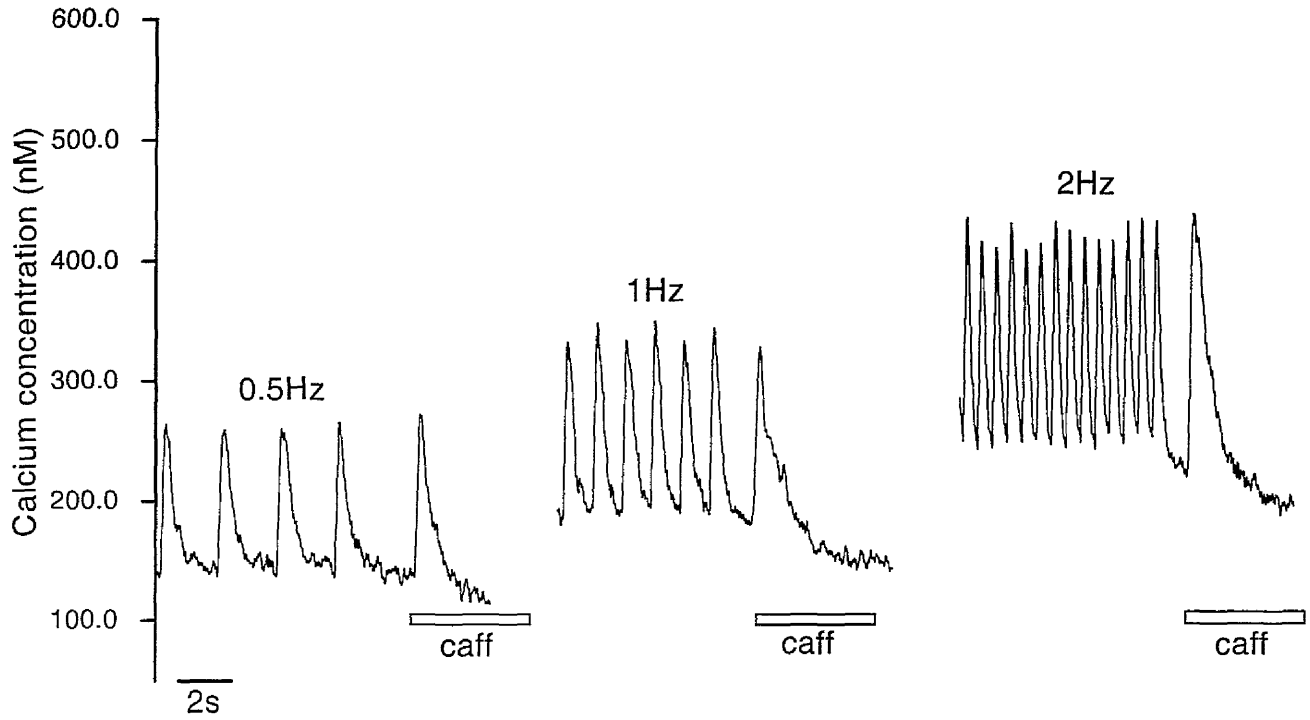

Figure 4.5. Typical example of calcium transients produced by electrical stimulation (0.5,1&2 Hz) and on the application of caffeine after stopping stimulation. Open bars represent caffeine application (5s).

4.4.2. Transmural differences in caffeine induced calcium transients

Increasing stimulation frequency leads to an increase in SR $[Ca^{2+}]$ content, and consequently a larger peak systolic $[Ca^{2+}]_i$. It follows that caffeine-induced Ca^{2+} transients associated with increasing stimulation frequencies would reflect this increase and would also produce a larger systolic $[Ca^{2+}]_i$ (Frampton *et al.* 1991).
As caffeine application assesses SR Ca^{2+}content, only peak systolic $[Ca^{2+}]_i$ results are detailed here. Similar to the trends observed in electrically elicited Ca^{2+} transients, a very similar frequency-dependent pattern in caffeine-induced transients was observed in both sham and LVD data sets.

Caffeine application produced peak systolic $[Ca^{2+}]_i$ ranging from 270.9 ± 30.0 at 0.5Hz to 464.6 ± 45.9 nM at 2Hz (sham; endocardial) and from 311.8 ± 35.3 to 691.1 ± 121.3nM respectively in sham epicardial myocytes (figure 4.6,A). The normal sham transmural difference observed in electrically stimulated myocytes (i.e. higher epicardial peak systolic $[Ca^{2+}]_i$ than endocardial) was maintained in caffeine induced transients. LVD endocardial peak systolic $[Ca^{2+}]_i$ ranged from 253.5 ± 19.8 (0.5Hz) to 452.5 ± 34.3nM (2Hz) and from 206.6 ± 21.2 (0.5Hz) to 361.5 ± 31.9nM (2Hz) in the epicardial data (figure 4.6,B). Again, the normal transmural difference observed in the sham data was not maintained in LVD as endocardial peak systolic $[Ca^{2+}]_i$ was higher than epicardial (figure 4.6). These LVD caffeine results are similar to those produced by electrical stimulation of LVD myocytes (figure 4.3).

4.4.3. Comparisons between Sham and LVD caffeine induced $[Ca^{2+}]_i$

Caffeine induced peak systolic $[Ca^{2+}]_i$ in endocardial sham and LVD myocytes were almost identical (figure 4.7,A). In contrast, there was a significant difference between sham and LVD epicardial peak systolic $[Ca^{2+}]_i$ at 0.5 ($p<0.05$), 1 & 2Hz ($p<0.01$) (figure 4.7,B). These results follow the same trend as the sham:LVD peak systolic $[Ca^{2+}]_i$ comparisons observed during electrical stimulation (figure 4.4).

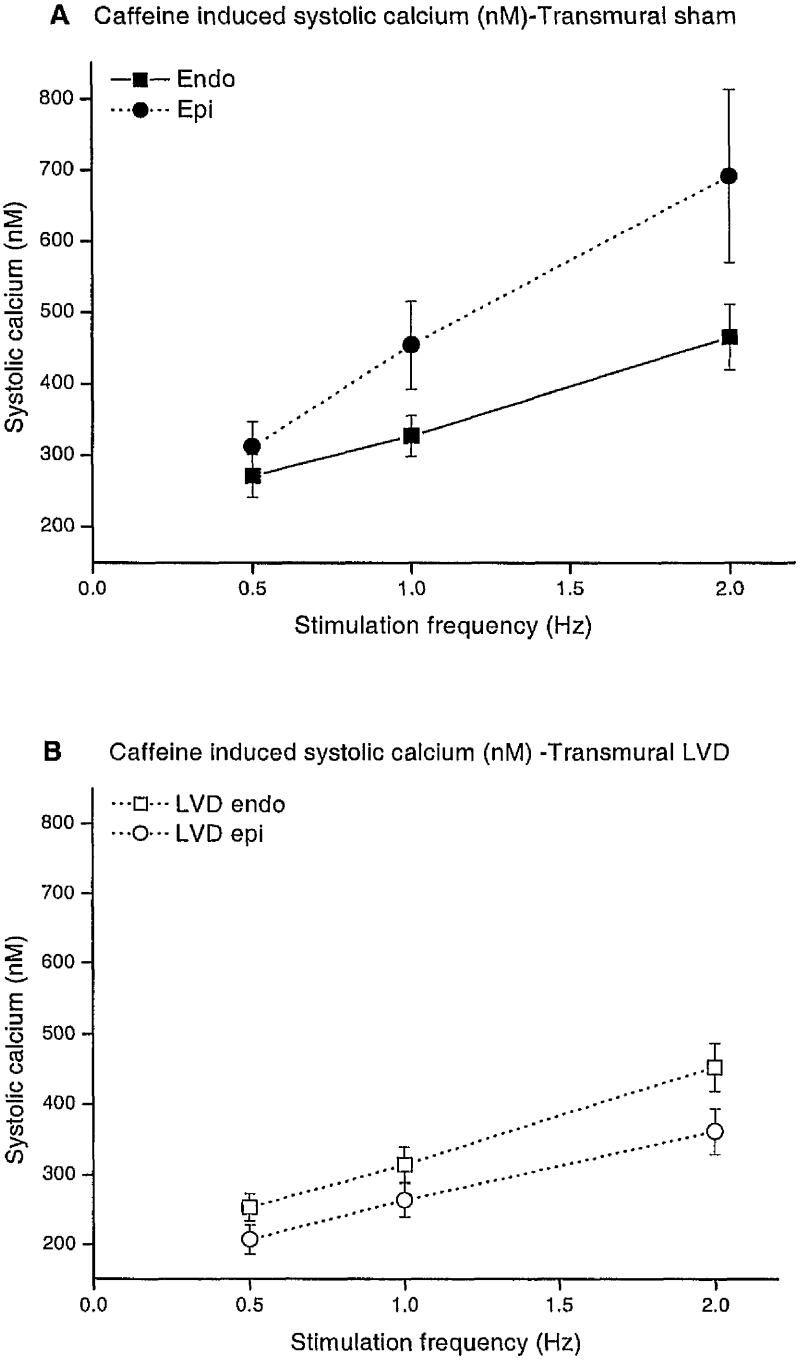

Figure 4.6. Effect of caffeine (20mM) on transmural peak systolic $[Ca^{2+}]_i$ (nM) following cessation of electrical stimulation at 0.5, 1 and 2Hz. Sham endo n=22,17, 15 and epi n=18,14,11. LVD endo n=27,26,21 and epi n=20,20,20 for 0.5, 1 and 2 Hz respectively. n= number of myocytes.

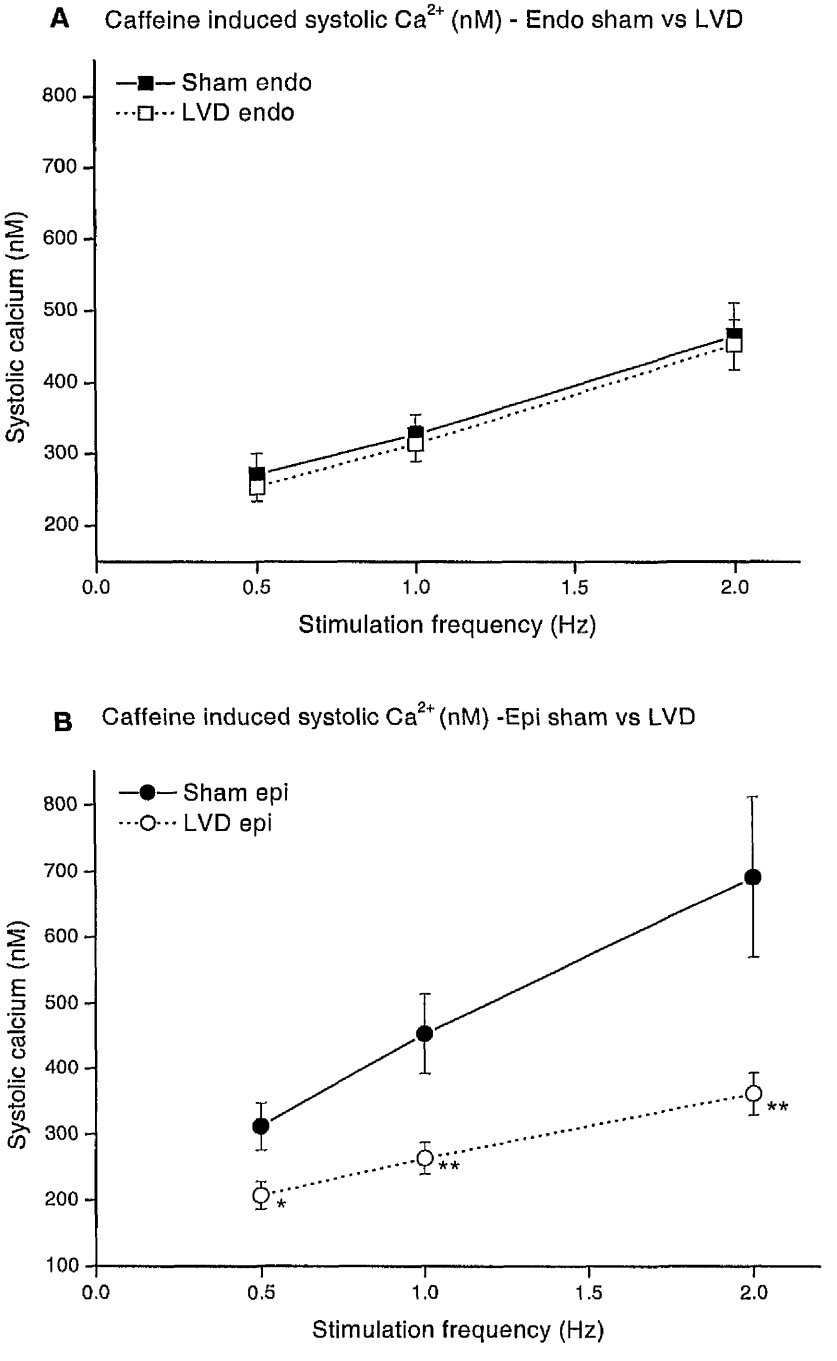

Figure 4.7. Sham and LVD comparisons of caffeine (20mM) induced systolic $[Ca^{2+}]_i$ (nM) following cessation of electrical stimulation (0.5, 1 and 2Hz). * indicates $p<0.05$, ** indicates $p<0.01$.

4.5. Discussion

4.5.1. Transmural differences in Ca^{2+} transients

In all sham myocytes, end diastolic and peak systolic $[Ca^{2+}]_i$ increased as stimulation frequency increased and no significant transmural differences in either parameter were observed, although epicardial $[Ca^{2+}]_i$ had a tendency to be higher than endocardial. Similar to sham myocytes, end diastolic and peak systolic $[Ca^{2+}]_i$ in LVD myocytes increased as stimulation frequency increased. In contrast to the sham data, LVD endocardial end diastolic and peak systolic $[Ca^{2+}]_i$ were higher than epicardial, although these differences were not significant. Therefore, the transmural difference in end diastolic and peak systolic $[Ca^{2+}]_i$ observed in sham was not maintained in LVD. These transmural differences may be due to either alterations in Ca^{2+} handling protein expression which subsequently affects SR Ca^{2+}content (see chapter 7) or to differences in SR Ca^{2+} release mechanisms.

4.5.2. Comparisons between sham and LVD Ca^{2+} transients

End diastolic and peak systolic $[Ca^{2+}]_i$ were similar in both sham and LVD endocardial myocytes, although there was a tendency for sham values to be marginally higher than LVD (figure 4.4). These diastolic results are similar to those published by McIntosh *et al.* (2000), who observed similar end diastolic values between moderate (EF $\geq$ 45%), severe failure (EF $\leq$ 45%) and sham operated animals. In contrast, McIntosh *et al.* observed higher endocardial systolic $[Ca^{2+}]_i$ in severely failing LVD myocytes in comparison to sham but no difference in systolic $[Ca^{2+}]_i$ was observed in the moderately failing myocytes. The reason for the differences in LVD endocardial systolic $[Ca^{2+}]_i$ between this and the McIntosh study may be due to differences between mean ejection fraction. A significant difference between EF values was observed between the severe LVD data (McIntosh *et al.* 2000) and the mean EF observed in this study ($p<0.05$). Furthermore, no significant difference in mean LVEDD values were observed between the two studies. No significant differences were observed in the echocardiographic data between the moderately failing myocytes (McIntosh study) and this study. This result suggests that the degree of change in systolic $[Ca^{2+}]_i$ may be linked to the severity of the failure (as assessed by EF). LVD epicardial end diastolic and peak systolic $[Ca^{2+}]_i$

were significantly smaller than sham epicardial values. These data are in agreement with the McIntosh study, although the diastolic differences are less distinct.

LVD endocardial myocytes displayed a trend to smaller peak systolic $[Ca^{2+}]_i$ in comparison to sham endocardial myocytes (not significant). LVD epicardial peak systolic $[Ca^{2+}]_i$ was significantly smaller at all three stimulation frequencies ($p<0.05$). These results are in line with previously published data on failing hearts (Siri *et al.*, 1991; Beuckelmann *et al.*, 1992;) and are consistent with reports of disruption of intracellular Ca^{2+} handling mechanisms in failing myocardium. Such disruption may be due to alterations in the expression of cardiac myocyte Ca^{2+} handling proteins. It appears that alterations of intracellular Ca^{2+} handling mechanisms has occurred in both LVD endocardial and epicardial myocytes, leading to a reduced end diastolic and peak systolic $[Ca^{2+}]_i$. As LVD epicardial peak systolic $[Ca^{2+}]_i$ is significantly reduced in comparison to endocardial this suggests that heterogeneous changes in Ca^{2+} handling mechanisms occurred across the left ventricle in LVD, i.e. greater changes in LVD epicardial Ca^{2+} handling mechanisms have occurred in comparison to endocardial. One possible factor that may be responsible for the transmural pattern of disruption of intracellular Ca^{2+} handling is that alterations in the expression and/or activity of intracellular Ca^{2+} handling proteins are heterogeneous in LVD myocytes (see chapter 7 and general discussion).

4.5.3. Transmural caffeine induced Ca^{2+} transients

Caffeine-induced Ca^{2+} transients demonstrate an almost identical trend in changes to peak systolic $[Ca^{2+}]_i$ as Ca^{2+} transients elicited by electrical stimulation, i.e. increasing peak systolic $[Ca^{2+}]_i$ as stimulation frequency increases. In normal sham myocytes epicardial peak systolic $[Ca^{2+}]_i$ had a tendency to be higher than endocardial, although this did not reach statistical significance. In contrast, LVD endocardial peak systolic $[Ca^{2+}]_i$ was higher than epicardial. Therefore, the normal transmural difference in caffeine induced peak systolic $[Ca^{2+}]_i$ was not maintained in LVD (figure 4.6). Larger peak systolic $[Ca^{2+}]_i$ are normally associated with a larger SR Ca^{2+} store suggesting that sham Epi and LVD endocardial myocytes have either a larger SR Ca^{2+} storage capacity or that the effect of caffeine application on SR Ca^{2+} release is greater in these myocytes. As the transmural trends in peak systolic $[Ca^{2+}]_i$ are similar for electrically stimulated and caffeine induced transients, this implies that the larger Ca^{2+} transients elicited by sham Epi and LVD endocardial myocytes

occur due to a higher SR Ca^{2+} content rather than these myocytes being differentially affected by caffeine application.

4.5.4. Comparisons between sham and LVD caffeine induced Ca^{2+} transients

Caffeine-induced peak systolic $[Ca^{2+}]_i$ in endocardial myocytes are virtually the same in sham and LVD (figure 4.7) and these results are similar to those observed in the electrically elicited Ca^{2+} transient data (figure 4.4,A). In contrast, there was a significant decrease in LVD epicardial peak systolic $[Ca^{2+}]_i$ at all stimulation frequencies in comparison to the sham data (figure 4.7,B). Again, these sham/LVD differences were present in the electrically elicited peak systolic $[Ca^{2+}]_i$ transient data (figure 4.4,B).

Comparisons between sham and LVD peak systolic $[Ca^{2+}]_i$ induced by caffeine application showed almost identical trends in peak systolic $[Ca^{2+}]_i$ as those elicited by electrical stimulation. As these results are similar it suggests that the significant differences observed between sham and LVD epicardial myocytes are a function of the myocytes themselves rather than the affect of caffeine application. As discussed earlier, the most likely explanation is that heterogeneous changes in Ca^{2+} handling mechanisms have occurred in LVD, and that these changes are greater in LVD epicardial myocytes.

4.6. Summary

In summary, a small transmural difference in diastolic and peak systolic $[Ca^{2+}]_i$ exists in sham myocytes, where $[Ca^{2+}]_i$ was slightly higher in epicardial in comparison to endocardial myocytes. This difference was reversed in LVD myocytes (endocardial higher than epicardial). Comparisons between sham and LVD showed overall lower diastolic and peak systolic $[Ca^{2+}]_i$ at all stimulation frequencies in the LVD data, reaching statistical significance in the epicardial data set. Both sham and LVD endocardial myocytes have similar diastolic and systolic $[Ca^{2+}]_i$ although there is a tendency for lower values in the LVD data. In contrast, LVD epicardial myocytes have a significantly lower diastolic and systolic $[Ca^{2+}]_i$ in comparison to sham. This may reflect greater alterations in intracellular Ca^{2+} handling mechanisms in epicardial in comparison to endocardial LVD myocytes.

Caffeine-induced calcium transients showed the same trend as electrically induced calcium transients, i.e. increasing peak systolic $[Ca^{2+}]_i$ as stimulation frequency increased. Similar to the electrically induced Ca^{2+} transients, the LVD data showed overall lower peak systolic $[Ca^{2+}]_i$ in comparison to the sham data. LVD endocardial peak systolic $[Ca^{2+}]_i$ induced by caffeine was similar to sham whereas epicardial values were significantly lower.

Caffeine is used as an indicator of SR Ca^{2+} content and the data suggest sham and LVD endocardial SR Ca^{2+} content was similar whereas LVD epicardial content was significantly lower than sham.

Ratiometric differences between electrical and caffeine induced peak systolic (PS) $[Ca^{2+}]$ (table 4.2) revealed no significant differences between endocardial and epicardial myocytes within experimental groups and between sham:LVD data sets. This data indicates that fractional release of SR Ca^{2+} is similar irrespective of the mode of release (electrical or caffeine).

	ES PS Ca /Caff PS Ca	**Number of myocytes**
Sham Endo	0.99 ± 0.02	17
Sham Epi	0.94 ± 0.02	14
LVD Endo	0.99 ± 0.02	26
LVD Epi	0.97 ± 0.02	20

Table 4.2. Ratio of electrically stimulated peak systolic Ca^{2+} (ES PS Ca) to caffeine induced peak systolic Ca^{2+} (Caff PS CA) in Sham and LVD endocardial and epicardial myocytes at 1Hz. ANOVA analysis revealed no statistical differences between any of the data sets ($p>0.05$).

Chapter 5

Assessment of protein retrieval from cardiac homogenates

5.1. Background

This biochemical study was performed to assess protein content and the efficiency of protein retrieval from homogenates of rabbit left ventricular myocardium and crude sarcoplasmic reticulum (SR) preparations derived from these samples. Left ventricular muscle samples were obtained from control (sham operated) hearts and those with left ventricular dysfunction (LVD). This study was also performed to compare homogenate and SR protein content between sham and LVD ventricular samples.

5.2. Methods

Initially, samples for protein assessment were prepared as described in the general methods section (2.3.1) and stored in ice cold Ringer solution until use. Total protein content (mg ml^{-1}) was assayed for homogenate and SR samples using the method described in 2.3.2 (chapter 2). Coomassie staining methods are described in section 2.3.4.1 (chapter 2).

5.2.1. Homogenate tissue samples for protein retrieval assessment

Transmural tissue sections of various weights (60, 125, 250, 500, 1000mg) were dissected from the left ventricular free wall, blotted to remove excess Ringer solution (prevents overestimation of actual wet tissue weight) and resuspended in 10 volumes of ice cold homogenisation buffer (see methods). Tissue samples were finely chopped with scissors and then homogenised for approximately 1 minute or until no tissue pieces were visible using either the Kimematica homogeniser for the large samples or the ultra-turrax T_8 (IKA Labortechnik) for the smaller samples. From each of these homogenate suspensions, 100µl was removed and frozen for future total protein analysis (total protein homogenate). Homogenate samples did not undergo any centrifugation therefore contained all ventricular proteins.

5.2.2. Crude SR vesicles for protein retrieval assessment

Crude SR vesicles were prepared from homogenate samples (1000, 500, 250 and 125mg). The protocol detailed in figure 5.1 is based upon the isolation technique by Chamberlain *et al.* (1983). All crude SR vesicle samples were used to calculate total SR protein content derived from wet weight homogenate samples of 1000, 500, 250 and 125 mg.

The following solutions were used in the preparation of SR vesicles:

Precipitation buffer contained in mM: 300 Sucrose, 600 KCl, 20 Histidine, 10 Imidazole, 1 DTT, and protease inhibitors; Leupeptin 5mg ml^{-1}, Aprotinin 10mg ml^{-1} at pH 7.2

Assay buffer contained in mM: 50 Tris base, 15 $MgCl_2$, 0.1 EGTA (Ethylene glycolbis (β-aminoethyl ether) N,N,N,N'- tetraacetic acid, 1 DTT and protease inhibitors; Leupeptin 5mg ml^{-1}, Aprotinin 10mg ml^{-1} at pH 7.4

5.2.3. Statistical analysis

All data are expressed as mean ± SEM. Statistical analysis was performed using student *t* test and linear regression analysis. Results were considered significant at $p<0.05$.

5.2.4. In vivo left ventricular echocardiographic parameters

Mean ejection fractions were 51.4 ± 1.61 and 40.9 ± 0.41% for moderate (n=13) and severe (n=9) LVD groups respectively with a combined mean of 47.1 ± 1.5% for the LVD group. Mean sham ejection fraction was 72.7 ± 1.9% (n=10). Mean LVEDD values were 21 ± 0.39 and 21.9 ± 0.33mm for moderate and severe LVD groups. The combined LVD group LVEDD was 21. 4 ± 0.3 and sham values were 17.7 ± 0.3mm.The above values were not statistically different from the mean EF and LVEDD values calculated for this whole study (table 2.1).

Isolation of crude SR vesicles

The SR preparation protocol is shown diagrammatically below (figure 5.1).

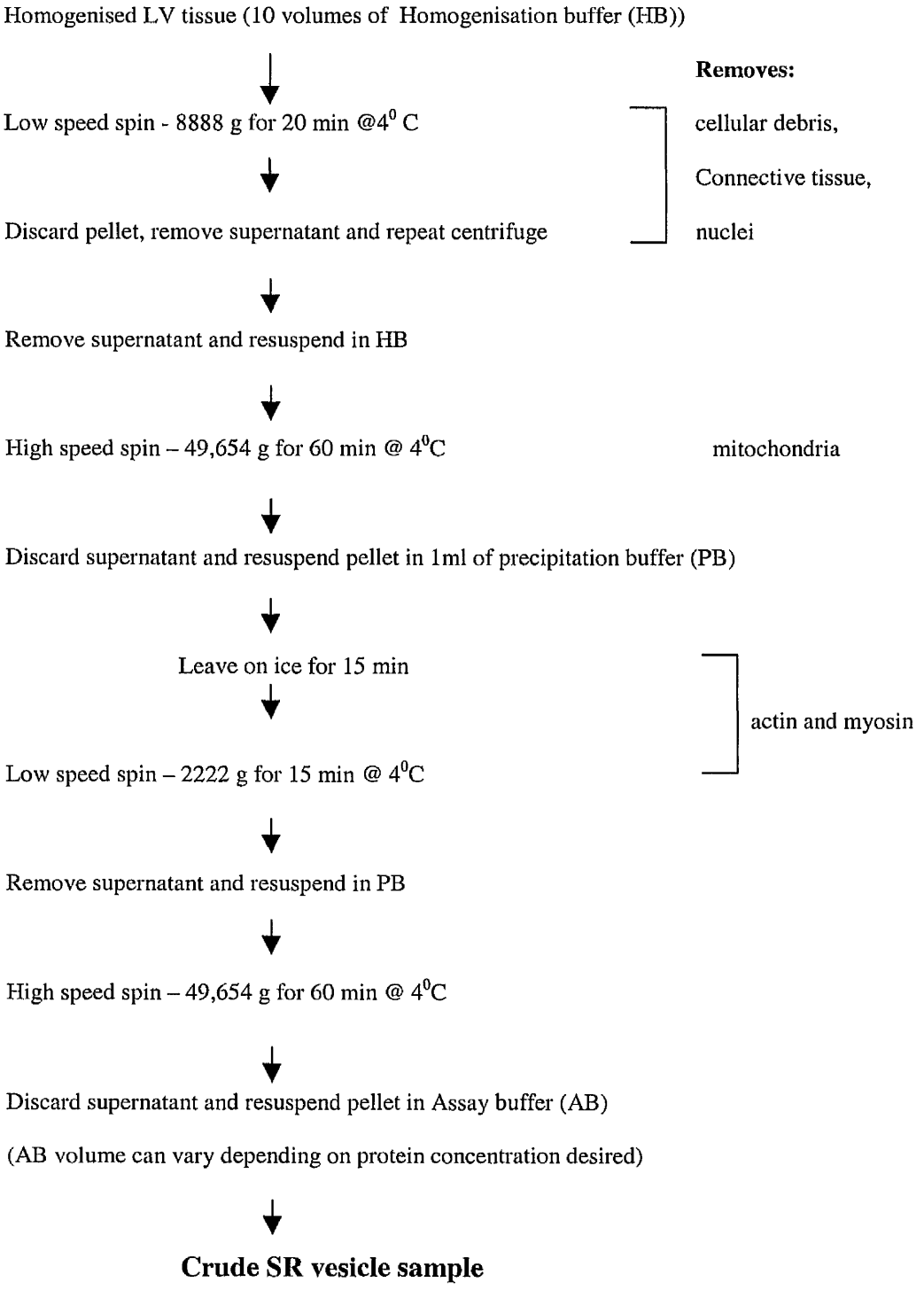

Figure 5.1. Flow diagram of SR vesicle preparation protocol

5.3. Homogenate verses SR total protein content

To assess the differences in protein content between homogenate and SR preparations, samples were subjected to gel electrophoresis and subsequent Coomassie staining. See general methods for protocol (chapter 2). A typical example of a Coomassie stained gel (figure 5.2) shows that overall, homogenate samples cover a large molecular weight range (25 to 200kDa) and have an abundance of proteins. In comparison, SR vesicle preparations possess fewer proteins overall and protein bands specific for SR proteins are more clearly defined. A lower protein density would be expected in SR preparations as these samples have undergone several centrifugal steps in order to remove excess cellular proteins such as connective tissue, actin and myosin and organelles such as mitochondria (figure 5.1).

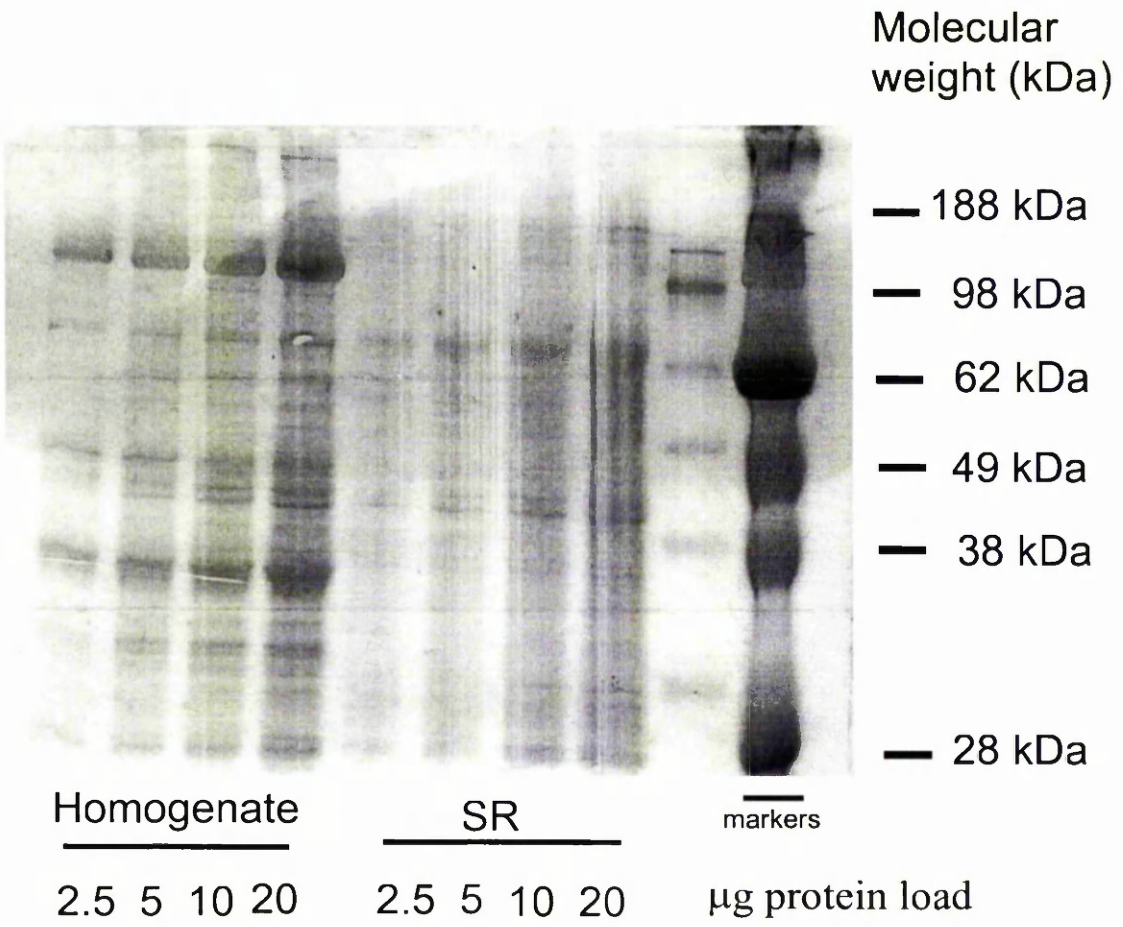

Figure 5.2. Typical example of a Coomassie stained Tris-glycine gel showing increasing protein loads (2.5 – 20 µg) of homogenate and SR samples. Molecular weight markers (kDa) are indicated with solid lines on the right hand side of the gel.

5.4. Homogenate protein retrieval and quantification

Left ventricular tissue samples weighing 60, 125, 250, 500 and 1000mg were isolated and analysed to determine whether homogenate protein retrieval was comparable when calculated from a range of tissue wet weights. In all experimental groups a linear increase in absolute protein homogenate retrieval (mg) was observed as tissue sample size increased from 60 to 1000mg (figure 5.3). This relationship was confirmed statistically by linear regression analysis and produced slopes of $0.10 \pm 6.4x10^{-4}$, $0.10 \pm 7.43x10^{-4}$, and 0.09 ± 0.002, for sham, moderate LVD and severe LVD groups respectively (values are mean ± SEM). Analysis showed that no statistically significant difference in protein retrieval throughout the range of tissue weights (60 to 1000mg) and between the three experimental groups (sham, moderate and severe LVD) was present. As no significant difference in protein retrieval was apparent between moderate and severe LVD samples (figure 5.3), data from these two groups were pooled and hereafter classed together as the LVD group.

Protein retrieval was also expressed per total homogenate protein (mg/g) and throughout the weight ranges and between groups no statistical differences were apparent (table 5.1). Total protein values in table 5.1 have been standardised to mg of protein retrieved per 1g of wet tissue weight.

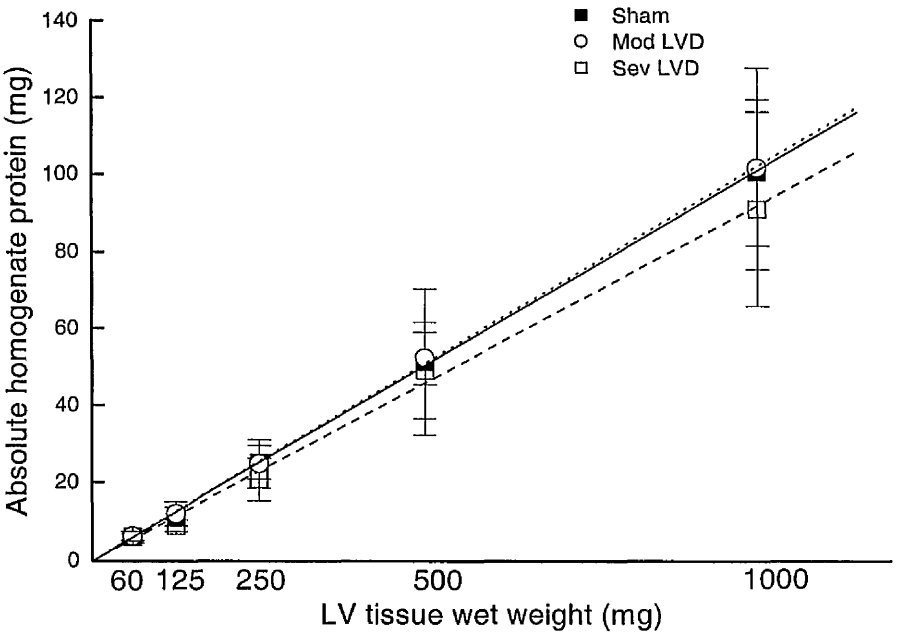

Figure 5.3. Absolute homogenate protein (mg) retrieved from various left ventricular tissue weights (mg) isolated from 3 experimental groups: sham, moderate and severe LVD. Slope data are expressed as mean ± SEM. Statistical analysis produced r values of 0.9, 0.99 and 0.99 for sham, moderate and severe LVD groups respectively and p values of <0.001 (all 3 experimental groups). n numbers as per table 5.1.

		Left ventricular wet weight (mg)				
		60	125	250	500	1000
Total Homogenate protein (mg/g)	Sham	103.2 ± 13 (n = 4)	91.2 ± 19 (n =8)	100.7 ± 15 (n =8)	102.5 ± 38 (n =8)	100.5 ± 19 (n =11)
	LVD	102.8 ± 23 (n = 12)	87.2 ± 23 (n = 11)	92.3 ± 24 (n =14)	98.9 ± 21 (n = 19)	97.6 ± 26 (n = 19)

Table 5.1. Total homogenate protein retrieved (mg/g) per left ventricular wet weight sample (mg) in sham operated and LVD rabbit hearts. Data are expressed as mean ± SD. n =indicates number of hearts.

These data suggest that homogenate protein retrieval via this protocol is reproducible even when using a broad range of tissue weights and that there were no significant differences in protein retrieval between sham and LVD preparations.

5.5. SR protein retrieval and quantification

All crude SR vesicles were isolated from homogenate samples of 125, 250, 500 and 1000mg as described in figure 5.1. Absolute SR protein retrieval showed a linear increase as tissue wet weight was increased from 125 to 1000mg (figure 5.4). This relationship was confirmed by linear regression analysis which produced slopes of $6.8 \pm 0.2 \times 10^{-4}$, $8.6 \pm 0.4 \times 10^{-4}$, and $7.2 \pm 0.3 \times 10^{-4}$, for sham, moderate LVD and severe LVD groups respectively (data are mean ± SEM). Again, no statistical differences in protein retrieval were observed between moderate and severe LVD preparations therefore the data were pooled and classed hereafter as the LVD group. The linear regression lines were fixed through zero, and it can be seen that the absolute protein content at 125 mg (all experimental groups) was less than the predicted value (figure 5.4).

Expressing SR protein retrieval in mg/g, showed no significant differences in the efficiency of protein retrieval in SR preparations isolated from samples weighing 250, 500, and 1000mg in both sham and LVD preparations. However, as seen in Table 5.2 and figure 5.4, SR protein retrieval from 125mg of both sham and LVD tissue samples was noticeably lower in comparison to the larger tissue samples although these values did not reach statistical significance.

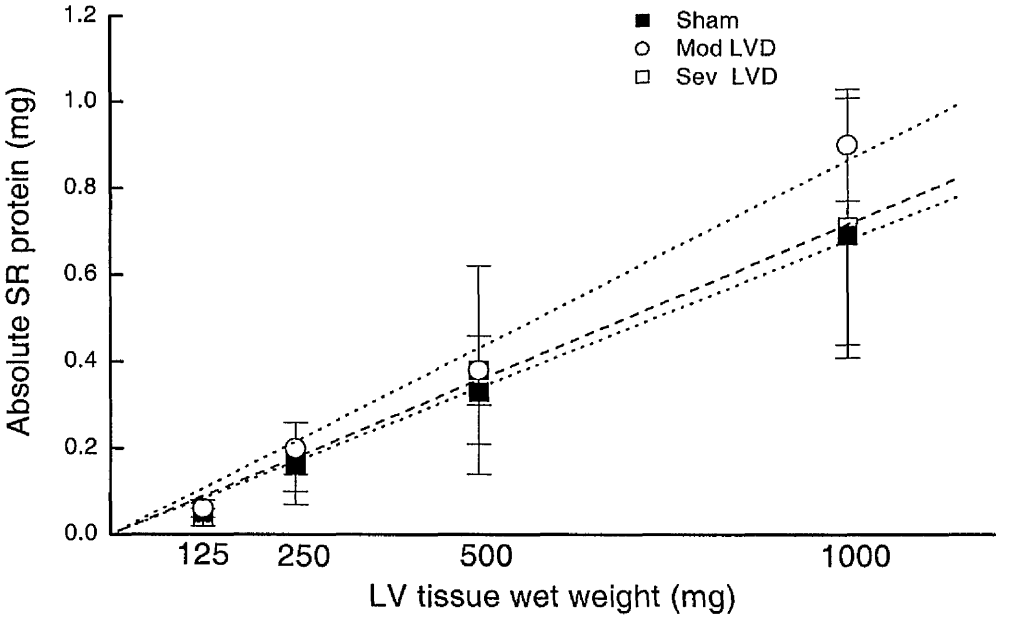

Figure 5.4. Absolute SR protein retrieved (mg) from various left ventricular tissue weights (mg) isolated from 3 experimental groups (sham, moderate and severe LVD). Statistical analysis produced r values of 0.99 for all 3 experimental groups and $p < 0.001$ (0.002, 0.0008 and 0.0005 for sham, moderate and severe LVD respectively). n numbers as per table 5.2.

		Left ventricular wet weight (mg)			
		125	**250**	**500**	**1000**
Total SR Protein (mg/g)	**Sham**	0.42 ± 0.21 (n =8)	0.65 ± 0.36 (n =8)	0.65 ± 0.25 (n =8)	0.69 ± 0.26 (n =8)
	LVD	0.44 ± 0.18 (n =10)	0.75 ± 0.27 (n =14)	0.77 ± 0.31 (n =16)	0.83 ± 0.22 (n =16)

Table 5.2. Protein content of SR fraction per gram wet weight of ventricle isolated from sham operated and LVD rabbit hearts. Values are means ± SD. n = indicates number of hearts.

Due to reduced SR protein retrieval efficiency below 250mg in both experimental groups, samples smaller than 250mg were deemed quantitatively unsuitable for SR vesicle preparations and further experimental purposes involving SR preparations.

Although linear increases in absolute homogenate and SR protein retrieval was associated with increasing tissue weight, SR protein content was some 100 fold smaller than that of the homogenate. This suggests that total SR protein is approximately 1% of total myocardial protein content in both normal and failing hearts. This value is comparable to that found in other studies (table 5.3). Quantification of homogenate and SR protein retrieval was performed by other research groups and has yielded similar results to those observed in this study (table 5.3). Interestingly, Schwinger *et al.* 1995 and Frank *et al.* 2002 also found an increase in the amount of protein retrieved from SR failing preparations as opposed to non-failing, although no additional comments regarding this finding were mentioned.

References	Species	Protein retrieval mg/g			
		Homogenate retrieval		SR retrieval	
		Non-failing	Failing	Non-failing	Failing
Meyer *et al.* 1995	Human	140 ± 3	136 ± 3		
Xu & Narayanan 1998	Rat			2	
Reddy *et al.* 1995	Canine			0.8 –1	
Schwinger *et al.* 1995	Human			1.32 ± 0.29	1.58 ± 0.38
Frank *et al.* 2002	Human	125.1 ± 6.4	123.1 ± 8.7	1.25 ± 6.4	1.31 ± 6.4
Hasenfuss *et al.* 1999	Human	134 ± 5	111 ± 7		
This study	Rabbit	100.5 ± 19	97.6 ± 26	0.66 ± 0.26	0.84 ± 0.27

Table 5.3. Quantification of total homogenate and SR protein retrieved per mg/g wet tissue weight in various experimental groups. Data are mean ± SD.

5.6. Homogenate protein variation

Examination of the data revealed a moderate amount of variation between tissue weights isolated from multiple samples in single hearts and those isolated from different hearts. Intracardiac samples are defined as tissue samples isolated from within the same heart whereas intercardiac samples are preparations that have been isolated from different hearts.

Combining intra and intercardiac samples (sham & LVD) to calculate protein retrieval per gram wet weight produced a normal distribution curve (bell shaped) with a mean value of 95.68 ± 21.93 (SD) suggesting a mean protein retrieval of approximately 100mg/g (figure 5.5, panel A). Differences between intracardiac and the combined intra/intercardiac data are representative of the intercardiac variation i.e. variation in protein retrieval between hearts. The mean relative intracardiac protein retrieval data produced a normal distribution curve with a mean value of 0.99 ± 0.19 (SD) (figure 5.5, panel B). All tissue samples (60 to 1000mg) were normalised to the protein retrieved from 1 gram wet weight. The combined intra/intercardiac data showed slightly more variation in protein retrieval in comparison to the intracardiac data although these differences were not statistically significant.

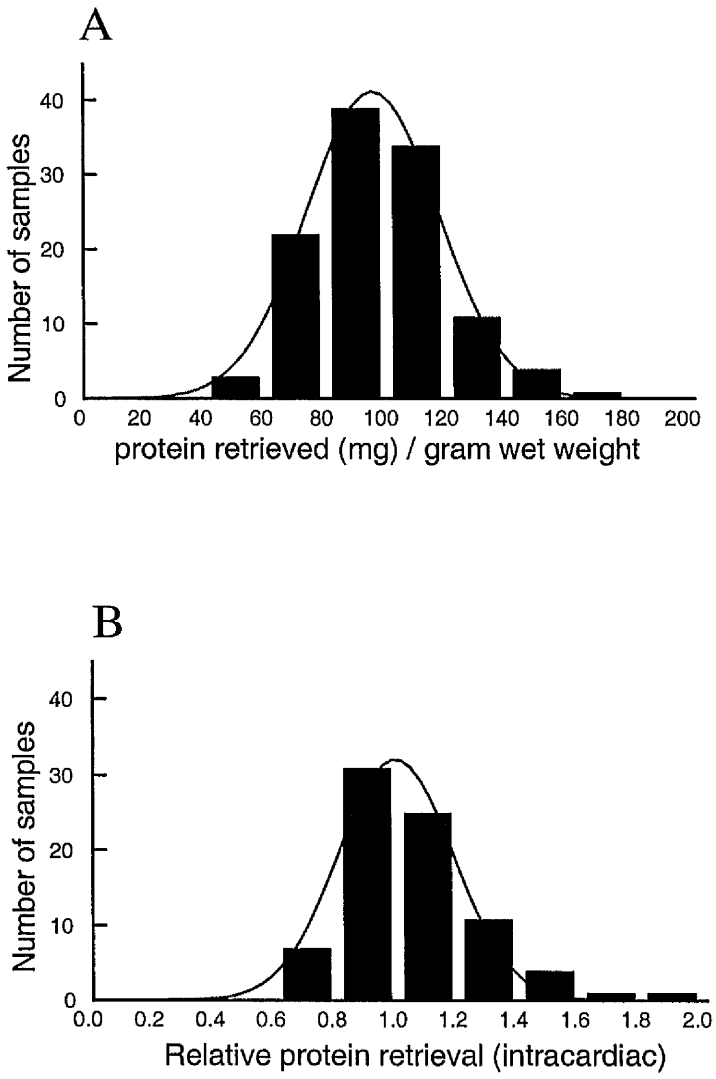

Figure 5.5. Protein retrieved (mg) per gram wet tissue weight (A) pooling both intracardiac and intercardiac samples (Mean 95.68 ± 21.93) and (B) relative intracardiac protein retrieval (Mean 0.99 ± 0.19). Intracardiac data are normalised to protein retrieved from 1 gram samples. Data are from all three experimental groups and are expressed as mean ± SD. A normal distribution curve is superimposed onto both histograms, confirming the normal distribution of the data.

5.7. SR protein variation

Figure 5.6. shows SR protein retrieved (mg) per gram tissue wet weight for sham and LVD samples respectively. Both data sets consist of pooled results for 250, 500 and 1000mg samples. Each set shows a normal distribution pattern with a mean value 0.66 ± 0.28 and 0.76 ± 0.25 for sham and LVD data respectively. T-test analysis on the two data sets produced a p value of 0.075. Calculating SR protein retrieval directly from tissue wet weight is likely to introduce variation into the data as there are many steps between the initial wet weight tissue sample and the final SR sample (figure 5.1). Therefore, variation in SR protein retrieval was corrected for by calculating the SR protein retrieval directly from the absolute protein homogenate values (figure 5.7). Mean values were 0.61 ± 0.29 for sham and 0.81 ± 0.21 for LVD, $p = 0.01$. This analysis suggests that SR protein retrieval from LVD samples is significantly greater than that retrieved from sham samples.

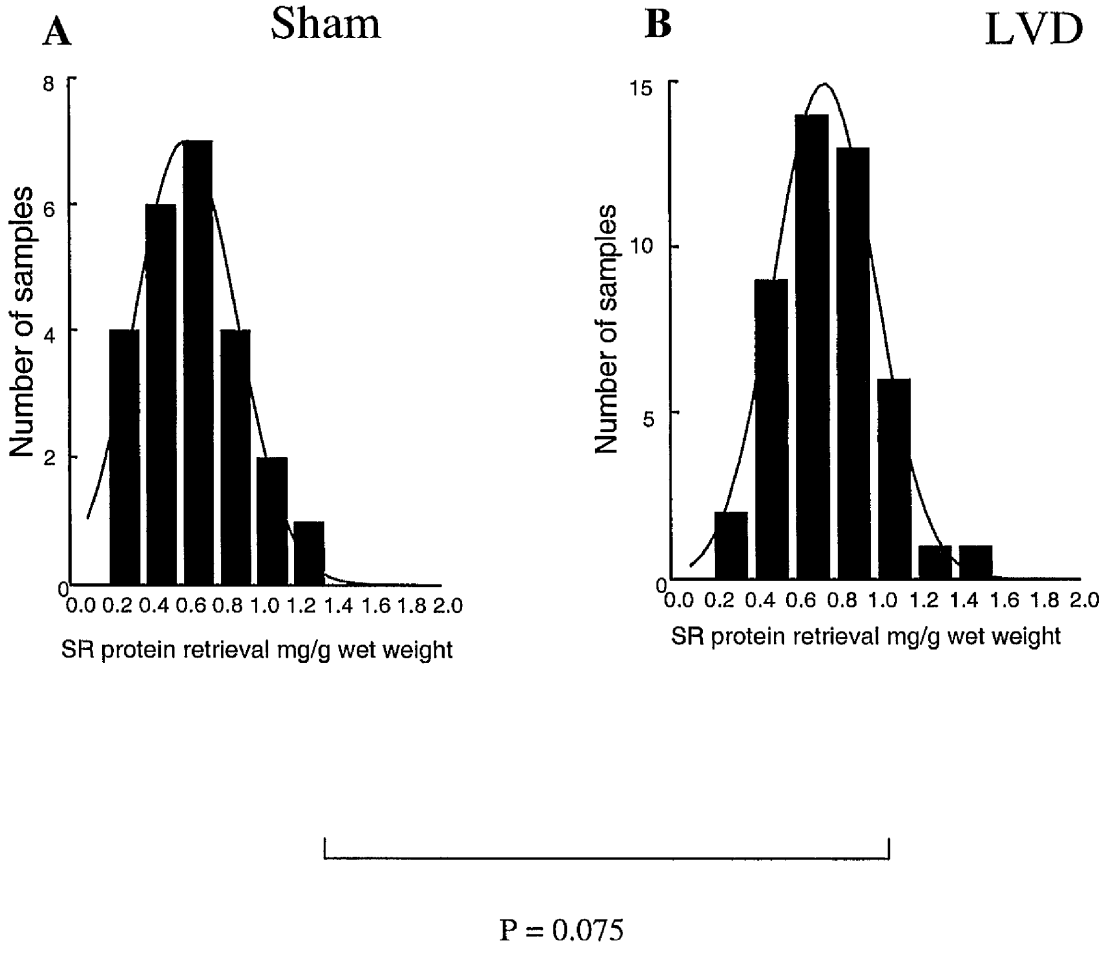

Figure 5.6. SR protein retrieved (mg) per gram tissue wet weight isolated from (A) sham and (B) LVD tissue samples. Data combines all SR protein retrieved from 250, 500 and 1000mg (n=24). Data are mean ± SD. Number of animals: N=24 and 46 for sham and LVD samples respectively. Mean values were 0.64 ± 0.28 (sham) and (LVD) 0.76 ± 0.25, p =0.075. A normal distribution curve is superimposed onto both histograms (solid line).

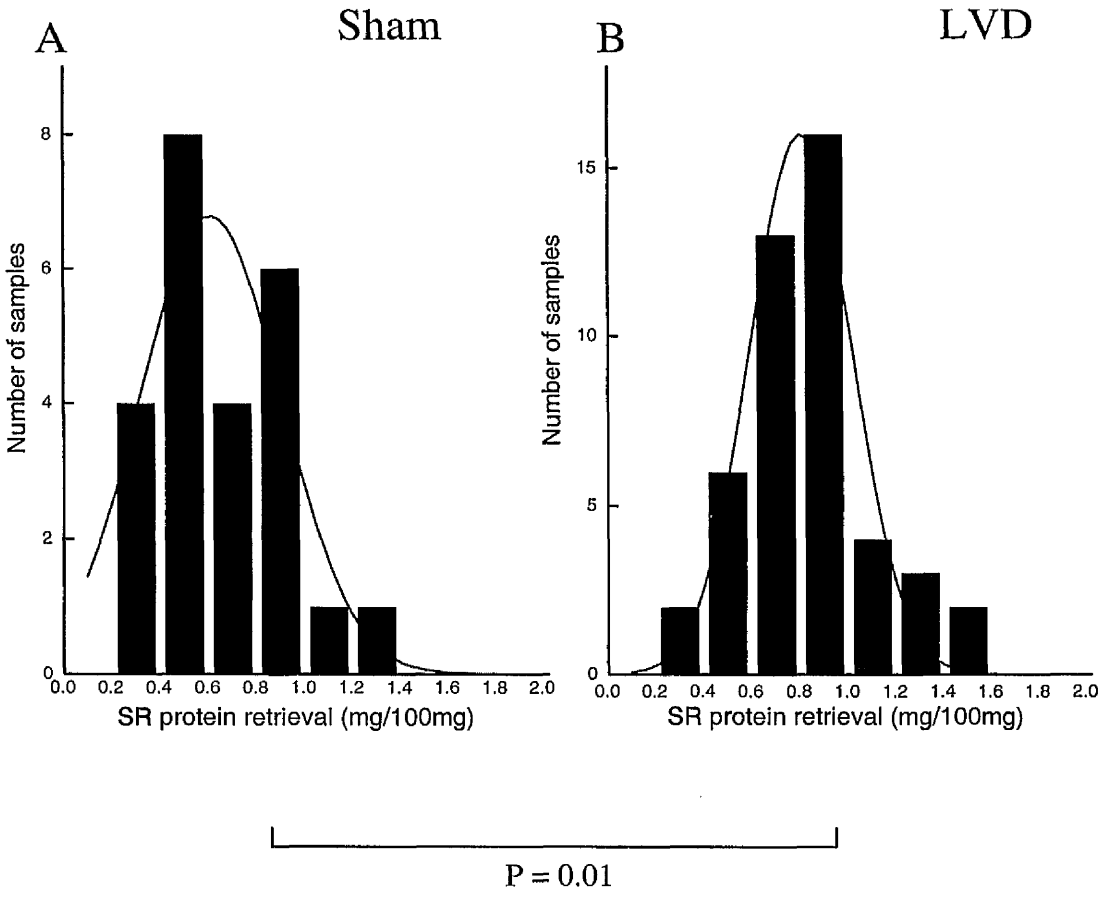

Figure 5.7. SR protein retrieved (mg) per 100mg sham (A) and LVD (B) homogenate. Data combines all SR protein retrieved from 250, 500 and 1000mg samples Sham. Data are represented as mean ± SD. Mean values were 0.61 ± 0.29 (sham) and 0.81 ± 0.21 (LVD), p = 0.01. A normal distribution curve is superimposed onto both histograms (solid line).

5.8. Discussion

5.8.1. Homogenate retrieval variation

The aim of this study was to assess the efficiency of protein retrieval in homogenate and SR samples produced from different tissue wet weights. The homogenate retrieval data suggests that it is possible to retrieve reproducible protein amounts (mg/g) from a large range of tissue weights (60 to 1000mg). This reproducibility was present in both sham and LVD tissue samples (table 5.1 and figure 5.3).

The results show that there is a moderate, yet similar amount of both intra and intercardiac variation in total protein homogenate content (figure 5.5). Such variation may arise from either differences in connective tissue content or in the homogenisation technique. Differences in connective tissue content seem unlikely as the amount of connective tissue throughout an individual heart should be uniform and would therefore not influence protein content. Therefore the most likely reason for the intracardiac variation is via differences in homogenisation technique. Potential variables in the homogenising technique were temperature, speed, resuspended volume, and homogenisation time. All of these variables were constant for each sample except for the homogenisation time. Homogenisation times varied slightly depending on how well the chunks of tissue were broken up, i.e. a longer time would be necessary if non muscle tissue (connective tissue) prevented adequate homogenisation of muscle tissue. Furthermore, differences in homogenisation time could alter sample viscosity, i.e. increased viscosity of sample if homogenisation time was inadequate. The more viscous a sample is the greater is the potential for pipetting errors, i.e. a reduced volume of sample being drawn up. Such pipetting error may be sufficient to produce quantifiable differences in calculated protein content. Excessive connective/adipose tissue was removed from the epicardial surface of all hearts to minimise variation in the homogenisation time required.

In addition, inaccuracies in the protein assay itself may influence protein content values. Protein concentration is determined using a calibration curve produced by BSA standards (general methods, 2.3.3). To minimise intracardiac variation, samples from the same heart were assayed on the same plate using one particular standard curve. Variation within individual plates would influence all of

the samples on each plate and could not explain the observed intracardiac variation. As calibration curves vary between plates variation in protein determination is inevitable, this may account for some of the observed intercardiac variation. Furthermore, additional errors may be introduced to both intracardiac and intercardiac samples as the mean of 3 optical density readings were calculated per sample, plus the mean of up to 3 optical density readings were calculated for various sample dilutions to produce the final protein concentration. Variation within any or all of these triplicate samples is likely to influence the final protein concentration reading, and hereafter any analysis performed on the data, i.e. calculating means.

In summary, the observed intracardiac variation is most likely due to variation in the homogenisation technique i.e. homogenisation time, combined with the variation produced when the mean of the optical density measurements are calculated. Intercardiac variation is most likely due to variations present within calibration curves and when calculating the mean of the optical density measurements. Figure 5.5. suggests that there are no significant differences in the amount of protein retrieved from different samples within one heart, than that which can be retrieved from samples from many different hearts. This suggests that protein content between hearts irrespective of experimental type i.e. sham or LVD is similar. In addition, protein retrieval from a range of tissue weights yields comparable protein levels.

5.8.2. SR retrieval variation

SR protein retrieved from both sham and LVD tissue samples was comparable throughout tissue weights between 250 and 1000mg although a tendency for higher LVD SR protein retrieval was observed. SR protein retrieval was slightly lower in 125mgs samples (table 5.2 & figure 5.4). This reduction in SR protein retrieval suggests that a moderate amount of error is introduced in the efficiency of protein retrieval when samples weighing less than 250mg are used. All tissue samples irrespective of weight were resuspended in x10 volumes of homogenisation buffer, therefore it follows that, the smaller the original tissue sample the smaller the volume of buffer it is resuspended in. The SR isolation protocol involved many steps and any loss of the resuspended sample (via pipetting or sticking of sample to the side of centrifuge tubes) would disproportionately affect the protein content retrieved

in smaller rather than larger volume samples. This may account for the decreased protein retrieval observed from 125mg samples. An additional factor may be the introduction of error when calculating protein content via the actual protein assay, as discussed earlier (homogenate retrieval variation). However, this error is likely to occur throughout all samples and is unlikely to be totally responsible for the decreased protein observed only in 125mg samples. For that reason, it was concluded that reduced SR protein retrieval at 125mg most likely arises from errors produced whilst dealing with small volume samples, rather than small variations introduced by assay and calculation techniques. Taking this into account, tissue samples less than 250mg were deemed unsuitable for experimental purposes involving SR preparations due to the inaccuracy of calculating actual protein content, e.g. quantitative assessment of SR proteins.

5.8.3. LVD vs sham SR retrieval

Overall SR protein retrieval was greater in LVD samples than in sham samples although these values are not statistically significant when calculated in mg/g wet weight (table 5.2 & figure 5.6). As all samples underwent the same preparation technique, and these results were the mean value of 16 samples it seems unlikely that the retrieval differences could arise from minor technical differences. Due to the multiple steps required to produce SR vesicles from tissue homogenates, SR protein retrieval was calculated directly from absolute homogenate values therefore reducing variation introduced by multiple preparation steps (figure 5.7). Statistical analysis comparing these results showed that SR protein retrieval from LVD samples was significantly greater ($p<0.05$) than from sham samples. Such a significant difference could not be accounted for simply by the observed small technical variation.

The question that now arises is: Why is SR protein retrieval greater in LVD samples in comparison to sham samples?

One possibility is that LVD tissue samples may in fact possess a higher SR protein amount per weight of tissue than sham samples. As LVD myocytes are known to hypertrophy during the compensatory phase of heart failure (Gerdes *et al.* 1992; Bryant *et al.* 1997; McIntosh *et al.* 1999 & 2000) it is possible that the size of their intracellular organelles would increase to compensate for such enlargement.

Therefore, the proportion of SR protein would remain constant per weight of tissue. Alternatively, the amount of SR protein in LVD samples may in fact be disproportionately smaller in comparison to sham samples as connective tissue content may be increased in LVD due to compensatory mechanisms (Schaper & Schaper, 1986; Olivetti *et al.* 1994). Ultracentrifugation steps during the SR vesicle isolation protocol (figure 5.1) removes excess intracellular organelles and connective tissue, therefore in LVD samples more protein, in the form of connective tissue would be removed leaving a reduced SR protein retrieval for any given wet weight. As this is not observed, it appears that greater SR protein is present in LVD tissue samples despite a potential increase in connective tissue protein content. To further explain these results additional biochemical investigations would be required.

In conclusion, homogenate protein retrieval from a variety of tissue weights (60 to 1000mg) and hearts (sham and LVD) yielded comparable protein amounts. No significant differences in protein retrieval were observed within or between heart samples in both sham and LVD samples. The minor differences in protein retrieval within samples was most likely caused by variations in the homogenisation technique and/or the accuracy of the protein assay, rather than actual differences in tissue protein content.

SR protein retrieval (mg/g) throughout a range of tissue weights (250 to 1000mg) was greater in LVD samples in comparison to sham. These values were significantly higher when SR protein retrieval was calculated directly per 100mg protein retrieved. Furthermore, SR preparations below 250 mg produced less than predicted amounts of protein retrieval due to inaccuracies when dealing with such small sample volumes.

Chapter 6

Quantification of protein expression using Western Blotting

As with many experimental techniques variability is introduced into the data by the technique itself. Western blotting is no exception. This chapter highlights the major sources of variation observed within this technique and details the experimental approach taken in order to minimise this variation hereafter optimising the technique and subsequent quantification. A variety of internal normalisation sources were also investigated.

6.1. Methods

The protocol for Western Blot technique and Commassie stained gels are described in the general methods (2.3.4).

6.1.1. Reproducibility of Western Blots

6.1.1.1. Assessment of experimental variation

SDS-polyacrylamide gel electrophoresis was performed on the same protein sample loaded in duplicate, i.e.1μg protein load across one gel. Normal transfer and subsequent probing for SERCA and calsequestrin proteins were carried out to assess the homogeneity of protein loading, transfer and antibody binding across the gel. This protocol was performed on two separate homogenate samples.

Assaying identical samples (complete western blotting procedure) i.e. 2 gels loaded with identical samples, assesses the amount of variation produced within one experiment (intra variation). All solutions, running, and transfer times were identical therefore narrowing any final variation in the blots to either pipetting, protein transfer or antibody binding. The same samples were also electrophoresed on different days to assess daily variation (inter variation).

6.1.2. Sources of normalisation

PAGE was performed on 2 identical gels run in parallel followed by Coomassie staining of one gel (untransferred) and normal Western blotting of the other. Individual protein content (SERCA/NCX/CSQ) and total lane protein content were calculated using optical density measurements as described in section 2.3.5. Total lane protein as a normalisation source for individual proteins was also assessed.

6.1.3. Statistical Analysis

All data are expressed as Mean ± SEM unless stated otherwise. Paired students *t*-tests were used to compare two groups and ANOVA multi variant analysis (parametric) was used to compare multiple groups. A value of $p<0.05$ was considered statistically significant.

6.2. Sources of experimental variation

Accurate quantification of individual proteins within tissue homogenates is a difficult task and variation may be introduced at several different stages.

These include:

- Homogenisation of tissue sample
- Assay for total protein content
- Sample preparation for electrophoresis
- Sample loading into gels
- Electroblotting of proteins from gel to nitrocellulose membranes (protein transfer)
- Primary and secondary antibody binding
- Optical density measurements

Repetitive loading of a tissue homogenate sample (1μg protein load) across a gel was performed to assess variation in sample loading, protein transfer and antibody binding (figure 6.1). Two separate tissue samples (1& 2) were run on two separate gels. Figure 6.1 shows the results of both gels. Panel A in figure 6.1 shows the variation in optical density of a largely untransferred protein (~200kDa molecular weight) observed in a Coomassie stained gel (stained after protein transfer). This graph shows minimal variation in optical density across the 15 well gel suggesting that sample loading was both accurate and reproducible. The Coefficient of variation (CV) (S.D./Mean) of the optical density was used to assess the degree of variation within each data set. CV of 0.09 and 0.05 were calculated for samples 1 and 2 respectively. The small variation present may be due to either loading error or inhomogeneity of the Coomassie staining. Additional evidence verifying accurate sample loading is shown in figure 6.2. In this example, a linear relationship exists between optical density and protein load, i.e., doubling the protein load doubles the optical density.

Panels B and C in figure 6.1 show the variation in optical density of 2 homogenate samples probed with SERCA and calsequestrin antibodies. Optical density variation was random for both experimental samples (1& 2) and protein detection across the gel suggesting that protein transfer and antibody binding does not depend on the

region of the gel. Antibody binding affinity is similar irrespective of antibody type and all areas of the nitrocellulose membrane appear equally exposed to the antibody solution. CV ranged between 0.25 and 0.11 for calsequestrin (sample 1& 2) and between 0.24 and 0.18 for SERCA (sample 1& 2). Since minimal variation is observed when loading reproducibility alone is assessed (0.05 –0.09), and the variation in optical density measurements increases considerably (almost doubles) after protein transfer and antibody incubation, these results suggest that the majority of variation found within this technique is introduced during protein transfer and antibody binding stages.

In a limited number of experiments, identical samples were assayed (complete western blotting procedure) on the same and different days to investigate the intra experimental variation (2 gels (same sample), same day) and inter experimental variation (same samples, different days) of this technique. CV in optical density readings from gels run on the same day and those run on different days were comparable. Inter-CV values ranged from 0.4 to 0.56. As CV did not differ markedly between daily experiments (inter) this again suggests that the largest amount of variation arises from the assay technique itself. An additional source of variation may be introduced from incomplete homogenisation of the tissue sample. Microscopic pieces of non-homogenised tissue within the sample solution may lead to inaccuracies in volume loading (see chapter 5).

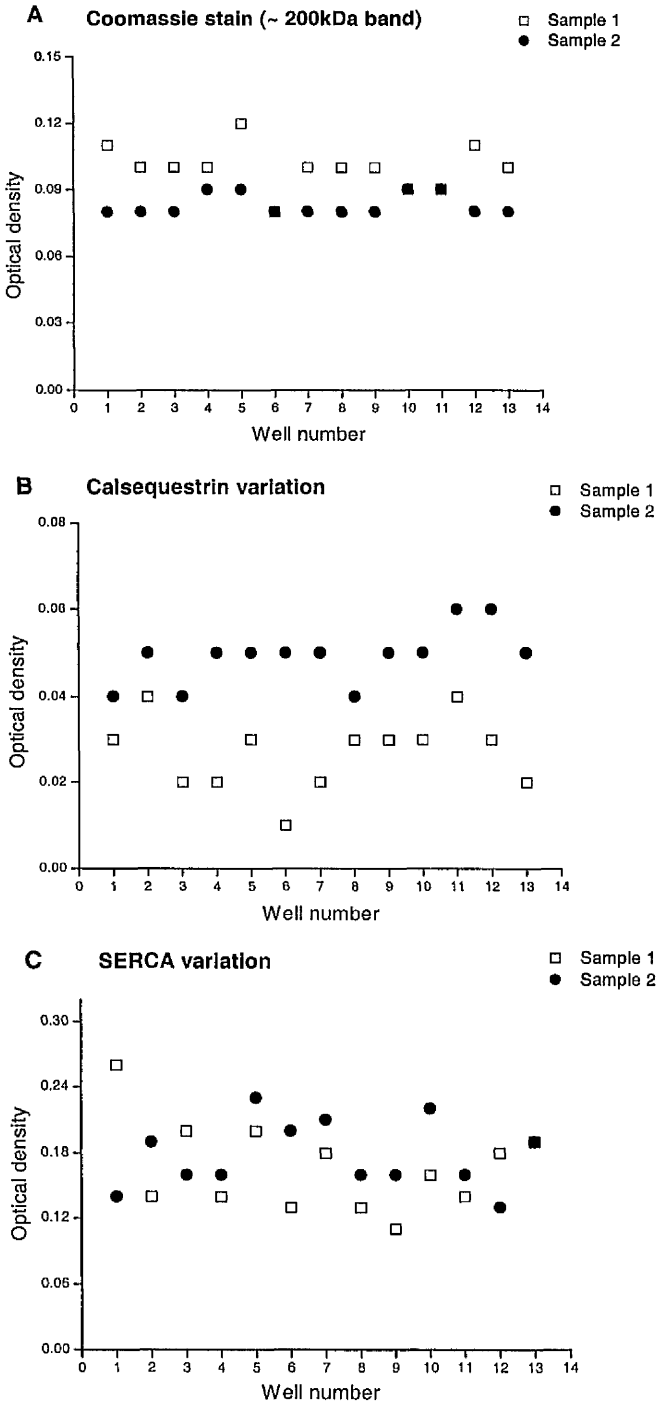

Figure 6.1. Repetitive loading of a 1μg protein sample across one gel. Two separate samples (1 & 2) were loaded and run on separate gels. Panel A is the resulting Coomassie stained gel after protein transfer. Nitrocellulose membranes were probed with Calsequestrin (B) and SERCA (C) antibodies. Co-efficient of variation (SD/mean): Coomassie variation; 0.09 and 0.05; calsequestrin variation; 0.25 and 0.11; SERCA variation; 0.24 and 0.18 for samples 1 and 2 respectively.

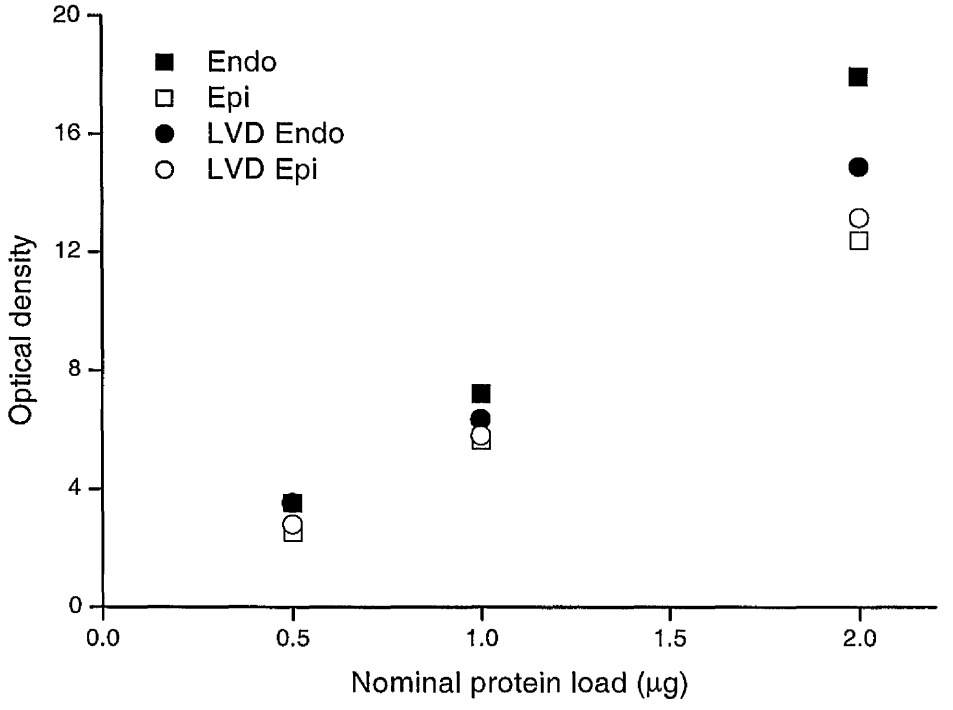

Figure 6.2. Linear relationship between optical density and protein load (µg). Data shown is from Sham; endocardial and epicardial and LVD endocardial and epicardial samples.

6.3. Normalisation of optical density measurements

At the beginning of this study it was the intention to normalise all protein expression data (sham endocardial /epicardial and LVD endocardial /epicardial) to the calsequestrin values of one sample within each gel. This normalisation was considered suitable as it is generally accepted in the literature that calsequestrin expression is unchanged in heart failure or left ventricular dysfunction (Movesian *et al.* 1994; Meyer *et al.* 1995; Schwinger *et al.* 1999). However, it has come to light in this study that this rabbit model of LVD was associated with a marked increase in calsequestrin protein expression. Furthermore, small transmural differences in calsequestrin expression were also observed in both sham and LVD samples (chapter 7). In agreement with this study, a recent paper by Naqvi *et al.* (2001) observed increased calsequestrin expression in their rabbit aortic banding model of hypertrophy. In contrast, Prestle *et al.* (1999) observed no changes in CSQ expression between either endocardial and epicardial myocardium or between non failing and failing human heart samples.

As calsequestrin appears to change across the ventricle wall (endocardial to epicardial) and between experimental groups it was considered unsuitable as a normalisation standard. Unfortunately, the unsuitability of calsequestrin as a standard was only discovered in the latter stages of this study when sufficient experiments had been performed to observe the changes in calsequestrin expression. As a result, alternative normalisation sources were investigated only towards the end of the study.

The following normalisation options were investigated:

6.3.1. Normalisation using a nominal protein load

Normalisation of protein optical density to the nominal protein load is a commonly used way of normalising data. In this study, nominal protein loads of 0.5,1 and 2 μg were used. Sample protein content was calculated using the Bradford method and BSA as standard (2.3.3).

6.3.2. Normalisation using relative lane protein

Another alternative was to run 2 identical gels in parallel, protein transfer was performed on one gel only whilst the other was stained with Coomassie stain. Staining an untransferred gel allows quantification of the total protein content found within each lane. It was thought that the total lane protein could be used to normalise the optical density of the protein bands, which were developed from the parallel transferred gel. These stained gels were also used to assess the accuracy of protein loading. As figure 6.2 shows, a linear relationship exists between protein content and optical density.

It is worth noting at this point that absolute protein content in each sample loaded may differ slightly from the total protein content calculated per lane due to the running conditions of the gel. Differences in gel running conditions determine how far the dye front migrates down the gel and how much sample enters the gel from the wells. In short, some lower molecular weight proteins may migrate off the gel and higher molecular weight proteins remain unresolved at the top end of the gel. Therefore, the estimate of total protein per lane is based on the running conditions of the particular gel and not solely on how much protein is actually loaded.

6.3.3. Normalisation using a non transferred protein band

Gels were stained after protein transfer and it was observed that consistently a 200 kDa protein remained on the gel. This largely nontransferred protein was subsequently investigated as a normalisation standard.

6.3.4. Comparisons between normalisation sources

In this study, protein loads ranged by a factor of 4; 0.5 to 2μg. A range of protein amounts was assessed prior to beginning experiments to find the optimum signal achieved under our standard immunoblot conditions. In order to allow multiple sample comparisons to be made across an individual gel only 3 different protein loads were used; 0.5, 1 and 2 μg.

The importance of using a suitable normalisation source is highlighted in figure 6.3. This figure shows the results of nitrocellulose membranes probed with a monoclonal antibody against SERCA. Panel A shows the optical density plotted against the nominal protein loads (0.5, 1,2 μg). This graph suggests that for the sham 2μg protein load, SERCA optical density is higher in epicardial than endocardial samples. Normalising this same data to total lane protein from the parallel stained gel is shown in panel B. This graph suggests that the higher optical density reading in the epicardial data was due to a larger amount of SERCA present in this sample. This high content was present despite an apparent lower total protein load in epicardial compared to endocardial sample; 12 as opposed to 18 optical density units. This result itself is feasible, however if you then compare SERCA optical density against the stained 200 kDa band from the same gel then the results appear quite different. Normalising SERCA optical density to the optical density of the 200 kDa band from the same gel suggests that the optical density of the epicardial sample is higher than endocardial because the actual protein loaded into the gel was greater. This is expressed as a higher optical density reading; 0.15 compared to 0.13. It appears that a small amount of variation is present between the 2 apparently identical gels. Furthermore, when comparisons of the 200 kDa protein bands were made between the transferred and the untransferred gels differences in optical density were present. It is the generally accepted view that optimum protein transfer occurs within the middle area of the gel (top to bottom). Under these running conditions minimal transfer occurs at the 200 kDa level therefore minimal differences in optical density should exist between the transferred and non transferred 200 kDa protein band. As small differences in optical density were observed this confirms along with the different normalisation results (figure 6.3) that variation in the loading between gels had occurred. This variation is most likely due to errors in micropipetting and or microscopic tissue pieces affecting the final loading volume. These results indicate that normalisation to total lane protein from a separate gel albeit a supposed "identical" gel is not accurate.

Clearly, very different conclusions can be drawn regarding protein expression depending on the normalisation source. Ideally, normalising to a protein within the same lane on the same gel is the most accurate as this corrects for non-uniformity in protein loading between different lanes and gels.

Due to the problems of finding a suitable normalisation standard in this study, protein optical densities were normalised to the nominal protein load. Nominal protein load is commonly used in the literature as a standard and the variation was not too dissimilar to the 200 kDa therefore it was chosen as the normalisation standard for this study. The slopes of the linear regression lines fitted to the data at 0.5, 1 and 2 μg determined the relative protein content of each sample.

Some non-linearity was observed in the optical density readings when the sample loads were doubled (figure 6.3). Such non-linearity was observed in many of the samples analysed. This non-linearity may be due to several factors. Pipetting errors should be minimal, as each volume added is simply double that of the previous sample. However, microscopic pieces of unhomogenised tissue may affect the actual volume drawn up giving rise to some variation. Homogenisation efficiency varies depending on technique. In addition, low optical density readings have a greater signal to noise ratio and high optical density readings may saturate the analysis system producing variability in these readings. Therefore, the inability of the densitometer to resolve small differences in optical density values at high and low readings may also add to the variation observed in the data.

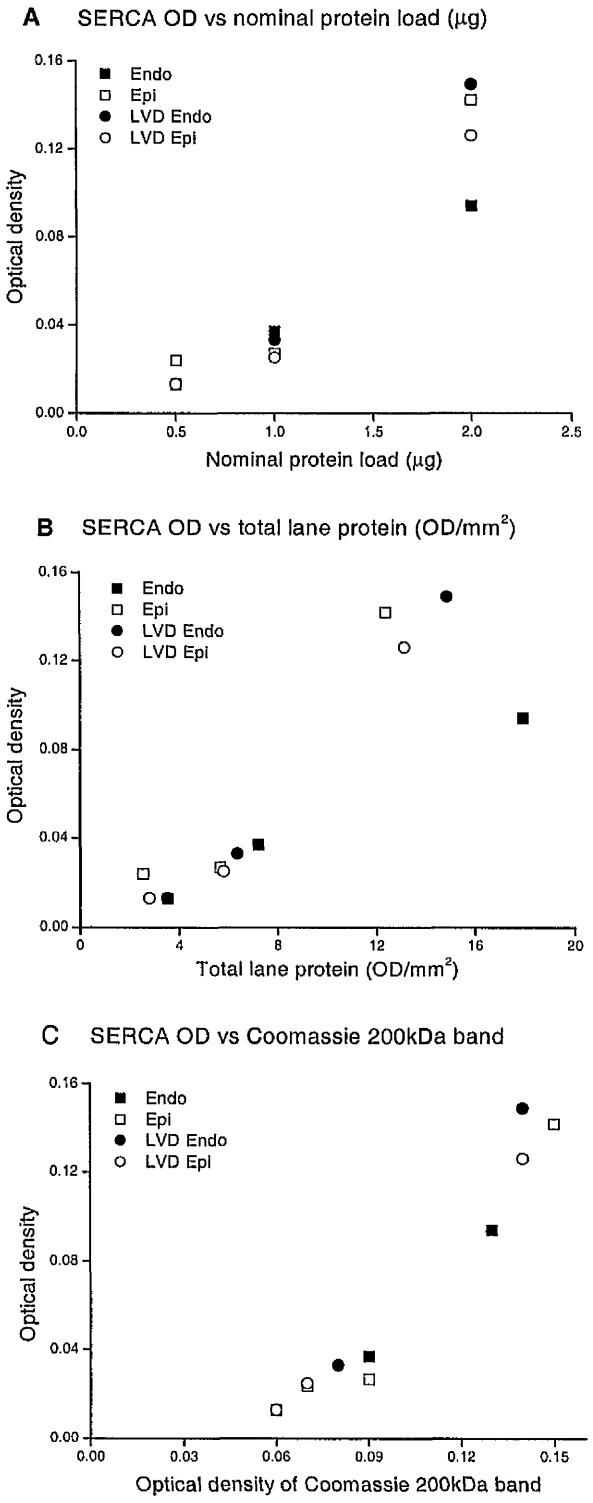

Figure 6.3. Relationship between intensity of immunochemical reaction (optical density - OD) of SERCA and A) nominal protein load (µg); B) total lane protein (OD/mm^2: OD x lane area) and C) OD of Coomassie stained 200kDa band.

6.4. Future technical improvements

Taking into account the sources of variation found within this Western Blotting technique current and future experiments have been modified to minimise where possible these sources.

Some of the most important modifications regarding protein normalisation will now be discussed. As detailed in the last section, protein normalisation is best achieved by normalisation to a specific protein/s within the same lane and/or gel as the experimental samples. This is the most accurate method as it corrects for non-uniformity in protein loading within different gels.

6.4.1. Single protein normalisation

A known amount of a purified protein run along with experimental samples (same gel) can be used as a normalisation standard. Purified proteins can be acquired from collaborators in other labs or bought commercially, although choice may be limited. It is also possible to make ones own purified proteins, however this depends on technical expertise and resources within the lab. As an alternative, normalisation to other proteins found in the tissue type being studied can be used. Proteins such as myosin, actin and GAPDH are commonly used as normalisation proteins. Normalisation proteins must be in a similar molecular weight range to the proteins that are being probed for in order that they can be run under the same gel conditions. However, their molecular weight must be sufficiently different to the proteins being investigated to allow adequate resolution of individual protein bands. Ensuring adequate band resolution avoids the additional problems associated with having to strip the nitrocellulose membrane of one antibody prior to incubation with another in order to determine protein expression. Unchanged protein density must be confirmed within the tissue sample or region of interest before any protein can be used as normalisation protein.

Alternatively, samples within each lane may be "spiked", i.e. a known amount of a specific protein (labelled or unlabelled) can be added into each lane along with the experimental sample and subsequently used as a normalisation source.

6.4.2. Total lane protein normalisation

Commercial stains such as *Amido black* (Biorad) are also available which can be used to stain the nitrocellulose membrane after probing with protein antibodies. This solution stains all proteins on the nitrocellulose membrane and allows quantification of total lane protein content. Normalisation to total protein on a lane to lane basis can then be performed. Recently, a new stain called *RedAlert* (Novagen) has become commercially available. In this case the nitrocellulose membrane is stained and total lane protein quantified prior to probing with antibodies. The advantage of both these methods is that normalisation is performed on the same nitrocellulose membrane from which the protein optical density readings are calculated. The suitability of both these stains would have to be assessed prior to use.

6.4.3. Use of Radiolabelled isotopes

An alternative experimental approach to quantifying individual protein expression is via the use of radiolabelled antibodies. The whole Western Blot procedure up to and including primary antibody incubated is the same as the Immunoblot technique. However the secondary antibody is conjugated with a radioactive isotope as opposed to Horseradish peroxidase used in the immunoblot technique. Radioactive decay is measured using a phosphoimager and is used as an indicator of protein expression. Again, the advantages and disadvantages of this technique would have to be investigated prior to use.

6.4.4. Linear protein detection range

To assess the linearity of the optical density/protein load relationship a large range of protein amounts (μg) can be loaded across one gel from a single sample. The complete Western Blotting procedure is performed and the data analysed. This establishes the linear range of protein detection. Optimum protein loading can be calculated by this method. The optimum protein load would have to be determined for every individual protein that was to be studied. It may also verify if particularly low or high optical density are disproportionately influenced by resolution limitations and/or high signal to noise ratios.

6.4.5. Additional points

As highlighted in Chapter 5 the homogenisation procedure used in this study was not ideal for the tissue type under investigation. Currently, a new homogenisation technique using a Mixermill (Qiagen) is being tested. Preliminary evidence suggests that this technique fully homogenises ventricular tissue samples, thereby minimising residual pieces of tissue within the solution.

Electroblotting of proteins from the gel to nitrocellulose membranes was optimised by using two blot modules instead of one. Earlier experiments had observed an inconsistency in protein transfer between the gels depending on their position in the blot module.

Variation caused by the transfer process and antibody binding appear to introduce the largest sources of variation. The wet transfer system used in this study produced a more homogeneous transfer than the alternative semidry system, therefore is more accurate and was used in this study.

In this study the mean Coefficient of variation (SD/Mean) in the protein expression data was 0.76. Using statistical power calculations (Instat statistical program, assumes mean of 1) it was estimated that in order to detect a 40% difference in protein expression at the 5% significance level n =29 would be required. To detect a 10% difference at the same significance level (5%) requires n = 454. For example, no significant difference in endo/epicardial LVD CSQ expression was detected even though the increase in expression was 35 – 43% higher than sham. Power calculations estimated n = 29 would be required to detect this difference. Endocardial/epicardial CSQ data was n =18 and 15 (respectively), consequently, with the observed error present in the data this number was insufficient to detect a 40% difference in expression. Sample numbers would approximately have to be doubled in order to detect a 40% difference.

6.5. Summary

Sources of variation within this Western Blotting technique include; protein assay, sample preparation and loading, electroblotting of proteins, antibody binding and optical density measurements.

It was concluded from this study that the major sources of variation arise from the electroblotting and antibody binding stages of the Western blotting technique.

Some sources of variation can be minimised by:

- Adequate homogenisation of tissue sample.
- Ensuring that protein sample readings are taken on the straight line section of the protein calibration curve and not at the highly non-linear sections of the curve.
- General consistency and accuracy in solution making, sample preparation, pipetting, running/transfer buffer solution levels, antibody dilutions, and adequate submerging and mixing of nitrocellulose membranes within antibody solutions.
- Ensuring optical density measurements are on the linear section of the optical density /protein concentration curve.

Chapter 7

Quantification of cardiac Ca^{2+} handling proteins

7.1. Background

Precise regulation of intracellular [Ca^{2+}] is critical for normal cardiac contractile function. There are several key proteins involved in the regulation of intracellular [Ca^{2+}] within cardiac myocytes. This study aimed to quantify protein expression of three of these proteins, calsequestrin (CSQ), SR Ca^{2+}-ATPase pump (SERCA2) and the sarcolemmal sodium-calcium exchanger (NCX). Expression of these three proteins was compared between endocardial and epicardial regions within each experimental group (sham & LVD) and between sham and LVD tissue samples.

The most commonly used and simplest method of quantify protein expression within tissue samples and the technique used in this study is via the Western blotting technique (general methods, 2.3.4.).

Calsequestrin (CSQ)

CSQ is a small protein with a molecular weight of 53kDa. CSQ is a relatively easy protein to quantify as it is stable, i.e. not particularly susceptible to proteolysis and the antibodies currently available against CSQ are fairly specific (i.e. minimal non-specific binding occurs). Using Western blotting, most current literature reports that CSQ protein expression is unchanged in human heart failure and left ventricular dysfunction (Takahashi *et al.* 1992; Meyer *et al.* 1995; Schwinger *et al.* 1999; Prestle *et al.* 1999). However, the results of animal studies are less well defined. In a rat animal model of cardiac hypertrophy CSQ mRNA levels were found to be unchanged over a range of severity of cardiac hypertrophy (Arai *et al.* 1996). In contrast, a recent study by Naqvi *et al.* (2001) observed a 65% increase in CSQ protein expression in their rabbit model of cardiac hypertrophy. In a separate rabbit cardiac hypertrophy study, Matsui *et al.* (1995) observed a decrease in mRNA for CSQ.

SR calcium-ATPase pump (SERCA)

SERCA is classed as a medium sized protein with a molecular weight of 110kDa. Similar to CSQ, SERCA is a reasonably stable protein, and the monoclonal antibodies currently available against SERCA are specific. Generally SERCA expression in human heart failure and animal models of failure and LV dysfunction shows a decrease in both protein and mRNA expression (Hasenfuss, 1998 and Ravens, 2000, for reviews). Again animal model results are less defined, decreases in SERCA protein expression (O'Rourke *et al.* 1999) and SERCA mRNA expression (Matsui *et al.* 1995) have been observed. In contrast, Pogwizd *et al.* (1999) observed no change in SERCA protein or mRNA in their pressure overloaded rabbit model of heart failure.

Sodium-calcium exchanger (NCX)

NCX protein expression has been difficult to quantify in general as it is not abundant and is relatively unstable during sample preparation i.e. proteolysis commonly occurs. A wide range of protease inhibitors was used during sample preparation in an attempt to minimise proteolysis, however this does not completely overcome the problem (see general methods). Throughout the literature several protein bands are reported to be associated with the NCX protein when heart preparations are assayed and even today the exact nature and function of the individual protein bands remains controversial. Gel electrophoresis reveals several major protein bands running at 70, 120 and 160 kDa (Philipson *et al.* 1988; and Iwata *et al.* 1995; Shigekawa & Iwamoto, 2001). The exact origin of the 120 and 160 kDa protein bands remains unknown. It is possible that they represent two different conformational states of the one protein although it remains unclear which is the native protein. The 160 kDa may represent an altered conformational state of the 120 kDa protein due to sample preparation for SDS-PAGE, this changed conformational state leads to an alteration in protein migration rate (Durkin *et al.* 1991). The 160 kDa protein appears under reduced (Durkin *et al.* 1991, Iwata *et al.* 1995) and non-reduced conditions (Philipson *et al.* 1988) and its origin has been proposed to be either a combination of 70 and 120 kDa protein dimers (Philipson *et al.* 1988) or may reflect glycosylation of the 120 kDa protein (Nicoll *et al.* 1990; Iwata *et al.* 1995). Evidence suggests that the 70 kDa protein is an active proteolytic fragment, most likely from the 120 band (Philipson *et al.* 1988, Saba, Bollen & Herchuelz 1999).

It is thought that either of the 120 and the 70 kDa proteins represents the main functional units of the NCX. Commonly quantification of immunoblots from both protein bands are combined and reflect NCX protein expression. Throughout this study, NCX protein expression combined optical density measurements calculated from both the 120 and the 70 kDa protein bands. In this study a polyclonal antibody was used as the currently available monoclonal does not pick up the 70kDa band.

NCX protein expression in heart failure (human & various animal models) remains controversial as studies have either observed no change (Schwinger *et al.* 1999; mRNA; Prestle *et al.* 1999) or an increase in protein (Reinecke *et al.* 1995; O'Rourke *et al* .1999; Pogwizd *et al.* 1999) and mRNA expression (Studer *et al.* 1994; Pogwizd *et al.* 1999).

7.2. Experimental approach

Tissue preparations and solutions used in the experiments described in this chapter are detailed in the general methods (chapter 2).

Throughout this study, 15 well gels were used to allow multiple sample comparisons to be made across an individual gel. For all 4 experimental samples (sham; endo/epi; LVD endo/epi) protein amounts of 0.5, 1 and 2μg were loaded into the gels. These protein loads were used as they produced readings within the optimum optical density range. Typical examples of some developed autoradiographs showing the gel set up are shown in figure 7.1. Gradient values were calculated for all experimental samples using these three protein loads. Examples of gradients calculated from these protein loads (0.5, 1 & 2μg) are shown in figure 7.2. Gradients were calculated for CSQ, SERCA and NCX proteins using sham endocardial and epicardial homogenate samples. In order to maximise the accuracy of the Western measurements (see chapter 6) protein results were expressed relative to either another sample within the gel (eg. endo: epi) or to another protein developed from the same gel (NCX:SERCA). Subsequent analysis directly compared sham and LVD transmural (endo/epi) and Sham/LVD (endo & epi) gradient differences. These ratios values reflect the relative protein expression of CSQ, SERCA and NCX.

7.2.1. Statistical analysis

All data are expressed as mean ± SEM. Statistical analysis was performed using either students *t* tests or ANOVA (repeated measures, parametric). $p<0.05$ was considered statistically significant.

7.2.2. In vivo left ventricular echocardiographic parameters

Mean ejection fractions were 72.2 ± 1.8 and 44.0 ± 1.6% with LVEDD values of 17.3 ± 0.3 and 21.4 ± 0.3mm for sham (n=10) and LVD hearts (n=20) respectively. These values were not significantly different from the mean ejection fraction and LVEDD values calculated for this whole study (table 2.1).

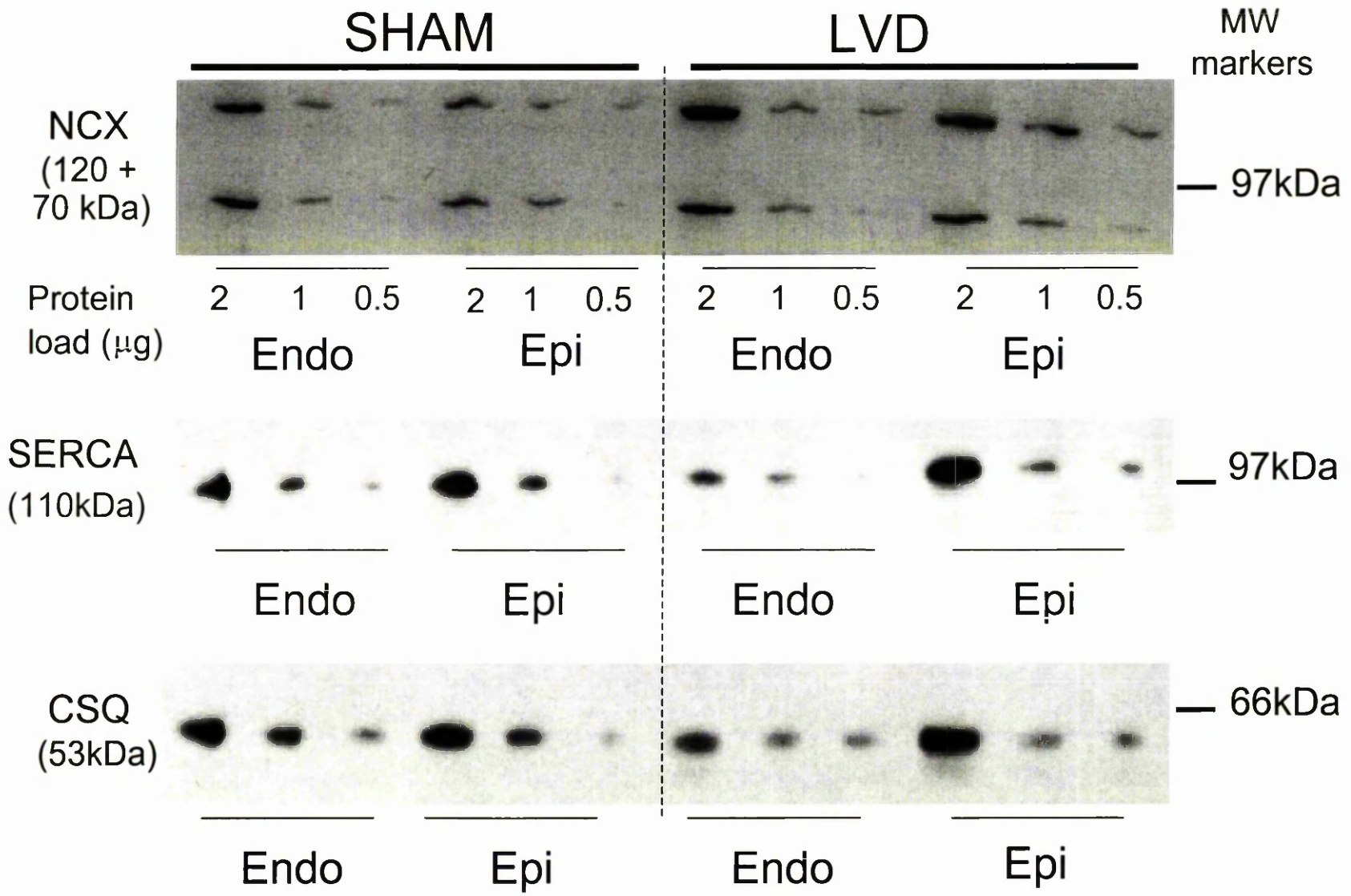

Figure 7.1. Typical example of developed Western Blot film probed for Sodium-Calcium exchange (NCX), Sarcoplasmic reticulum Ca^{2+} -ATPase pump (SERCA) and Calsequestrin (CSQ)proteins. All gels were set-up as shown above: Sham : endo/epi and LVD endo:epi to allow multiple sample comparisons to be made within one gel.Protein loads of 0.5, 1 and 2µg were loaded for all four experimental samples.Molecular weights are shown on the right hand side (kDa).

7.3. Protein expression results

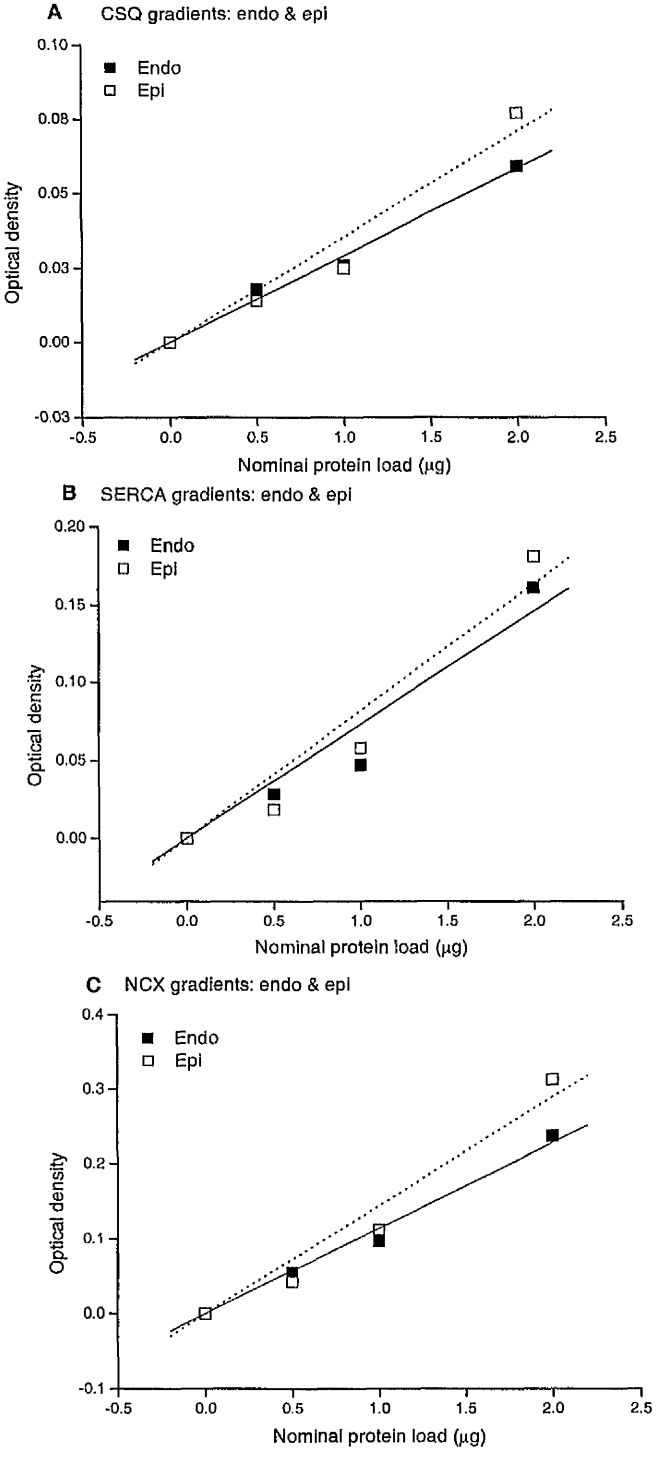

Figure 7.2. Typical examples of gradient values calculated from three protein loads for CSQ, SERCA & NCX. The examples shown are sham endocardial and epicardial samples.

7.3.1. Calsequestrin protein expression

Transmural or epi/endo ratios for CSQ protein expression are shown in panel A of figure 7.3. As reference, a ratio value of 1.0 shown as the dotted line represents equal epicardial CSQ expression. It follows that, a ratio value of less than 1.0 indicates lower epicardial protein expression whereas a ratio value more than 1.0 indicates higher epicardial protein expression. Panel A shows that both sham and LVD epicardial CSQ expression is lower than endocardial by approximately 9 ± 8 % (sham) and 7 ± 7 % (LVD). Comparisons between sham and LVD CSQ expression are shown in panel B. Both LVD endocardial and epicardial data showed a large increase in CSQ expression of 43 ± 19% (endocardial) and 35 ± 18% (epicardial). This increased expression although marked was not statistically significantly using ANOVA analysis. As no significant transmural difference in CSQ expression was observed endocardial and epicardial data could be treated as one homogeneous population (i.e. could be combined as one data set). The combined LVD data showed a significance increase in CSQ expression of 39 ± 13% ($p < 0.001$) in comparison to sham.

It is worth noting at this point that combining endocardial and epicardial data does not necessarily reflect the results that assaying CSQ expression from whole transmural left ventricular samples would yield. This is because the combined endocardial and epicardial data represents only a small portion of left ventricular mass and does not contain mid myocardial sample data which makes up the majority of the left ventricle. It is possible that assaying CSQ expression in ventricular homogenate samples from the whole left ventricle may show different results. To date this assay has not been performed on this rabbit LVD model.

7.3.2. SERCA protein expression

Transmural (epi/endo ratio) SERCA protein expression showed no difference in both sham and LVD data, i.e. all ratio values are approximately one. Comparisons between sham and LVD data revealed a small decrease in SERCA expression in both LVD endocardial (8 ±11%) and epicardial data (8 ±10%). This was not statistically significant (ANOVA). Again, treating endocardial and epicardial data as one homogeneous population revealed a significant decrease in LVD SERCA expression of $8 \pm 7\%$ ($p < 0.05$) (figure 7.4).

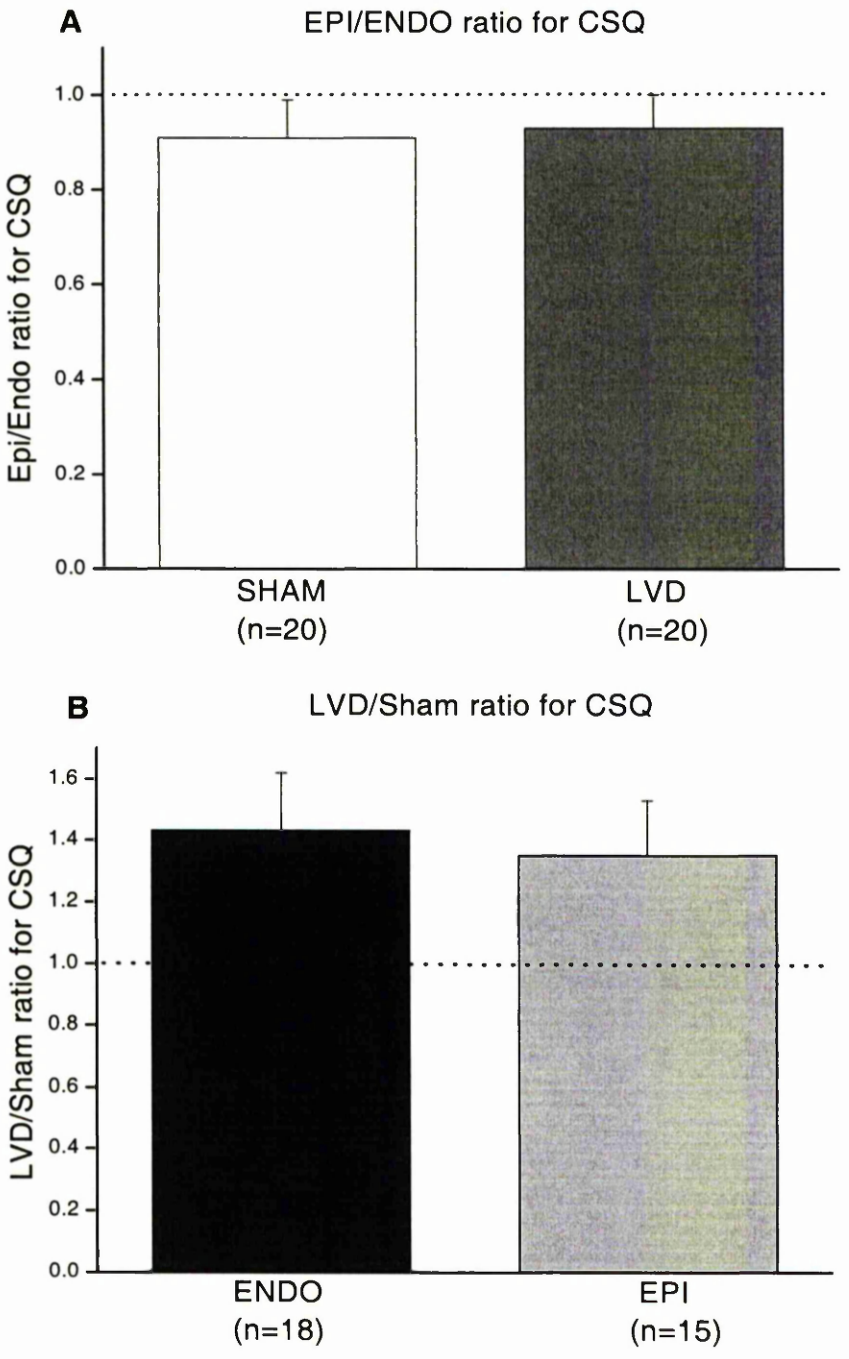

Figure 7.3. Transmural (epi/endo) and LVD/Sham ratios for calsequestrin expression are shown in panels A and B respectively. n denotes number of hearts.

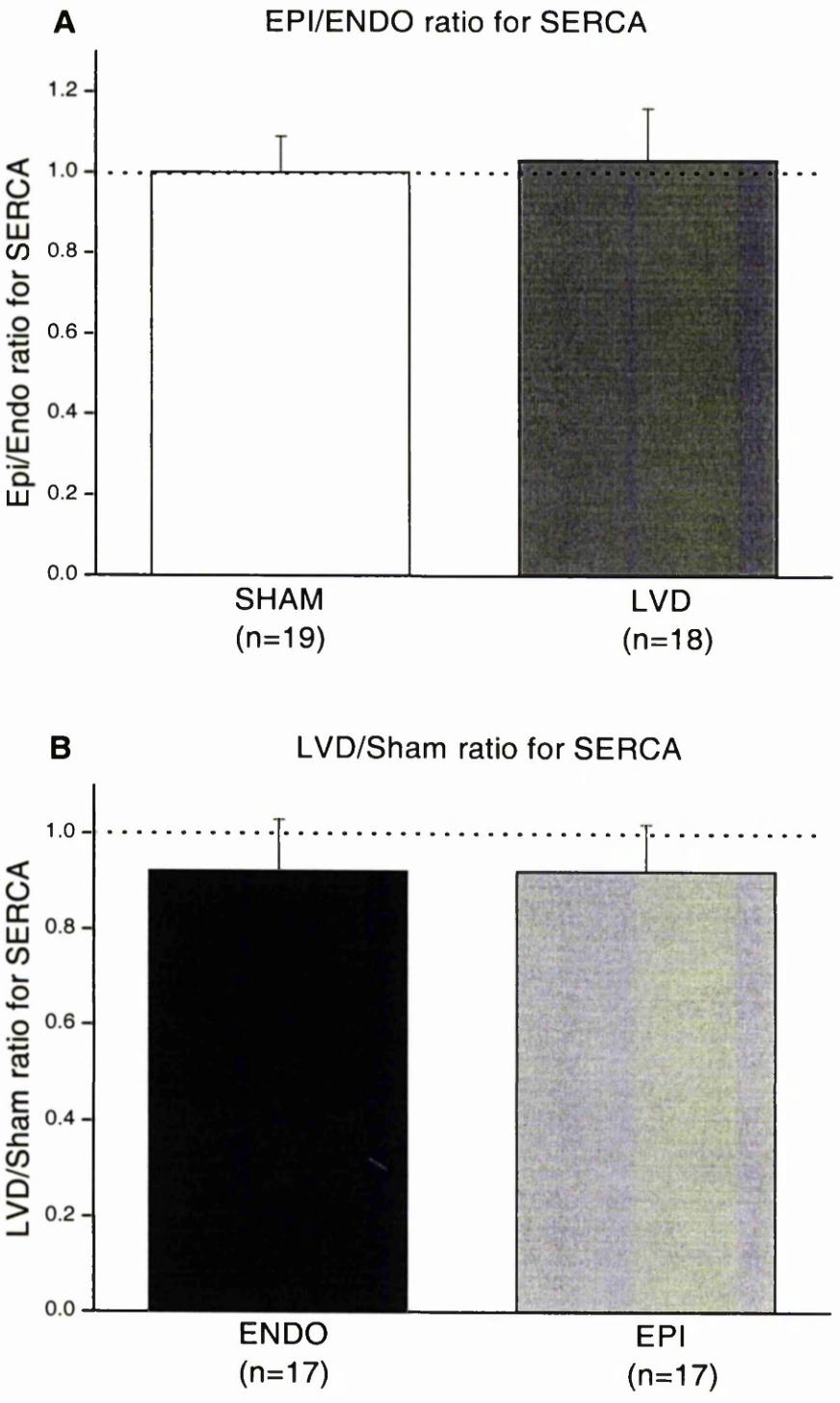

Figure 7.4. Transmural (epi/endo) and LVD/Sham ratios for SERCA expression are shown in panels A and B respectively. n denotes number of hearts.

7.3.3. Sodium-Calcium exchanger protein expression (NCX)

Transmural (epi/endo) NCX expression showed a small decrease in sham epicardial NCX expression of 14 ± 10% in comparison to sham endocardial data. This transmural difference is not as marked in the LVD data which showed minimal decrease in expression 3 ± 12 % (panel A, figure 7.5)

Comparisons between sham and LVD NCX expression are shown in panel B, where an increase in NCX protein expression was observed in both endocardial and epicardial LVD data sets. NCX expression in the LVD endocardial data was 11 ± 15% higher than sham whereas LVD epicardial NCX expression was 29 ± 18% higher. Statistical analysis (ANOVA) revealed no significant differences between the data sets. Again statistical analysis on the combined endocardial and epicardial data sets for sham and LVD revealed a significant increase in LVD NCX expression of 21 ± 12 % ($p < 0.05$).

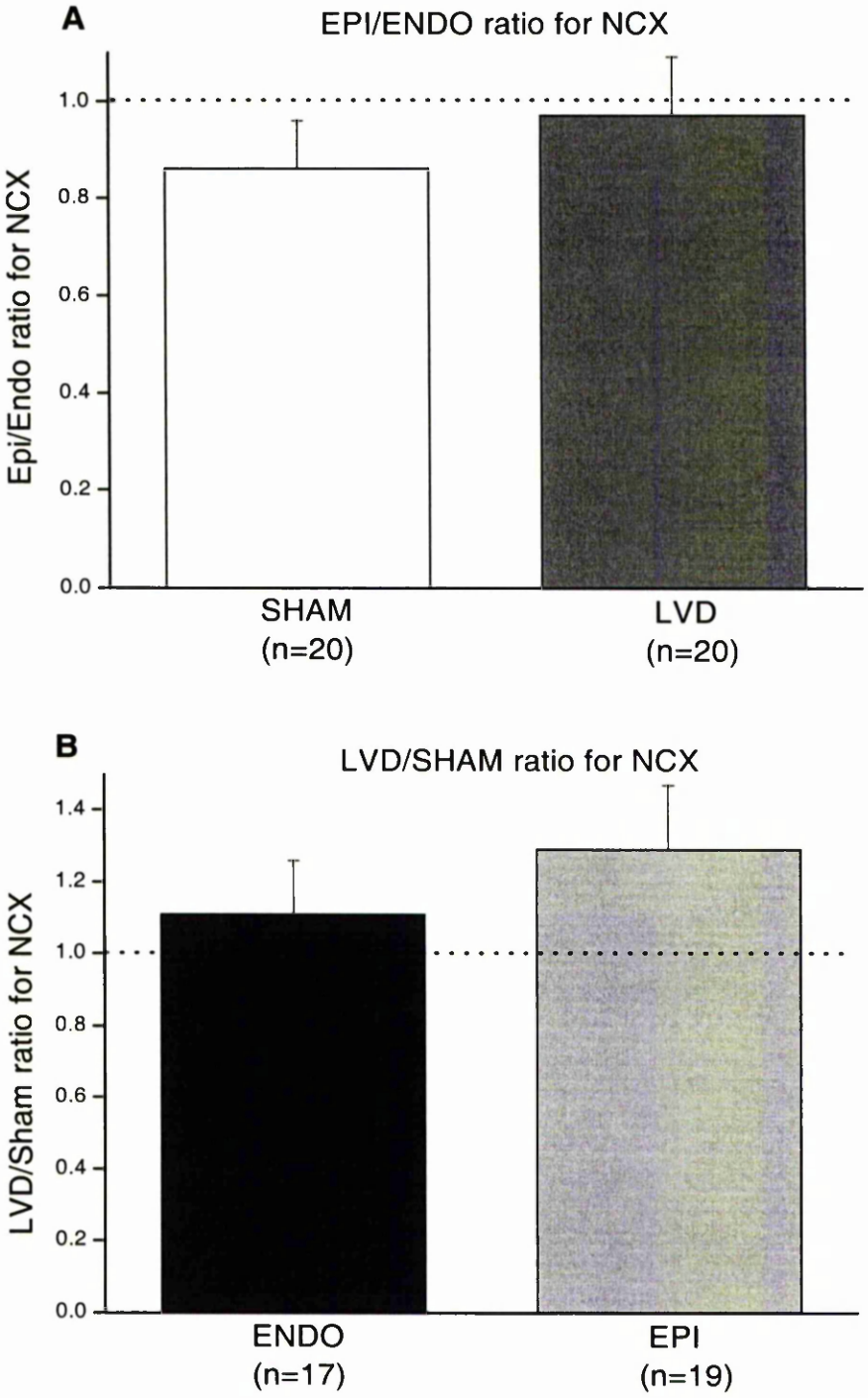

Figure 7.5. Transmural (epi/endo) and LVD/Sham ratios for NCX expression are shown in panels A and B respectively. n denotes number of hearts.

7.3.4. Sodium-calcium exchanger/SERCA ratio

As discussed in chapter 6, an alternative method to maximise accuracy (minimise variation) of the Western technique and to confirm changes in protein expression is to normalise one protein to another developed from the same gel. The NCX/SERCA and SERCA/CSQ ratios were calculated in transmural (endo:epi) and Sham/LVD samples to confirm the changes in NCX, SERCA and CSQ protein expression observed when the data was normalised to other samples within the gel, i.e., epi:endo, and LVD:sham. NCX and SERCA are the two major proteins responsible for reducing cytosolic Ca^{2+} levels back to resting values during diastole. In rabbit, approximately 28% of cytosolic Ca^{2+} is extruded from the cell by NCX, 70% is resequestered into the SR by SERCA mediated Ca^{2+} uptake and the remaining 2% is taken up by mitochondria or extruded from the cell by the sarcolemmal Ca^{2+}-ATPase pump (Bassani *et al.* 1994). Assessment of the NCX/SERCA ratio gives some indication of changes in the ratio of the two major proteins responsible for removal of cytoplasmic Ca^{2+} during diastole. A small transmural difference in NCX/SERCA ratio was present in sham but not in the LVD data. Sham epicardial NCX/SERCA ratio was 15 ± 9% lower than endocardial whereas the NCX/SERCA ratio in LVD was only 4 ± 14% lower (figure 7.6; panel A). LVD and sham comparisons of NCX/SERCA ratio revealed an 18 ±16% and a 34 ± 14% increase in endocardial and epicardial samples respectively (figure 7.6, panel B). The combined LVD endocardial and epicardial data revealed a 26 ± 11% increase in NCX /SERCA expression ratio ($p < 0.05$).

7.3.5. SERCA/CSQ ratio

As it is commonly observed that CSQ protein expression is unchanged in heart failure or LVD it is often used as a normalisation source when quantifying other proteins. As this study observed changes in CSQ protein expression in LVD CSQ was not used as a normalisation source.

A normal transmural difference (sham) in SERCA/CSQ was observed with a 34 ± 15% higher epicardial SERCA/CSQ ratio. LVD data showed minimal transmural differences (epicardial 4 ± 10% higher than endocardial). These data suggest that a small normal transmural difference in SERCA/CSQ exists but it is lost in LVD (figure7.7; panel A). Both endocardial and epicardial LVD samples showed a decrease in the SERCA/CSQ ratio in comparison to sham (endo; 9 ± 17% & 28 ± 13%). This decreased ratio was more pronounced in LVD epicardium (figure 7.7; panel B). The combined LVD endocardial and epicardial data revealed a 19 ± 11% decrease in SERCA/CSQ expression ratio ($p < 0.05$).

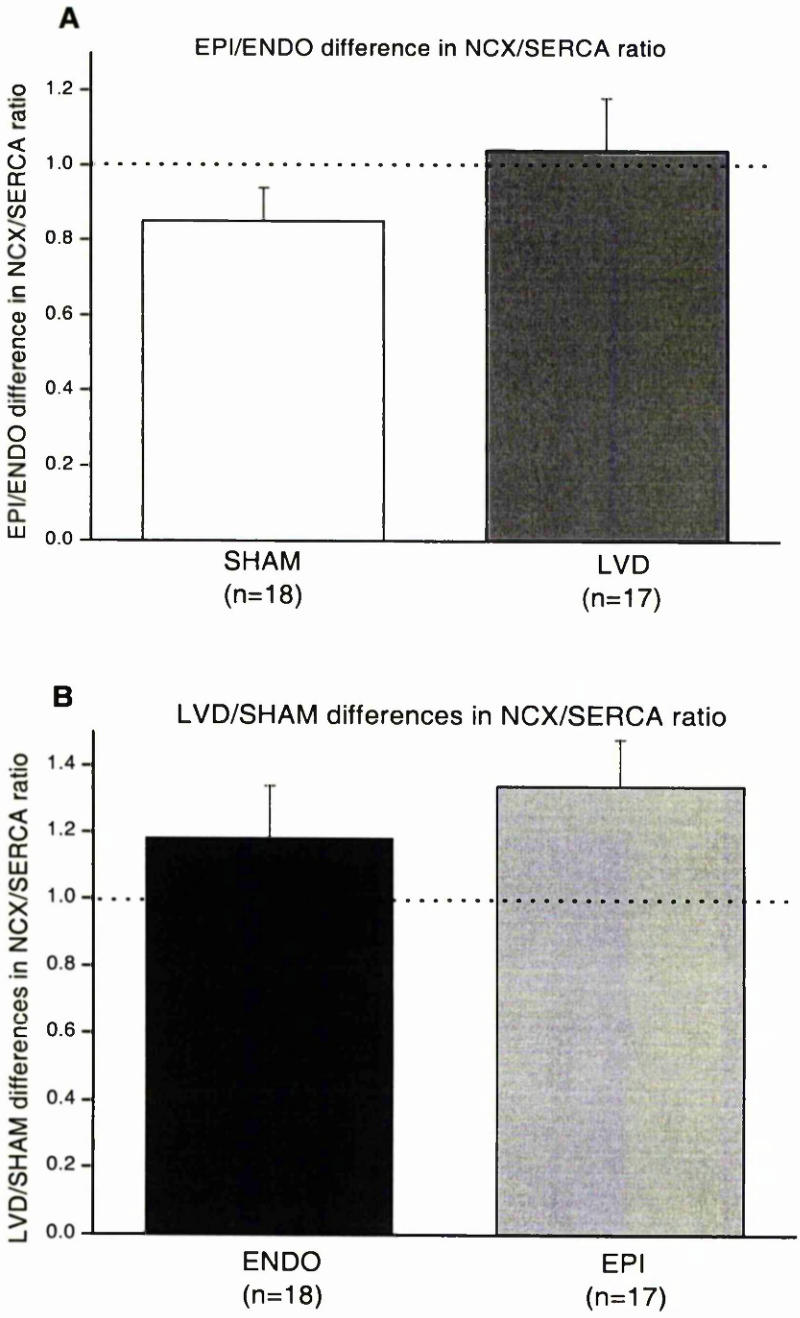

Figure 7.6. Transmural (epi/endo) and LVD/Sham ratios for NCX/SERCA expression are shown in panels A and B respectively. n denotes number of experimental samples.

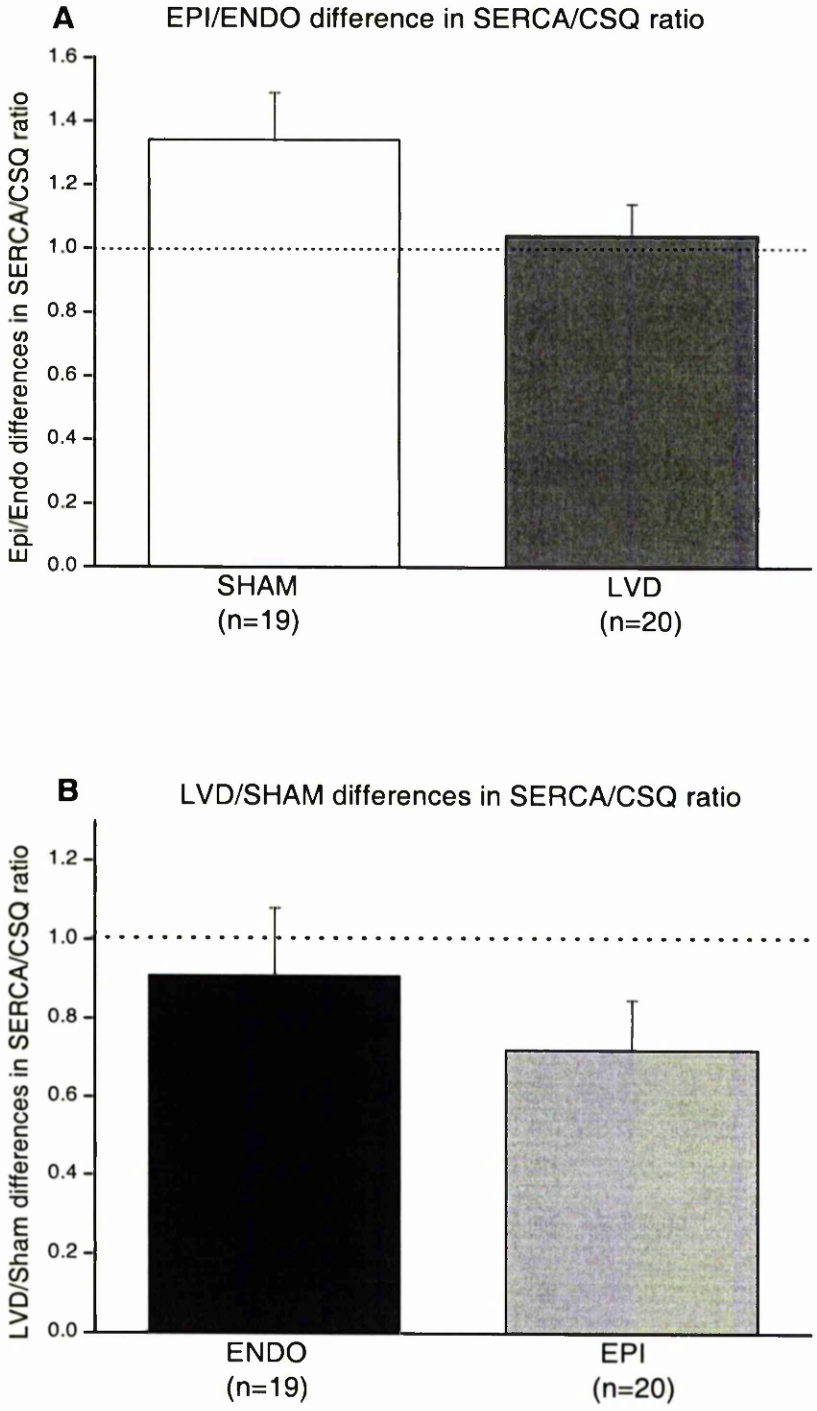

Figure 7.7. Transmural (epi/endo) and LVD/Sham ratios for SERCA/CSQ expression are shown in panels A and B respectively. n denotes number of experimental samples.

7.4. Discussion

The purpose of the experiments described in this chapter was to quantify Ca^{2+} handling protein expression between endocardial and epicardial regions and between sham and LVD experimental groups in the model of LVD featured in this study. Previous studies have reported alterations in protein expression of Ca^{2+} handling proteins linked to disruption in diastolic and systolic Ca^{2+} regulation and contractile dysfunction. However, prior to this study, no work has featured this particular rabbit model of LVD.

7.4.1. Transmural protein expression

Most studies investigating transmural differences in heart have concentrated on functional and electrophysiological changes and minimal work has been published on protein expression. This study observed only minor differences in transmural protein expression in all three proteins studied. The data suggest that there is a trend towards lower CSQ in epicardial tissue samples (sham and LVD), no transmural difference in SERCA expression (sham and LVD) and that NCX expression was slightly lower in sham epicardial samples but this trend was not present in LVD epicardial samples. With such small differences in transmural protein expression for all three proteins, it is unclear whether any normal transmural difference in expression actually exists. To verify any transmural differences a significantly larger sample size would be required. A study by Prestle *et al.* (1999) investigated transmural protein expression in failing human hearts. In agreement with the results in this study they observed a slight increase in endocardial CSQ expression in non-failing and failing hearts in comparison to epicardial although this was not significant. In contrast, they observed lower SERCA expression in endocardial in comparison to epicardial in both failing and non-failing hearts. This difference was statistically significantly in the failing group. Northern blot analysis quantified SERCA mRNA expression and observed a similar trend to that of protein expression. No assessment of NCX protein expression was performed in the Prestle study although quantification of mRNA revealed no transmural differences in mRNA expression in failing or non-failing hearts. The difference in results between these two studies may be due to a species difference (human vs rabbit), the degree of severity of failure/dysfunction and/or a difference in the aetiology of the underlying

disease. Although, direct extrapolation between mRNA and protein expression cannot be made due to possible post translational modifications it may give some indication of the trend in protein expression. Igarashi-Saito *et al.* (1999) investigated transmural gene expression in canine myocardium and observed a significant reduction in SERCA mRNA in endocardium in comparison to epicardium, but observed no change in CSQ mRNA. In failing canine myocardium they observed the same trend to lower SERCA mRNA in endocardium, but the endo:epi ratio was the same in control as heart failure. CSQ mRNA in heart failure showed no transmural differences. However, overall SERCA mRNA expression was lower in heart failure, and CSQ mRNA was slightly higher in heart failure.

The NCX/SERCA ratio in the sham epicardial data is lower than endocardial suggesting epicardial samples normally have either higher SERCA or lower NCX expression. As no sham transmural differences were observed in SERCA expression (figure 7.4, A) and NCX was slightly lower in epicardial samples (figure 7.5, B) it is likely that the lower NCX expression is responsible for the transmural differences in ratio values. The small transmural differences observed in the sham NCX/SERCA ratio was not present in the LVD data due to higher NCX expression in LVD epicardial samples.

The sham epicardial SERCA/CSQ ratio is higher than endocardial suggesting either a decrease in epicardial CSQ or an increase in SERCA expression. Epicardial CSQ is very slightly lower than endocardial and SERCA is unchanged. The decreased epicardial CSQ expression may be responsible for the ratio difference although the changes in CSQ expression (<10%) are not directly proportional to the changes in SERCA/CSQ ratio (34%). The SERCA/CSQ ratio in LVD endocardial and epicardial samples is similar as may be expected by minimal endocardial/epicardial differences in both SERCA and CSQ protein expression.

7.4.2. Comparisons between Sham and LVD protein expression

The most striking result in this study was the large increase in CSQ expression observed in LVD endocardial and epicardial samples. To date most studies have concentrated on whole ventricular samples and have observed no change in CSQ expression from failing or hypertrophied hearts (Takahashi *et al.*

1992; Meyer *et al.* 1995; Schwinger *et al.* 1999; Prestle *et al.* 1999;). The combined endocardial and epicardial samples showed a 35-40% increase in CSQ expression.

It should be noted that the combined data do not contain cells from the mid myocardium therefore do not necessarily reflect the results that would be produced from a whole ventricular sample. However, in agreement with these results, a recent study by Naqvi *et al* (2001) observed a 65% increase in CSQ expression in their rabbit aortic banding model of hypertrophy.

The small decrease in LVD SERCA protein expression (~10%) in this model is consistent with the general literature view in which a small decrease in SERCA expression is observed (Hasenfuss, 1998 and Ravens, 2000, for reviews). Previous investigations using the same rabbit model of LVD observed a significant decrease in SERCA expression (by 53 ± 9%) (Currie & Smith 1999). The reason for the more profound reduction in SERCA expression is not known. In vivo echocardiography revealed similar average ejection fractions for both studies, suggesting no gross differences in the degree of LVD in both groups. One possible explanation for the differences in SERCA expression may be that in this current study, tissue samples were only dissected from basal regions of sham and LVD hearts whereas samples in the Currie & Smith study (1999) where dissected from both apical and basal regions. Furthermore, whole ventricular samples were assayed by Currie & Smith (1999) whereas the results presented here are a combination of only endocardial and epicardial samples (no mid-myocardium).

NCX expression is slightly higher in LVD (endo & epi) than sham which is in line with literature results. Pogwizd *et al.* (1999) in a pressure over load rabbit model observed no change in SERCA protein expression and a large increase in NCX protein expression (93%). The differences in changes in protein expression between this study and Pogwizd's may be due to differences in the type or duration of animal model, i.e. volume vs pressure overload. Overall there is more uncertainty regarding the direction of change in NCX protein expression in heart failure and/or hypertrophy, as it appears to vary depending on species, severity, duration and aetiology of the underlying disease. Either no change in protein expression (Schwinger *et al.* 1999; mRNA; Prestle *et al.* 1999) or an increase in protein expression (Reinecke *et al.* 1995; O'Rourke *et al.* 1999; Pogwizd *et al.* 1999) has been observed.

Alterations from the normal transmural NCX/SERCA protein ratio will disrupt normal diastolic and systolic Ca^{2+} homeostasis. The NCX/SERCA ratio is higher in both endocardial and epicardial LVD samples suggesting either a lower SERCA expression and/or a higher NCX expression or both. In fact, both of these changes occurred in the LVD data samples and are likely to be responsible for the increased ratio. This ratio represents protein expression only and does not take into account the functional activity of the proteins. These results are in agreement with Hasenfuss *et al.* (1999) who also observed an increase in NCX/SERCA ratio in failing human myocardium. Interestingly no change in CSQ expression was observed in their study. Hasenfuss *et al.* (1999) identified different phenotypes according to diastolic function which were determined by various combinations of changes in protein expression. Disturbed diastolic function occurred in hearts with decreased SERCA and unchanged NCX expression. In contrast, diastolic function was preserved in hearts where NCX was increased and SERCA expression was unchanged. They concluded that increased NCX expression serves to preserve diastolic function in failing human myocardium and suggested that regulation of expression of both proteins occurred by different independent signals. Verifying this, Prestle *et al.* (1999) showed that transmural differences in SERCA but not NCX expression exist across failing and non-failing human hearts.

A marked decrease in SERCA/CSQ ratio is observed in both endocardial and epicardial LVD data sets. A decreased ratio suggests either increases in CSQ or decreases in SERCA protein expression. As both an increase in CSQ (figure 7.3) and a decrease in SERCA (figure 7.4) are observed in both LVD endocardial and epicardial data sets it appears that these changes are directly responsible for the changes in SERCA/CSQ ratio. Therefore, both the NCX/SERCA and the SERCA/CSQ ratio results confirm the protein expression changes observed in the averaged transmural and LVD/Sham data sets (figures 7.3.; 4 & 5).

7.4.3. Implications of altered Ca^{2+} handling protein expression

As discussed in chapter 1, CSQ distribution is mainly concentrated around the Ryanodine receptor (RyR) in the junctional SR where it is increasingly believed to have some regulatory influence on RyR activity either directly or indirectly (Szegedi *et al.* 1999). Given the high buffering capacity of CSQ, the overall affect of increased CSQ protein expression will be to increase SR Ca^{2+} content, i.e. increased CSQ expression would be expected to provide more Ca^{2+} buffering within the SR. This reduces free $[Ca^{2+}]_i$ and subsequently stimulates SERCA pump activity, leading to a rise in SR Ca^{2+} content. However, as NCX expression is higher and SERCA expression is lower in this model of LVD this will counteract to a certain extent the affect of increased CSQ expression. Increased expression of NCX would partially counter the effect of increased CSQ assuming that the NCX is working in forward mode (Na^+in/Ca^{2+}out). However, if NCX was working in reverse mode (Na^+out/Ca^{2+}in) then it would increase $[Ca^{2+}]_i$ and may promote Ca^{2+} loading into the SR. Furthermore, SERCA is influenced by the amount of and the phosphorylation status of the regulatory protein phospholamban (PLB). PLB expression and phosphorylation state may either counteract a decrease in SERCA expression or partially alleviate it. To date, transmural expression of PLB has not been studied in this model.

Clearly, it is difficult to estimate what the net effect on SR Ca^{2+} content would be following such changes in Ca^{2+} handling protein expression. Quantification of protein expression reflects only the amount of protein present within a tissue and does not take into account the functional activity of the protein. SR functional measurements would be required to accurately quantify SR Ca^{2+} content.

The use of transgenic animal models is becoming an important method in which researchers can study the affects of specific protein knockout or overexpression. Mouse models specifically overexpressing CSQ have also observed additional changes in the expression of other proteins. Transgenic mice overexpressing CSQ by 10 fold showed a decrease in protein expression of the ryanodine receptor, junctin, triadin and demonstrated minimal change or a small increase in SERCA and phospholamban expression (Jones *et al.* 1998). In another CSQ over expressing mouse study, a 20-fold increase in CSQ was produced (Sato *et*

al. 1998). In contrast, the Sato study observed an increase in SERCA and phospholamban expression, without alterations in ryanodine receptor, junctin and triadin expression. These studies suggested that CSQ overexpression might be directly responsible for alterations in the expression of other proteins. Alternatively, as CSQ is closely associated with the RyR, increased CSQ may disrupt the functional properties of the ryanodine receptor complex which may produce alterations in the expression of other Ca^{2+} handling proteins. Whichever mechanism is responsible, such alterations in expression probably constitute a compensatory mechanism, the degree of which is dependent on the extent of CSQ overexpression. Interestingly, transgenic animals overexpressing CSQ show signs of cardiac hypertrophy (Jones *et al.* 1998; Sato *et al.* 1998; Schmidt *et al.* 2000).

Studies overexpressing SERCA (Baker *et al.* 1998) observed no changes in phospholamban protein expression and He *et al.* (1997) observed no changes in the ryanodine receptor, CSQ, phospholamban or NCX protein expression, although the mRNA expression for phospholamban and NCX were increased 1.4 and 1.8 fold respectively. Transgenic animal models overexpressing NCX demonstrated no changes in the protein expression of CSQ, SERCA and phospholamban (Terracciano *et al.* 1998; Kiriazis & Kranias, 2000). It appears from transgenic animal studies that CSQ expression has a strong influence on cellular form and function and may play a regulatory role in the expression of other proteins. In contrast, overexpressing NCX and SERCA proteins does not appear to exert such influence on the expression of other intracellular proteins.

Finally, it is not possible to determine from this study whether the alterations in SERCA and NCX expression observed in this model are triggered by cellular changes activated as a compensatory mechanism due to LVD or are a secondary affect induced by alterations in CSQ protein expression.

7.4.4. Summary

In summary, the three proteins quantified in this study CSQ, SERCA and NCX , showed minimal transmural differences in protein expression in both sham and LVD samples. The most interesting and unexpected finding from these experiments was the significant increase (~ 40%) in CSQ protein expression observed in LVD. This finding is unusual, as most studies have reported unchanged CSQ protein expression in heart failure or LVD. The increase in CSQ protein expression may be specific to this particular animal model (severity, duration and aetiology). SERCA protein expression was slightly lower (~10%) and NCX protein expression was higher (15%) in LVD than sham. These findings are consistent with most literature observations.

Chapter 8

General discussion

8.1. Relationship between myocyte contractility and intracellular $[Ca^{2+}]$.

The aim of this study was to characterise and interrelate transmural differences in normal myocyte contractility with intracellular $[Ca^{2+}]$ and Ca^{2+} handling protein expression. Furthermore, the effects of chronic myocardial infarction on the above parameters were investigated and compared to normal (sham) myocytes. Table 8.1 below summarises the changes reported in earlier chapters (3 & 4).

	Sham Epi/Endo ratio	**LVD Epi/Endo ratio**	**Endo LVD/Sham ratio**	**Epi LVD/Sham ratio**
Diastolic L. Δ	= 1	=1	≤ 1	≤ 1
Diastolic Ca	> 1	< 1	< 1	< 1
Fractional shortening	< 1	≤ 1	< 1	⇔
Peak systolic Ca^{2+}	≥ 1	< 1	=1	< 1

Table 8.1. Summary changes in Epi/Endo and LVD/Sham ratios of diastolic length change, fractional shortening and associated changes in diastolic and peak systolic $[Ca^{2+}]_i$. The ratios are indicated by < 1 and > 1, =1 indicates no change. Equal ratios with a trend to lower or higher ratios are indicated by ≤ 1 and ≥ respectively.

8.1.1. Transmural comparisons

Relating changes in myocyte length to $[Ca^{2+}]_i$ can give some indication of myocyte myofilament Ca^{2+} sensitivity. Frequency-dependent changes in diastolic length were of a similar magnitude between endocardial and epicardial sham myocytes, yet sham epicardial diastolic $[Ca^{2+}]_i$ was slightly higher than endocardial. These results may indicate a transmural difference in myofilament Ca^{2+} sensitivity, with epicardial myofilaments less sensitive to Ca^{2+} than endocardial myofilaments (table 8.1). LVD endocardial and epicardial diastolic length changes were also similar yet in contrast to the sham data, LVD epicardial diastolic $[Ca^{2+}]_i$ was lower than endocardial suggesting higher myofilament Ca^{2+} sensitivity in LVD epicardial myocytes in comparison to endocardial. These data suggest that the normal myofilament Ca^{2+} sensitivity gradient observed in sham myocytes is not maintained in LVD.

Correlation between fractional shortening and peak systolic $[Ca^{2+}]_i$ in the sham data indicate a similar transmural myofilament Ca^{2+} sensitivity gradient to that observed with the diastolic length/Ca^{2+} relationship. Fractional shortening was less in sham epicardial myocytes in comparison to endocardial yet peak systolic $[Ca^{2+}]_i$ was similar if not greater in epicardial myocytes. These results indicate lower sham epicardial myofilament Ca^{2+} sensitivity. Transmural fractional shortening was very similar in the LVD data set, yet peak systolic $[Ca^{2+}]_i$ was slightly lower in epicardial myocytes, although not significantly. These results are in agreement with the diastolic data where LVD epicardial myofilament Ca^{2+} sensitivity appears higher than LVD endocardial myofilament Ca^{2+} sensitivity.

8.1.2. Sham/ LVD comparisons

The trend towards less relative diastolic myocyte length changes with increasing frequency of stimulation in LVD myocytes (table 8.1) could reflect either lower diastolic $[Ca^{2+}]_i$ or reduced myofilament Ca^{2+} sensitivity in LVD myocytes. Endocardial and epicardial LVD myocytes display lower diastolic $[Ca^{2+}]_i$ than corresponding shams myocytes suggesting that the increased resting length is due to lower diastolic $[Ca^{2+}]_i$ rather than altered myofilament Ca^{2+} sensitivity (table 8.1). Comparisons between LVD/Sham relative diastolic length changes suggests a slightly higher sensitivity in both LVD endocardial and epicardial myocytes as

relative diastolic length changes are small or unchanged, yet LVD diastolic [Ca^{2+}] is lower, significantly so in LVD epicardial myocytes.

Fractional shortening is lower in endocardial LVD in comparison to sham although not significantly, yet LVD endocardial peak systolic [Ca^{2+}]$_i$ is unchanged. This suggests that myofilament Ca^{2+} sensitivity is lower in LVD endocardial myocytes in comparison to sham. In contrast, the opposite occurs in epicardial myocytes (table 8.1), where LVD epicardial fractional shortening is unchanged yet the peak systolic [Ca^{2+}] is lower. This result suggests that epicardial myofilament Ca^{2+} sensitivity is higher in LVD than sham. The diastolic data suggest that both LVD endocardial and epicardial myofilament Ca^{2+} sensitivity is greater than sham whereas in contrast, the fractional shortening data suggests that only LVD epicardial sensitivity is higher. The reason for this difference is unknown.

To further investigate myofilament Ca^{2+} sensitivity changes in LVD, the correlation between relative diastolic length and [Ca^{2+}]$_i$ with increasing stimulation frequency was examined. Figure 8.1 compares the relative diastolic length changes associated with changing [Ca^{2+}]$_i$ (nM) in both sham and LVD myocytes. Although this approach may not be the ideal way of measuring myofilament Ca^{2+} sensitivity due to dynamic changes in both diastolic length and [Ca^{2+}]$_i$ under these conditions it may give some indication of myofilament Ca^{2+} sensitivity changes. Both endocardial and epicardial results were combined for sham and LVD groups. Relative diastolic length changes for each group are expressed relative to diastolic length at 0.3Hz of each myocyte subtype. The diastolic length – [Ca^{2+}] relationship showed a trend towards greater length changes (gradient = $-11.2 \pm 1.29 \times 10^{-5}$) in LVD myocytes in comparison to the sham (gradient = $-9.7 \pm 1.56 \times 10^{-5}$) data set, although no significant differences were observed. These results suggest that myofilament Ca^{2+} sensitivity is similar between LVD and sham myocytes.

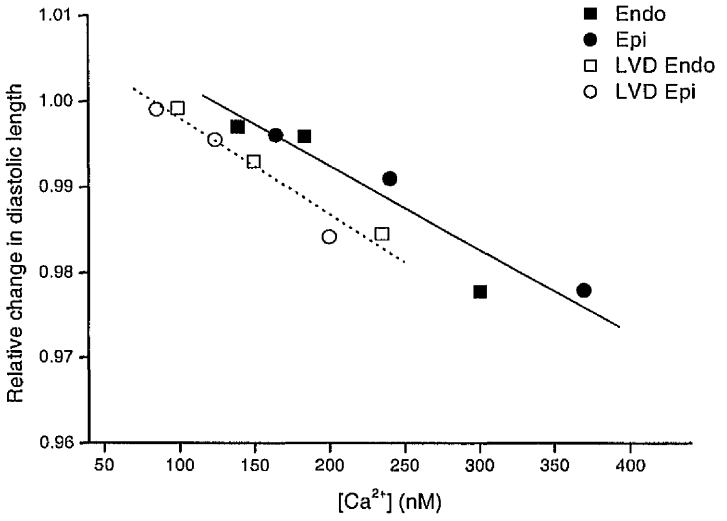

Figure 8.1. Relationship between changes in relative diastolic length and $[Ca^{2+}]_i$. Solid lines represent best linear fits of the data. Slope of linear fit were $-9.76 \pm 1.56 \times 10^{-5}$ and $-11.2 \pm 1.29 \times 10^{-5}$ for sham and LVD respectively.

To date, published reports of changes in myofilament Ca^{2+} sensitivity in failing myocardium have been conflicting. Unchanged myofilament Ca^{2+} sensitivity in hypertrophic guinea-pig (Naqvi & Macleod, 1994), rabbit trabeculae (Denvir *et al.* 1996), dog (Kinugawa *et al.* 1999), and human muscle strips (Gwathmey & Hajjar, 1990; Hajjar *et al.* 2000) have been reported. Decreased sensitivity in failing rat myocytes (Li *et al.* 1997; Wisloff *et al.* 2002), and trabeculae (Perez *et al.* (1999) have also been reported. In contrast, increased myofilament Ca^{2+} sensitivity has been reported in human (Schwinger *et al.* 1994; Wolff *et al.*1996) and canine myocardium (Wolff *et al.*1995).

An alternative cause of the altered relationship between intracellular $[Ca^{2+}]$ and length in failing myocytes is a change in the resistance to myocyte shortening. Increased passive resistance would result in decreased myocyte shortening in the face of constant myofilament force production. Passive resistance within myocytes is dependent on the density and distribution of the cytoskeleton. Increased density and disorganisation of cytoskeletal proteins (Schaper *et al.* 1991) and membrane

associated proteins (Hein *et al.* 2000) have been observed. Increased cytoskeletal density impedes sarcomere motion, increases intracellular loading and produces contractile dysfunction. Contractile dysfunction, in the form of reduced extent and velocity of sarcomere shortening (Tsutsui *et al.* 1994) and loss of compliance (increased cytoskeletal stiffness) (Tagawa *et al.* 1997) have been reported in a feline pressure overloaded hypertrophic model. The degree of cytoskeletal accumulation and disorganisation may be species, severity of failure, load and chamber dependent (Hein *et al.* 2000). Cytoskeletal changes may be an alternative reason for the differences in contraction amplitude observed in this study between LVD and Sham myocytes. Further, cytoskeleton density and organisation may vary across the left ventricle due to differences in transmural myocyte load.

8.2. Relationship between Ca^{2+} handling protein expression and intracellular $[Ca^{2+}]$.

As mentioned previously, intracellular $[Ca^{2+}]$ homeostasis is governed by SR Ca^{2+} release/uptake and sarcolemmal Ca^{2+} influx and efflux. The major mechanisms responsible for intracellular Ca^{2+} movement are the Ca^{2+} handling proteins, most importantly SERCA, RyR, and NCX. Alterations in expression of these proteins are likely to have adverse affects on intracellular Ca^{2+} homeostasis. Table 8.2 below summarises the changes in protein expression between endocardial and epicardial samples and between sham and LVD groups. Peak systolic $[Ca^{2+}]_i$ (electrically induced) and caffeine-induced peak systolic $[Ca^{2+}]_i$ are included in this table to try to determine if a correlation between protein expression and peak systolic $[Ca^{2}]_i$ exists, i.e. are the changes in protein expression responsible for changes in peak systolic $[Ca^{2+}]_i$.

	Sham Epi/Endo ratio	**LVD Epi/Endo ratio**	**Endo LVD/Sham ratio**	**Epi LVD/Sham ratio**
Peak systolic Ca^{2+}	≥ 1	< 1	$=1$	< 1
Caffeine peak systolic Ca^{2+}	> 1	< 1	$=1$	< 1
CSQ	≤ 1	≤ 1	> 1	> 1
SERCA	$=1$	$=1$	≤ 1	≤ 1
NCX	< 1	$=1$	≥ 1	> 1

Table 8.2. Summary of changes in Epi/Endo and LVD/Sham ratio of peak systolic Ca^{2+}, caffeine-induced peak systolic Ca^{2+} and protein expression. Increases and decreases in the ratios are indicated by < 1 and > 1, $=1$ indicates no change. Equal ratios with a trend to lower or higher ratios are indicated by ≤ 1 and ≥ 1 respectively.

8.2.1. Transmural and LVD/Sham comparisons.

As explained in chapter 7, it is difficult to correlate intracellular changes with protein expression directly as the net intracellular effect of a change in a given amount of protein is unknown unless the functional activity of the protein has been determined quantitatively. Furthermore, it is also possible that the expression of more than one protein will change in any given situation, therefore directly relating a specific intracellular event to a change in expression of one specific protein is almost impossible.

The use of transgenic animals to artificially overexpress or knockout specific proteins allows researchers to investigate the physiological role played by these proteins. Over expression of CSQ in transgenic mice produced a decreased calcium transient amplitude even though SR Ca^{2+} content was increased (assayed by caffeine application) (Sato *et al.* 1998; Jones *et al.* 1998). In these cases, increased CSQ expression was associated with increased SR Ca^{2+} capacity but a decreased efficiency of Ca^{2+} induced SR Ca^{2+} release, i.e. decreased peak systolic $[Ca^{2+}]_i$.

In this study, a marked increase in CSQ expression was observed in both endocardial and epicardial LVD myocytes (table 8.2). A reduced peak systolic $[Ca^{2+}]_i$ was observed in epicardial but not in endocardial LVD myocytes and in addition no differences in the caffeine-induced peak systolic $[Ca^{2+}]_i$ was observed. One explanation for the apparent differences between these studies is that the CSQ overexpression in the Sato & Jones models was increased 10 and 20 fold whereas, the increased CSQ expression in this LVD model was increased by only ~1.5 fold. Therefore, the small increase in CSQ expression observed in this study appears to be having a negligible affect on SR Ca^{2+}content.

Another study observed doubling of the calcium transient amplitude when SERCA was overexpressed ~1.5 fold (Baker *et al.* 1998). Therefore, one may predict that decreased SERCA expression would lead to decreased calcium transient amplitudes. In agreement, LVD endocardial and epicardial myocytes showed a ~ 10% decrease in SERCA expression (table 8.2) and a small decrease in calcium and caffeine-induce calcium transient amplitude. Studies overexpressing NCX (Terracciano *et al.* 1998) observed no significant changes in calcium transient amplitude, although transgenic myocytes showed a tendency to smaller calcium transient amplitudes, yet SR Ca^{2+} content was 69% higher (caffeine application). In

addition, contraction kinetics were significantly faster in transgenic myocytes in comparison to control myocytes. In contrast Schillinger *et al.* (2000) observed smaller caffeine-induced calcium transients in their NCX overexpression model (adenoviral upregulation). The tendency for unchanged or smaller calcium transient amplitude observed in LVD may reflect increased NCX activity as a result of increased NCX expression.

The peak systolic $[Ca^{2+}]_i$ and protein expression changes reported in this study agree with previously published data regarding trends between these two factors. Obviously, with the combination of protein expression changes in this LVD model it is impossible to specify which if any single protein is solely responsible for the changes in peak systolic $[Ca^{2+}]_i$. Furthermore, as the activity of these proteins is unknown, one cannot assume that there is direct correlation between protein expression and activity (Quinn *et al.* 2001).

It is likely that the effect on SR Ca^{2+}content and subsequent peak systolic $[Ca^{2+}]_i$ is the net effect of the combined protein expression changes. In addition, intracellular disruption of normal signalling pathways, biochemical changes, such as protein phosphorylation may also influence changes in overall cellular and/or protein function.

8.3. Future work

In this study, indirect evidence was presented to suggest that a transmural gradient in myofilament sensitivity in normal rabbit myocardium exists and that is subsequently altered in this model of LVD.

The most obvious set of experiments to be performed in the future on this LVD model is the assessment of transmural sham and LVD myofilament Ca^{2+} sensitivity. Altered myofilament Ca^{2+} sensitivity may arise from changes in intracellular conditions such as pH, $[Mg^{2+}]$ and [Pi] which act directly on myofilaments to alter force production. Therefore it would be useful to establish which intracellular conditions changed in this LVD model and how they subsequently affect Ca^{2+} myofilament sensitivity.

Alternatively, changes in myosin isoform expression may alter the intrinsic activity of the myofilaments in hypertrophy (Bugaisky, *et al.* 1990). Furthermore, alterations in troponin quantity (Westfall & Solaro 1992) and phosphorylation state (Solaro & Van Eyk, 1996) may also affect myofilament function and Ca^{2+}

sensitivity. Assessment of myofilament protein biochemistry and cytoskeletal expression in this model of dysfunction may help establish causative factors involved in cellular dysfunction.

In addition, quantification of RyR protein expression and activity in sham and LVD endocardial and epicardial regions may help to explain differences in SR Ca^{2+} release. RyRs are thought to be modulated by many intracellular proteins, one of which is FKBP. Hyperphosphorylation of FKBP has been reported in heart failure (Marx *et al.* 2000), this hyperphoshorylated state results in defective channel function and subsequently alters SR Ca^{2+} release. Assessment of FKBP protein expression and phosphorylation status in sham and LVD endocardial and epicardial regions could be an important determinant of RyR modulation and may help to explain the differences in peak systolic $[Ca^{2+}]_i$.

References

ALLEN, B.G. & KATZ, S. (2000). Calreticulin and Calsequestrin are differentially distributed in canine heart. *Journal of molecular and cellular cardiology* **32**, 2379-2384.

ALLEN, D.G., JEWELL, B.R. & WOOD, E.H. (1976). Studies of the contractility of mammalian myocardium at low rates of stimulation. *Journal of Physiology* **254**, 1-17.

ANTZELEVITCH, C., SICOURI, S., LITOVSKY, S.H., LUKAS, A., KRISHNAN, S.C., DI DIEGO, J.M.,GINANT.G.A & LUI, D. (1991). Heterogeneity within the ventricular wall. *Circulation research* **69**, -1427

ARAI, M., ALPERT, N., MACLENNAN, D.H., BARTON, P. & PERIASAMY, M. (1993). Alterations in sarcoplasmic reticulum gene expression in human heart failure. *Circulation research* **72**, 463-469.

ARAI, M., SUZUKI, T. & NAGAI, R. (1996). Sarcoplasmic reticulum genes are upregulated in mild cardiac hypertrophy but downregulated in severe cardiac hypertrophy induced by pressure overload. *Journal of molecular and cellular cardiology* **28**, 1583-1590.

BAKER.D.L, HASHIMOTO, K., GRUPP, I.L., JI, Y., REED, T., LOUKIANOV, E., GRUPP, G., BHAGWHAT, A., HOIT, B., WALSH, R., MARBAN, E. & PERIASAMY, M. (1998). Targeted overexpression of the sarcoplasmic reticulum Ca^{2+}-ATPase increases cardiac contractility in transgenic mouse hearts. *Circulation* **83**, 1205-1214.

BASSANI, J.W., BASSANI, R.A. & BERS, D.M. (1994). Relaxation in rabbit and rat cardiac cells: species-dependent differences in cellular mechanisms. *Journal of Physiology* **476.2**, 279-293.

BASSANI, J.W., BASSANI, R.A. & BERS, D.M. (1995). Calibration of Indo-1 and resting intracellular $[Ca]_i$ in intact rabbit cardiac myocytes. *Biophysical Journal* **68**, 1453-1460.

BASSANI, R.A. & BERS, D.M. (1994). Na-Ca exchange is required for rest-decay but not rest-potentiation of twitches in rabbit and rat ventricular myocytes. *Journal of molecular and cellular cardiology* **26**, 1335-1347.

BELTRAMI, C.A., FINATO, N., ROCCO, M., FERUGLIO, G.A., PURICELLI, C., CIGOLA, F., QUAINI, F., SONNENBLICK, E.H., OLIVETTI, G. & ANVERSA, P. (1994). Structural basis of end-stage failure in ishaemic cardiomyopathy in humans. *Circulation* **89**, 151-163.

BERS, D.M. (1985). Ca influx and sarcoplasmic reticulum Ca release in cardiac muscle activation during postrest recovery. *American journal of physiology* **248**, H366-H381

BERS, D.M. (1987). Ryanodine and the calcium content of cardiac SR assessed by caffeine and rapid cooling contractures. *American journal of physiology* **253**, C408-C415

BERS, D.M. (1989). SR Ca loading in cardiac muscle preparations based on rapid-cooling contractures. *American journal of physiology* **256**, C109-C120

BERS, D.M., BASSINI.J.W.M & BASSANI.R.A (1993). Competition and redistribution among calcium transport systems in rabbit cardiac myocytes. *Cardiovascular research* **27**, 1772-1777.

BERS, D.M. (1993). *Excitation-contraction coupling and cardiac contractile force.* Kluwer Academic Publishers.

BERS, D.M., BASSANI, R.A., BASSANI, J.W., BAUDET, S. & HRYSHKO, L.V. (1993). Paradoxical twitch potentiation after rest in cardiac muscle: increased fractional release of SR calcium. *Journal of molecular and cellular cardiology* **25**, 1047-1057.

BERS, D.M. & BERLIN, J.R. (1995). Kinetics of $[Ca]_i$ decline in cardiac myocytes depend on peak $[Ca]_i$. *American journal of physiology* **268**, C271-C277

BERS, D.M. (2000). Calcium fluxes involved in control of cardiac myocyte contraction. *Circulation research* **87**, 275-281.

BEST, P.M., BOLITHO DONALDSON, S.K. & KERRICK, W.G.L. (1977). Tension in mechanically disrupted mammalian cardiac cells: effects of magnesium adenosine triphosphate. *Journal of Physiology* **265**, 1-17.

BEUCKELMANN, D.J., NABAUER, M. & ERDMANN, E. (1992). Intracellular calcium handling in isolated ventricular myocytes from patients with terminal heart failure. *Circulation* **85**, 1046-1055.

BISHOP, S.P., OPARIL, S., REYNOLDS, R.H. & DRUMMOND, J.L. (1979). Regional myocyte size in normotensive and spontaneously hypertensive rats. *Hypertension* **1**, 378-383.

BLOCK, B.A., IMAGAWA, T., CAMPBELL, K.P. & FRANZINI-ARMSTRONG, C. (1988). Structural evidence for direct interaction between the molecular components of the transverse tubule/Sarcoplasmic reticulum junction in skeletal muscle. *Journal of Cellular biology* **107**, 2587-2600.

BRIDGE, J.H. (1986). Relationships between the sarcoplasmic reticulum and sarcolemmal calcium transport revealed by rapidly cooling rabbit ventricular muscle. *Journal of General Physiology* **88**, 437-473.

BRILLANTES, A.M., ONDRIAS, K., SCOTT, A., KOBRINSKY, E., ONDRIASOVA, E., MOSCHELLA, M.C., JAYARAMAN, T., LANDERS, M., EHRLICH, B.E. & MARKS, A.R. (1994). Stabilisation of calcium release channel (Ryanodine receptor) function by FK506-binding protein. *Cell* **77**, 513-523.

BRILLANTES, A.M., ALLEN, P., TAKAHASHI, T., IZUMO, S. & MARKS, A.R. (1992). Differences in cardiac calcium release channel (ryanodine receptor) expression in myocardium from patients with end-stage heart failure caused by ischaemic versus dilated cardiomyopathy. *Circulation research* **71**, 18-26.

BRUZZONE, R., WHITE, T.W. & PAUL, D.L. (1996). Connections with connexins: the molecular basis of direct intercellular signalling. *European journal of Biochemistry* **238**, 1-27.

BRYANT, S.M., SHIPSEY, S.J. & HART, G. (1997). Regional differences in electrical and mechanical properties of myocytes from guinea-pig hearts with mild left ventricular hypertrophy. *Cardiovascular research* **35**, 315-323.

BUGAISKY, L.B., ANDERSON, P.G., HALL, R.S. & BISHOP, S.P. (1990). Differences in myosin isoform expression in the subepicardial and subendocardial myocardium during cardiac hypertrophy in the rat. *Circulation research* **66**, 1127-1132.

BURTON, F.L., MCPHADEN, A.R. & COBBE, S.M. (2000). Ventricular fibrillation threshold and local dispersion of refractoriness in isolated rabbit hearts with left ventricular dysfunction. *Basic research in cardiology* **95**, 359-367.

CAMPBELL, S.E. & GERDES, A.M. (1988). Regional changes in myocyte size during the reversal of thyroid-induced cardiac hypertrophy. *Journal of molecular and cellular cardiology* **20**, 379-387.

CARAFOLI, E. (1985). The homeostasis of calcium in heart cells. *Journal of molecular and cellular cardiology* **17**, 203-212.

CHAMBERLAIN, B.K., LEVITSKY, D.O. & FLEISCHER, S. (1983). Isolation and characterisation of canine cardiac SR with improved Ca^{2+} transport properties. *Journal of Biological Chemistry* **258**, 6602-6609.

CHAMUNORWA, J.P. & O'NEILL, S.C. (1995). Regional differences in rest decay and recoveries of contraction and the calcium transient in rabbit ventricular muscle. *Pflügers Archives-European Journal Of Physiology* **430**, 195-204.

COLYER.J (1993). Control of the calcium pump of cardiac sarcoplasmic reticulum. A specific role for the pentameric structure of phospholamban. *Cardiovascular research* **27**, 1766-1771.

COOK, S.J., CHAMUNORWA, J.P., LANCASTER, M.K. & O'NEILL, S.C. (1997). Regional differences in the regulation of intracellular sodium and in action potential configuration in rabbit left ventricle. *Pflügers Archives-European Journal Of Physiology* **433**, 515-522.

COWIE, M.R., MOSTERD, A., WOOD, D.A., DECKERS, J.W., POOLE-WILSON, P.A., SUTTON, G.C. & GROBBEE, D.E. (1997). The epidemiology of heart failure. *European Heart Journal* **18**, 208-225.

CURRIE, S. and SMITH, G. L. Enhanced phosphorylation of phospholamban and down regulation of SERCA 2 in cardiac sarcoplasmic reticulum from rabbits with heart failure. Cardiovascular research 41, 135-146. 1999.

DAVIES, C.H., DAVIA, K., BENNETT, J.G., PEPPER, J.R., POOLE-WILSON, P.A. & HARDING, S.E. (1995). Reduced contraction and altered frequency response of isolated ventricular myocytes from patients with heart failure. *Circulation* **92**, 2540-2549.

DAVIES, C.H., HARDING, S.E. & POOLE-WILSON, P.A. (1996). Cellular mechanisms of contractile dysfunction in human heart failure. *European Heart Journal* **17**, 189-198.

DE MULDER, P.A., VAN KERCKHOVEN, R.J., ADRIAENSEN, H.F., GILLEBERT, T.C. & DE HERT, S.G. (1997). Continuous total intravenous anaesthesia, using Propofol and Fentanyl in an open-thorax rabbit model: Evaluation of cardiac contractile function and biochemical assessment. *Laboratory Animal Science* **47**, 367-375.

DEL MONTE, F., O'GARA, POOLE-WILSON, P.A., YACOUB, M. & HARDING, S.E. (1995). Cell geometry and contractile abnormalities of myocytes from failing human left ventricle. *Cardiovascular research* **30**, 281-290.

DENVIR, M.A., MacFARLANE. N.G., MILLER,D.J., & COBBE.S.M. (1996). Enhanced SR function in saponin-treated ventricular trabeculae from rabbits with heart failure *American journal of physiology* **271**, H850 –H859.

DIXON, I.M., HATA, T. & DHALLA, N.S. (1992). Sarcolemmal calcium transport in congestive heart failure due to myocardial infarction in rats. *American journal of physiology* **262**, H1387-H1394

DURKIN, J.T., AHRENS, D.C., PAN, Y.-C.E. & REEVES, J.P. (1991). Purification and amino-terminal sequence of the bovine cardiac sodium-calcium exchange: Evidence for the presence of a signal sequence. *Archives of Biochemistry and Biophysics* **290**, 369-375.

EISENBERG, B.R., EDWARDS, J.A. & RADOVAN, Z. (1985). Transmural distribution of Isomyosin in rabbit ventricle during maturation examined by immunofluorescence and staining for calcium activated adenosine triphosphatase. *Circulation research* **56**, 548-555.

EZZAHER, A., BOUANANI, N. & CROZATIER, B. (1992). Force-frequency relations and response to ryanodine in failing rabbit hearts. *American journal of physiology* **263**, H1710-H1715

FABIATO, A. (1983). Calcium-induced release of calcium from the sarcoplasmic reticulum. *American journal of physiology* **245**, C1-C14

FABIATO, F. & FABIATO, A. (1978). Effects of pH on the myofilaments and the sarcoplasmic reticulum of skinned cells from cardiac and skeletal muscles. *Journal of Physiology* **276**, 233-255.

FABIATO, A. & FABIATO, F. (1975). Effects of magnesium on contractile activation of skinned cardiac cells. *Journal of Physiology* **249**, 497-517.

FABIATO, A. (1985). Use of aequorin for the appraisal of the hypothesis of the release of calcium from the sarcoplasmic reticulum induced by a change of pH in skinned cardiac cells. *Cell Calcium* **6**, 95-108.

FEDIDA, D. & GILES, W.R. (1991). Regional variations in action potentials and transient outward current in myocytes isolated from rabbit left ventricle. *Journal of Physiology* **442**, 191-209.

FIGUEREDO, V.M., BRANDES, R., WEINER, M.W., MASSIE, B. & CAMACHO, S.A. (1993). Endocardial versus epicardial differences of intracellular free calcium under normal and ischaemic conditions in perfused rat heart. *Circulation research* **72**, 1082-1090.

FLESCH, M., SCHWINGER, R.H.G., SCHNABEL, P., SCHIFFER, F., VEN GELDER, I., BAVENDIEK, U., SUDKAMP, M., KUHN-REGNIER, F. & BOHM, M. (1996). Sarcoplasmic reticulum Ca^{2+}-ATPase and phospholamban mRNA and protein levels in end stage heart failure due to ischaemic or dilated cardiomyopathy. *Journal of Molecular Medicine* **74**, 321-332.

FRANK, K., BRIXIUS, K. & SCHWINGER, R.H.G. (2002). Effect of Omega- 3 polyunsaturated fatty acids on force frequency relationship and sarcoplasmic Ca^{2+}-ATPase activity in human myocardium. *In press*

GERDES, A.M., KELLERMAN.S.E, MOORE, J.A., MUFFLY, K.E., CLARK, L.C., REAVES, P.Y. & MALEC, K.B. (1992). Structural remodelling of cardiac myocytes in patients with ischaemic cardiomyopathy. *Circulation* **86**, 426-430.

GERDES, A.M. (1979). Differences in regional capillary distribution and myocyte sizes in normal and hypertrophic rat hearts. *American Journal of Anatomy* **156**, 523-532.

GERDES, A.M. & CAPASSO, J.M. (1995). Structural remodelling and mechanical dysfunction of cardiac myocytes in heart failure. *Journal of molecular and cellular cardiology* **27**, 849-856.

GERDES, A.M., ONODERA, T., WANG, X. & MCCUNE, S.A. (1996). Myocyte remodelling during the progression to failure in rats with hypertension. *Hypertension* **28**, 609-614.

GO, L.O., MOSCHELLA, M.C., WATRES, J., HANDA, K.K., FYFE, B.S. & MARKS, A.R. (1995). Differential regulation of two types of intracellular calcium release channels during end-stage heart failure. *Journal of Clinical Investigation.* **95**, 888-894.

GRAY, R.P., MCINTYRE, H., SHERIDAN, D.S. & FRY, C.H. (2001). Intracellular sodium and contractile function in hypertrophied human and guinea-pig myocardium. *Pflügers Archives-European Journal Of Physiology* **442**, 117-123.

GRYNKIEWICZ, G., POENIE, M. & TSIEN, R.Y. (1985). A new generation of Ca indicators with greatly improved fluorescence properties. *The Journal of Biological Chemistry* **260**, 3440-3450.

GWATHMEY, J.K., COPELAS, L., MACKINNON, R., SCHOEN, F.J., FELDMAN, M.D., GROSSMAN, W. & MORGAN, J.P. (1987). Abnormal intracellular calcium handling in myocardium from patients with end-stage heart failure. *Circulation research* **61**, 70-76.

GWATHMEY, J.K., SLAWSKY, M.T., HAJJAR, R.J., BRIGGS, G.M. & MORGAN, J.P. (1990). Role of intracellular calcium handling in force-interval relationships of human ventricular myocardium. *Journal of Clinical Investigation.* **85**, 1599-1613.

GWATHMEY, J.K. & HAJJAR, R.J. (1990). Relation between steady state force and intracellular Ca^{2+}. Index of myofibrillar responsiveness to Ca^{2+}. *Circulation* **82**, 1266-1278.

GWATHMEY, J.K., WARREN.S.E, BRIGGS, G.M., COPELAS, L., FELDMAN, M.D., PHILLIPS.P.J, CALLAHAN.M, SCHOEN, F.J., GROSSMAN, W. & MORGAN, J.P. (1991). Diastolic dysfunction in hypertrophic cardiomyopathy. Effect on active force generation during systole. *Journal of Clinical Investigation.* **87**, 1023-1031.

HAJJAR, R.J., SCHWINGER, R.H.G., SCHMIDT, U., KIM, C.S., LEBECHE, D., DOYE, A.A. & GWATHMEY, J.K. (2000). Myofilament calcium regulation in human myocardium. *Circulation* **101**, 1679-1685.

HARDING, S.E., VESCOVO, G., JONES, S.M., BENNETT, G., YACOUB, M.H. & POOLE-WILSON, P.A. (1989). Morphological and functional characteristics of myocytes isolated from human left ventricular aneurysms. *Journal of Pathology* **159**, 191-196.

HARRISON, S.M. & BERS, D.M. (1989). Influence of temperature on the calcium sensitivity of the myofilaments of skinned ventricular muscle from the rabbit. *Journal of General Physiology* **93**, 411-428.

HART, G. (1994). Cellular electrophysiology in cardiac hypertrophy and failure. *Cardiovascular research* **28**, 933-946.

HASENFUSS, G., REINECKE, H., STUDER, R., MEYER, M., PIESKE, B., HOLTZ, J., HOLUBARSCH, C., POSIVAL, H., JUST, H. & DREXLER, H. (1994). Relation between myocardial function and expression of sarcoplasmic reticulum Ca^{2+}-ATPase in failing and nonfailing human myocardium. *Circulation research* **75**, 434-442.

HASENFUSS, G. (1998). Alterations of calcium-regulatory proteins in heart failure. Cardiovascular research 37, 279-289.

HASENFUSS, G., SCHILLINGER, W., LEHNART, S.E., PREUSS, M., PIESKE, B., MAIDAN, R., PRESTLE, J., MINAMI, K. & JUST, H. (1999). Relationship between Na^+-Ca^{2+}-exchanger protein levels and diastolic function of failing human myocardium. *Circulation* **99**, 641-648.

HATEM, S.N., SHAM, J.S.K. & MORAD, M. (1994). Enhanced Na^+-Ca^{2+} exchange activity in cardiomyopathic Syrian hamster. *Circulation research* **74**, 253-261.

HE, H., GIORDANO, F.J., HILAL-DANDAN, R., CHOI, D.-J., ROCKMAN, H.A., MCDONOUGH, P., BLUHM, W.F., MEYER, M., SAYEN, M.R., SWANSON, E. & DILLMANN, W.H. (1997). Overexpression of the rat sarcoplasmic reticulum Ca2+ ATPase gene in the heart of transgenic mice accelerates calcium transients and cardiac relaxation. *Journal of Clinical Investigation.* **100**, 380-389.

HEIN, S., KOSTIN, S., HELING, A., MAENO, Y. & SCHAPER, J. (2000). The role of the cytoskeleton in heart failure. *Cardiovascular Re*search **45**, 273-278.

HILGEMANN, D.W. (1990). Regulation and deregulation of cardiac Na^+-Ca^{2+} exchange in giant excised sarcolemmal membrane patches. *Nature* **344**, 242-245.

HISAMATSU, Y., OHKUSA, T., KIHARA, Y., INOKO, M., UEYAMA, T., YANO, M., SASAYAMA, S. & MATSUZAKI, M. (1997). Early changes in the functions of cardiac sarcoplasmic reticulum in volume-overloaded cardiac hypertrophy in rats. *Journal of molecular and cellular cardiology* **29**, 1097-1109.

HOFFMAN, J.I.E. (1995). Heterogeneity of myocardial blood flow. *Basic research in cardiology* **90** , 103-111.

HRYSHKO, L.V., STIFFEL, V. & BERS, D.M. (1989). Rapid cooling contractures as an index of sarcoplasmic reticulum calcium content in rabbit ventricular myocytes. *American journal of physiology* **257**, H1369-H1377

HUMPHREY, S.M., VANDERWEE, M.A. & GAVIN, J.B. (1988). Transmural differences in the postischaemic recovery of cardiac energy metabolism. *American journal of pathology* **131**,

IGARASHI-SAITO.K, TSUTSUI.H, TAKAHASHI.M, KINUGAWA.S, EGASHIRA.K & TAKESHITA.A (1999). Endocardial verses epicardial differences of sarcoplasmic reticulum Ca^{2+} -ATPase gene expression in the canine failing myocardium. *Basic research in cardiology* **94**, 267-273.

IKEMOTO, N., RONJAT, M., MESZAROS, L.G. & KOSHITA, M. (1989). Postulated role of Calsequestrin in the regulation of calcium release from sarcoplasmic reticulum. *Biochemistry* **28**, 6771

IWATA, T., GALLI, C., DAINESE, P., GUERINI.D & CARAFOLI, E. (1995). The 70 kDa component of the heart sarcolemmal Na^+/Ca^{2+}-exchanger preparation is the C-terminal portion of the protein. *Cell Calcium* **17**, 263-269.

JELICKS, L.A. & SIRI, F.M. (1995). Effect of hypertrophy and heart failure on $[Na^+]_i$ in pressure-overloaded guinea-pig heart. *American journal of Hypertension* **8**, 934-943.

JONES, L.R., SUZUKI, Y.J., WANG, W., KOBAYASHI, Y.M., RAMESH, V., FRANZINI-ARMSTRONG, C., CLEEMANN, L. & MORAD, M. (1998). Regulation of Ca^{2+} signalling in transgenic mouse cardiac myocytes overexpressing calsequestrin. *Journal of Clinical Investigation* **101**, 1385-1393.

KENTISH, J.C., TER KEURS, H.E.D.J., RICCIARDI, L., BUCX, J.J.J. & NOBLE, M.I.M. (1986). Comparison between the sarcomere length-force relations of intact and skinned trabeculae from rat right ventricle. *Circulation research* **58**, 755-768.

KENTISH, J.C. (1986). The effects of inorganic phosphate and creatine phosphate on force production in skinned muscles from rat ventricle. *Journal of Physiology* **370**, 585-604.

KEUNG, E.C. (1989). Calcium current is increased in isolated adult myocytes from hypertrophied rat myocardium. *Circulation research* **64**, 753-763.

KINUGAWA, S., TSUTSUI, H., SATOH, S., TAKAHASHI, M., IDE, T., IGARASHI-SAITO, K., ARIMURA, K., EGASHIRA, K. & TAKESHITA, A. (1999). Role of Ca^{2+}availability to myofilaments and their sensitivity to Ca^{2+} in myocyte contractile dysfunction in heart failure. *Cardiovascular research* **44**, 398-406.

KIRIAZIS, H. & KRANIAS, E.G. (2000). Genetically engineered models with alterations in cardiac membrane calcium -handling proteins. *Annual reviews in physiology* **62**, 321-351.

KISS, E., BALL, N.E. & KRANIAS, E.G. (1995). Differential changes in cardiac phospholamban and sarcoplasmic reticulum Ca-ATPase protein levels - effects on Ca^{2+} transport and mechanics in compensated pressure overload and mechanics in compensated pressure overloaded hypertrophy and congestive heart failure. *Circulation research* **77**, 759-764.

KOSS, K.L. & KRANIAS, E.G. (1996). Phospholamban: a prominent regulator of myocardial contractility. *Circulation research* **79**, 1059-1063.

LEVI, A.J. & ISSBERNER, J. (1996). Effect of the fura-2 transient of rapidly blocking the Ca^{2+} channel in electrically stimulated rabbit heart cells. *Journal of Physiology* **493**, 19-37.

LEVICK, J.R. (1995). *An introduction to Cardiovascular physiology.* Butterworth-Heinmann Ltd.

LI, P., HOFMANN, P.A., LI, B., MALHOTRA, A., CHENG, W., SONNENBLICK, E.H., MEGGS, L.G. & ANVERSA, P. (1997). Myocardial infarction alters myofilament calcium sensitivity and mechanical behaviour of myocytes. *American journal of physiology* **272**, H360-H370

LINCK, B., BOKNIK, P., ESCHENHAGEN, T., MULLER, F.U., NEUMANN, J., NOSE, M., JONES, L.R., SCHMITZ, W. & SCHOLZ, H. (1996). Messenger RNA expression and immunological quantification of phospholamban and SR-Ca^{2+} -ATPase in failing and nonfailing human hearts. *Cardiovascular research* **31**, 625-532.

LINDNER, M., ERDMANN, E. & BEUCKELMANN, D.J. (1998). Calcium content of the sarcoplasmic reticulum in isolated ventricular myocytes from patients with terminal heart failure. *Journal of molecular and cellular cardiology* **30**, 743-749.

LIU, Z., HILBELINK, D.R., CROCKETT, W.B. & GERDES, A.M. (1991). Regional changes in hemodynamics and cardiac myocyte size in rats with aortocaval fistulas (1.Developing and established hypertrophy). *Circulation Research.* **69**, 52-58.

LIU, Z., HILBELINK, D.R. & GERDES, A.M. (1991). Regional changes in hemodynamics and cardiac myocyte size in rats with aortocaval fistulas (2. Long-term effects). *Circulation Research.* **69**, 59-65.

MACLEOD,K.T. & Bers, D.M. (1987). Effects of rest duration and ryanodine on changes of extracellular [Ca] in cardiac muscle from rabbits. American journal of physiology **253,** C398 – C407

MAIER, L.S., BERS, D.M. & PIESKE, B. (2000). Differences in Ca^{2+}-handling and sarcoplasmic reticulum Ca^{2+}-content in isolated rat and rabbit myocardium. *Journal of molecular and cellular cardiology* **32**, 2249-2258.

MARX, S.O., REIKEN, S., HISAMATSU, Y., JAYARAMAN, T., BURKHOFF, D., ROSEMBLIT, N. & MARKS, A.R. (2000). PKA Phosphorylation dissociates FKB12.6 from the calcium release channel (Ryanodine Receptor):Defective Regulation in Failing Hearts. *Cell* **101**, 365-376.

MARX, S.O., GABURJAKOVA, J., GABURJAKOVA.M., HENRIKSON, C., ONDRIAS, K. & MARKS, A.R. (2001). Coupled gating between cardiac calcium release channels (Ryanodine receptors). *Circulation research* **88**, 1151-1158.

MATSUI, H., BARRY W.H, SPITZER K.W. & LIVSEY C (1995). Angiotensin II stimulates Na/H exchange in adult rabbit ventricular myocytes. *Cardiovascular physiology* **29**, 215

MATSUI, H., MACLENNAN, D.H., ALPERT, N.R. & PERIASAMY, M. (1995). Sarcoplasmic reticulum gene expression in pressure overload-induced cardiac hypertrophy in rabbit. *American journal of physiology* **268**, C252-C258

MCINTOSH, M.A., COBBE, S.M. & SMITH, G.L. (1999). Heterogeneous calcium current and intracellular calcium transients in ventricular myocyte sub-types from normal and failing rabbit hearts. *Journal of Physiology* 521P

MCINTOSH, M.A., COBBE, S.M. & SMITH, G.L. (2000). Heterogeneous changes in action potential and intracellular Ca^{2+} in left ventricular myocyte sub-types isolated from rabbits with heart failure. *Cardiovascular research* **45**, 397-409.

MEISSNER, G. (1994). Ryanodine receptor/Ca^{2+} release channel and their regulation by endogenous effectors. *Annual reviews in physiology* **56**, 485-508.

MERCADIER, J.-J., LOMPRE, A.-M., DUC, P., BOHELER, K.R., FRAYSSE, J.-B., WISNEWSKY, C., ALLEN, P.D., KOMAJDA, M. & SCHWARTZ, K. (1990). Altered sarcoplasmic reticulum Ca^{2+}-ATPase gene expression in the human ventricle during end-stage heart failure. *Journal of Clinical Investigation* **85**, 305-309.

MEYER, M., SCHILLINGER, W., PIESKE, B., HOLUBARSCH, C., HEILMANN, C., POSIVAL, H., KUWAJIMA, G., MIKOSHIBA, K., JUST, H. & HASENFUSS, G. (1995). Alterations of SR proteins in failing human dilated cardiomyopathy. *Circulation* **92**, 778-784.

MILNES, J.T. & MACLEOD, K.T. (2001). Reduced ryanodine receptor to dihydropyridine receptor ratio may underlie slowed contraction in a rabbit model of left ventricular hypertrophy. *Journal of molecular and cellular cardiology* **33**, 485

MING, Z., NORDIN, C., SIRI, F.M. & ARONSON, R. (1994). Reduced calcium current density in single myocytes isolated from hypertrophied failing guinea pig hearts. *Journal of molecular and cellular cardiology* **26**, 1133-1143.

MORGAN, J.P., GROSSMAN, W., SCHOEN.F.J, CALLAHAN.M, PHILLIPS.P.J, FELDMAN, M.D., WARREN.S.E & GWATHMEY, J.K. (1991). Diastolic dysfunction in hypertrophic cardiomyopathy (Effect on active force generation during systole). *Journal of Clinical Investigation* **87**, 1023-1031.

MOVSESIAN, M.A., KARIMI, M., GREEN, K. & JONES, L.R. (1994). Ca^{2+} -transporting ATPase, phospholamban and calsequestrin levels in nonfailing and failing human myocardium. *Circulation* **90**, 653-657.

MULIERI, L.A., HASENFUSS, G., LEAVITT, B., ALLEN, P.D. & ALPERT, N.R. (1992). Altered myocardial force-frequency relation in human Heart Failure. *Circulation* **85**, 1743-1750.

NAQVI, R.U. & MACLEOD, K.T. (1994). Effect of hypertrophy on mechanisms of relaxation in isolated cardiac myocytes from guinea pig. *American journal of physiology* **267**, H1851-H1861

NAQVI, R.U., TWEEDIE, D. & MACLEOD, K.T. (2001). Evidence for the action potential mediating the changes to contraction observed in cardiac hypertrophy in the rabbit. *International Journal of Cardiology* **77**, 189-206.

NG, G.A., COBBE, S.M. & SMITH, G.L. (1998). Non-uniform prolongation of intracellular Ca^{2+} transients recorded from the epicardial surface of isolated hearts from rabbits with heart failure. *Cardiovascular research* **37**, 489-502.

NICOLL, D.A., LONGONI, S. & PHILIPSON, K.D. (1990). Molecular cloning and functional expression of the cardiac sarcolemmal Na^{+}-Ca^{2+} exchanger. *Science* **250**, 562-564.

O'NEILL, S.C. (1993). Differences in twitch decay of isolated cells from epicardial and endocardial layers of rabbit ventricular muscle. *Journal of Physiology* **467**, 331P

O'ROURKE, B., KASS, D.A., TOMASELLI, G.F., KAAB, S., TUNIN, R. & MARBAN, E. (1999). Mechanisms of altered Excitation-Contraction coupling in canine tachycardia-induced heart failure, 1 Experimental studies. *Circulation Res.* **84**, 562-570.

OLIVETTI, G., MELISSARI, M., BALBI, T., QUAINI, F., CIGOLA, E., SONNENBLICK, E.H. & ANVERSA, P. (1994). Myocyte cellular hypertrophy is responsible for ventricular remodelling in the hypertrophied heart of middle aged individuals in the absence of cardiac failure. *Cardiovascular research* **28**, 1199-1208.

ORCHARD, C.H. & LAKATTA, E.G. (1985). Intracellular calcium transients and developed tension in rat heart muscle. *Journal of General Physiology* **86**, 637-651.

ORCHARD.C.H & KENTISH.J.C (1990). Effects of changes of pH on the contractile function of cardiac muscle. *American journal of physiology* **258**, C967-C981

OUADID, H., ALBAT, B. & NARGEOT, J. (1995). Calcium currents in diseased human cardiac cells. *Journal of cardiovascular pharmacology* **25**, 282-291.

PEREZ, N.G., HASHIMOTO, K., MCCUNE, S., ALTSCHULD, R.A. & MARBAN, E. (1999). Origin of contractile dysfunction in heart failure. *Circulation* **99**, 1077-1083.

PESSAH, I.N., MOLINSKI, T.F., MELOY, T.D., WONG, P., BUCK, E.D., ALLEN, P.D., MOHR, F.C. & MACK, M.M. (1997). Bastadins relate ryanodine-sensitive and -insensitive Ca^{2+} efflux pathways in skeletal SR and BC3H1 cells. *American journal of physiology* **272**, C601-C614

PHILIPSON, K.D., BERSOHN, M.M. & NISHIMOTO, A.Y. (1982). Effect of pH on Na^{+}-Ca^{2+} exchange in canine cardiac sarcolemmal vesicles. *Circulation research* **50**, 287-293.

PHILIPSON, K.D., LONGONI, S. & WARD, R. (1988). Purification of the cardiac Na^{+} - Ca^{2+} exchange protein. *Biochemica et Biophysica Acta* **945**, 298-306.

PHILIPSON, K.D. & NICOLL, D.A. (2000). Sodium-calcium exchange: A molecular perspective. *Annual reviews in physiology* **62**, 111-133.

PIESKE, B., MAIER, L.S., BERS, D.M. & HASENFUSS, G. (1999). Ca^{2+} handling and sarcoplasmic reticulum Ca^{2+} content in isolated failing and non failing myocardium. *Circulation research* **85**, 38-46.

POGWIZD, S.M., YUAN, M.Q., SAMAREL, A.M. & BERS, D.M. (1999). Upregulation of Na^{+}/Ca^{2+} exchanger expression and function in an arrhythmogenic rabbit model of heart failure. *Circulation research* **85**, 1009-1019.

PRESTLE, J., DIETERICH, S., PREUSS, M., BIELIGK, U. & HASENFUSS, G. (1999). Heterogeneous transmural gene expression of calcium-handling proteins and natriuretic peptides in the failing human heart. *Cardiovascular research* **43**, 323-331.

PYE, M.P., BLACK, M. & COBBE, S.M. (1996). Comparison of in vivo and in vitro haemodynamic function in experimental heart failure - use of echocardiography. *Cardiovascular research* **31**, 873-881.

QUINN, F.R., MCINTOSH, M.A., COBBE, S.M. & SMITH, G.L. (2001). Altered calcium handling and sarcoplasmic reticulum (SR) Ca^{2+} content in a rabbit model of left ventricular dysfunction. *Journal of Physiology* 536P

RAVENS, U. & DOBREV, D. (2000). Regulation of sarcoplasmic reticulum Ca^{2+} -ATPase and phospholamban in the failing and nonfailing heart. *Cardiovascular research* **45**, 245-252.

REDDY, L.G., JONES, L.R., PACE, R.C. & STOKES, D.L. (1996). Purified, reconstituted cardiac Ca^{2+}-ATPase is regulated by phospholamban but not by direct phosphorylation with Ca^{2+}/Calmodulin- dependent protein kinase. *Journal of Biological Chemistry* **271**, 14964-14970.

REEVES, J.P. & HALE, C.C. (1984). The stoichiometry of the cardiac sodium-calcium exchange system. *Journal of Biological Chemistry* **259**, 7733-7739.

REINECKE, H., STUDER, R., VETTER, R., HOLTZ, J. & DREXLER, H. (1996). Cardiac Na^{+}/Ca^{2+} exchange activity in patients with end-stage heart failure. *Cardiovascular research* **31**, 48-54.

ROBITAILLE, P.M., MERKLE, H., LEW, B., PATIL, G., HENDRICH, K., LINDSTROM, P., FROM, A.H.L., GARWOOD, M., BACHE, R.J. & UGURBIL, K. (1990). Transmural high energy phosphate distribution and response to alterations in workload in the normal canine myocardium as studied with spatially localized ^{31}P NMR spectroscopy. *Magnetic Resonance in Medicine* **16**, 91-116.

SABA, R.I., BOLLEN, A. & HERCHUELZ, A. (1999). Characterization of the 70kDa polypeptide of the Na/Ca exchanger. *Biochemical journal* **338**, 139-145.

SATO, Y., FERGUSON, D.G., SAKO, H., DORN, G.W., KADAMBI, V.J., YATANI, A., WALSH, R.A. & KRANIAS, E.G. (1998). Cardiac-specific overexpression of mouse cardiac calsequestrin is associated with depressed cardiovascular function and hypertrophy in transgenic mice. *The Journal of Biological Chemistry* **43**, 28470-28477.

SCHAPER, J. & SCHAPER, W. (1986). Morphological changes in myocardium from patients with coronary heart disease and cardiac hypertrophy. *Advances in cardiology* **34**, 16-24.

SCHAPER, J., FROEDE, R., HEiN, S., BUCK, A., HASHIZUME, H., SPEISER, B., FRIEDL, A. & BLEESE, N. (1991). Impairment of the myocardial ultrastructure and changes of the cytoskeleton in dilated cardiomyopathy. *Circulation* **83**, 504-514.

SCHILLINGER, W., JANSSEN, P.M.L., EMAMI, S., HENDERSON, S.A., ROSS, R.S., TEUCHER, N., ZEITZ, O., PHILIPSON, K.D., PRESTLE, J. & HASENFUSS, G. (2000). Impaired contractile performance of cultured rabbit ventricular myocytes after Adenoviral gene transfer of Na^{+}-Ca^{2+} exchanger. *Circulation research* **87**, 581-587.

SCHMIDT, A.G., KADAMBI, V.J., BALL, N.E., SATO, Y., WALSH, R.A., KRANIAS, E.G. & HOIT, B.D. (2000). Cardiac-specific overexpression of calsequestrin results in left ventricular hypertrophy, depressed force -frequency relation and pulses alternans In vivo. *Journal of molecular and cellular cardiology* **32**, 1735-1744.

SCHMIDT, U., SCHWINGER, R.H.G., BOHM, M. & ERDMANN, E. (1994). Alterations of the force-frequency relation depending on stages of heart failure in humans. *American Journal of Cardiology* **74**, 1066-1068.

SCHMIDT, U., HAJJAR, R.J., HELM, P.J., KIMC.S., DOYE, A.A. & GWATHMEY, J.K. (1998). Contribution of abnormal sarcoplasmic reticulum ATPase activity to systolic and diastolic dysfunction in human heart failure. *Journal of molecular and cellular cardiology* **30** , 1929-1937.

SCHWINGER, R.H.G., BOHM, M., MULLER-EHMSEN, J., UHLMANN, R., SCHMIDT, U., STABLEIN, A., UBERFUHR, P., KREUZER, E., REICHART, B., EISSNER, H.J. & ERDMANN, E. (1993). Effect of inotropic stimulation on the negative force-frequency relationship in the failing human heart. *Circulation* **88**, 2267-2276.

SCHWINGER, R.H.G., BOHM, M., KOCH, A., SCHMIDT, U., MORANO, I., EISSNER, H.J., UBERFUHR, P., REICHART, B. & ERDMANN, E. (1994). The failing human heart is unable to use the Frank-Starling mechanism. *Circulation research* **74**, 959-969.

SCHWINGER, R.H.G., BOHM, M., SCHMIDT, U., KARCZEWSKI, P., BAVENDIEK, U., FLESCH, M., KRAUSE, E.-G. & ERDMANN, E. (1995). Unchanged protein levels of SERCAII and phospholamban but reduced Ca^{2+} uptake and Ca^{2+}- ATPase activity of cardiac SR from dilated cardiomyopathy patients compared with patients with non-failing hearts. *Circulation* **92**, 3220-3228.

SCHWINGER, R.H.G., WANG, J., FRANK, K., MULLER-EHMSEN, J., BRIXIUS, K., MCDONOUGH, A. & ERDMANN, E. (1999). Reduced sodium pump α_1, α_3 and Beta-isoform protein levels and Na^{+}/K^{+}-ATPase activity but unchanged Na^{+}-Ca^{2+} exchanger protein levels in human heart failure. *Circulation* **99**, 2105-2112.

SHATTOCK, M.J. & BERS, D.M. (1989). Rat vs. rabbit ventricle Ca flux and intracellular Na assessed by ion-selective microelectrodes. *American journal of physiology* **256**, C813-C822

SHIGEKAWA, M. & IWAMOTO, T. (2001). Cardiac Na^{+}-Ca^{2+} exchange Molecular and pharmacological aspects. *Circulation Res.* **88**, 864-876.

SHIPSEY, S.J., BRYANT, S.M. & HART, G. (1997). Effects of hypertrophy on regional action potential characteristics in rat left ventricle. *Circulation* **96**, 2061-2068.

SIMMERMAN.H.K.B & JONES.L.R (1998). Phospholamban: Protein structure, mechanism of action, and role in cardiac function. *Physiological reviews* **78**, 921-947.

SIRI, F.M., KRUEGER, J., NORDIN, C., MING, Z. & ARONSON, R.S. (1991). Depressed intracellular calcium transients and contraction in myocytes from hypertrophied and failing guinea pig hearts. *American journal of physiology* **261**, H514-H530

SITSAPESAN, R. & WILLIAMS, A.J. (1990). Mechanisms of caffeine activation of single calcium-release channels of sheep cardiac sarcoplasmic reticulum. *Journal of Physiology* **423**, 425-439.

SMITH, S.H., MCCASLIN, M., SREENAN, C. & BISHOP, S.P. (1988). Regional myocyte size in two-kidney, one clip renal hypertension. *Molecular & Cellular Cardiology* **20**, 1035-1042.

SOLARO.R.J (1995). Control mechanisms regulating contractile activity of cardiac myofilaments. In *Physiology and Pathophysiology of the heart*, Ed: SPERLAKIS.N, Kluwer Academic publishers.

SOLARO.R.J & VAN EYK, J. (1996). Altered interactions among thin filament proteins modulate cardiac function. *Journal of molecular and cellular cardiology* **28**, 217-230.

SPOTNITZ, H.M., SONNENBLICK, E.H. & SPIRO, D. (1966). Relation of ultrastucture to function in the intact heart: sarcomere structure relative to pressure volume curves of intact left ventricles of dog and cat. *Circulation research* XVIII, 49-66.

STUDER, R., REINECKE, H., BILGER, J., ESCHENHAGEN, T., BÖHM, M., HASENFUSS, G., JUST, H., HOLTZ, J. & DREXLER, H. (1994). Gene expression of the cardiac Na^{+}-Ca^{2+} exchanger in end-stage human heart failure. *Circulation research* **75**, 443-453.

SUN, X., PROTASI, F., TAKAHASHI, M., TAKESHIMA, H., FERGUSON, D.G. & FRANZINI-ARMSTRONG, C. (1995). Molecular architecture of membranes involved in excitation-contraction coupling of cardiac muscle. *The Journal of Cell biology* **129**, 659-671.

SZEGEDI, C., SARKOZI, S., HERZOG, A., JONA, I. & VARSANY, M. (1999). Calsequestrin: more than 'only' a luminal Ca^{2+} buffer inside the sarcoplasmic reticulum. *Biochemical Journal* **337**, 19-22.

TAGAWA, H., WANG, N., NARISHIGE, T., INGBER, D.E., ZILE, M.R. & COOPER, G. (1997). Cytoskeletal mechanics in pressure-overload cardiac hypertrophy. *Circulation research* **80**, 281-289.

TAKAHASHI, T., ALLEN, P.D., LACRO, R.V., MARKS, A.R., DENNIS, A.R., SCHOEN, F.J., GROSSMAN, W., MARSH, J.D. & IZUMO, S. (1992). Expression of dihydropyridine receptor (Ca^{2+} channel) and calsequestrin genes in the myocardium of patients with end-stage heart failure. *Journal of Clinical Investigation.* **90**, 927-935.

TERRACCIANO, C.M.N., SOUZA, A.L., PHILIPSON, K.D. & MACLEOD, K.T. (1998). Na^+-Ca^{2+}-exchange and the sarcoplasmic reticular Ca^{2+} regulation in ventricular myocytes from transgenic mice over-expressing the Na^+-Ca^{2+} exchanger. *Journal of Physiology* **512**, 651-667.

TSUTSUI, H., TAGAWA, H., KENT, R.L., MCCOLLAM, P.L., ISHIHARA, K., NAGATSU, M. & COOPER, G. (1994). Role of microtubules in contractile dysfunction of hypertrophied cardiocytes. *Circulation* **90**, 533-555.

VAN DER VUSSE, G.J., ARTS, T., GLATZ, J.F.C. & RENEMAN, R.S. (1990). Transmural differences in energy metabolism of the left ventricular myocardium: Fact or fiction. *Journal of molecular and cellular cardiology* **22**, 23-37.

VARRO, A., NEGRETTI, N., HESTER, S.B. & EISNER, D.A. (1993). An estimate of the calcium content of the sarcoplasmic reticulum in rat ventricular myocytes. *Pflugers Archives-European Journal of Physiology* **423**, 158-160.

WESTFALL, M.V. & SOLARO.R.J (1992). Alterations in myofibrillar function and protein profiles after complete global ischemia in rat hearts. *Circulation research* **70**, 302-313.

WINEGRAD, S. (1965). The location of muscle calcium with respect to the myofibrils. *The Journal of General Physiology* **48**, 997-1002.

WISLOFF, U., LOENNECHEN, J.P., CURRIE, S., SMITH, G.L. & ELLINGSEN, O. (2002). Aerobic exercise reduces cardiomyocyte hypertrophy and increases contractility, Ca^{2+} sensitivity and SERCA-2 in rat after myocardial infarction. *Cardiovascular research* **54**, 162-174.

WOLFF, M.R., WHITESELL, L.F. & MOSS, R.L. (1995). Calcium sensitivity of isometric tension is increased in canine experimental heart failure. *Circulation research* **76**, 781-789.

WOLFF, M.R., BUCK, S.H., STOKER, S.W., GREASER, M.L. & MENTZER, R.M. (1996). Myofibrillar calcium sensitivity of isometric tension is increased in human dilated cardiomyopathies. *Journal of Clinical Investigation* **98**, 167-176.

WOLSKA, B.M. & SOLARO.R.J (1996). Method for isolation of adult mouse cardiac myocytes for studies of contraction and microfluorimetry. *American journal of physiology* **271**, H1250-H1255

XU, A. & NARAYANAN, N. (1998). Effects of aging on sarcoplasmic reticulum Ca^{2+}-cycling proteins and their phosphorylation in rat myocardium. *American journal of physiology* **275**, H2087-H2094

YU, L., PRAGAY, D.A., CHANG, D. & WICHER, K. (1979). Biochemical parameters of Normal Rabbit serum. *Clinical Biochemistry* **12**, 83-87.

ZHANG.L., KELLEY.J., SCHMEISSNER.G., KOBAYASHI, Y.M. & JONES, L.R. (1997). Complex formation between Junctin, Triadin, Caisequestrin and the Ryanodine receptor. *Journal of Biological Chemistry* **272**, 23389-23397.